WARWICK
THE UNIVERSITY OF WARWICK

A Thesis Submitted for the Degree of EngD at the University of Warwick

Permanent WRAP URL:

http://wrap.warwick.ac.uk/153553

Copyright and reuse:
This thesis is made available online and is protected by original copyright.
Please scroll down to view the document itself.
Please refer to the repository record for this item for information to help you to cite it.
Our policy information is available from the repository home page.

For more information, please contact the WRAP Team at: wrap@warwick.ac.uk

warwick.ac.uk/lib-publications

New prospects on ammonia recovery technologies from wastewater

EngD Innovation Report

by

Lavinia Bianchi

(1590317)

EngD International

WMG

University of Warwick

Submitted December, 2019

Abstract

Water pollution is rising due to the increase in human population. This represents a serious danger for the environment and human health. The wastewater sector is facing stricter regulations on environmental discharge limits, which result in higher energy and costs to remove contaminants. Thus, there is the need to develop more sustainable technologies that promote circularity by recovering valuable products and reusing resources. Amongst them, ammonia is a valuable resource widely used as a fertiliser, which can be recovered and exploited from wastewater.

This innovative research project focuses on two different ammonia recovery technologies that can be applied in different ranges of concentrations.

The first contribution regards the optimisation of the chemical precipitation technique, which is commonly applied in ammonium-rich streams. In particular, optimal conditions are defined to: (i) thermally decompose the precipitate (struvite) and recover higher quality products; (ii) recover the chemical employed for the precipitation. A kinetic mechanism of the thermal decomposition is also developed, which is key for a thorough understanding of the chemical process and to design the technology.

The second contribution focuses on lower concentration streams with the development of a new material for the adsorption technology. In this regard, innovation is needed due to high operational costs of conventional adsorbents. In this work, the Metal-Organic Framework ZIF-67 is used for the first time for this application. ZIF-67 demonstrates to: (i) successfully remove ammonium with an adsorption capacity comparable to natural zeolites; (ii) achieve 85 % removal efficiency at 35 °C; (iii) be effectively used in a continuous system; and (iv) be used in a composite configuration with recycled carbon fibres, which will facilitate the use of this material at large scale. ZIF-67 removes ammonia upon heating, thus reducing the need of chemicals required for zeolites regeneration. A cost analysis is also presented to discuss the conditions to make this material competitive for industrial application.

Acknowledgements

Firsty, I would like to thank my supervisors, Dr Stuart Coles and Professor Kerry Kirwan for the guidance they provided throughout the doctorate. I would like to express you my gratitude because you helped me to become a competent researcher and develop a critical mindset.

I would also like to thank Dr Marc Pidou for dedicating time to this project and for his valuable knowledge of the wastewater treatment sector. With your support I had the opportunity to improve the quality of this research.

I would like to acknowledge the Engineering and Physical Sciences Research Council (EPSRC) and Severn Trent Water for funding this project.

I would also like to thank my industrial mentors Peter Vale, Luca Alibardi and Keiron Maher that helped me to give industrial relevance to this research.

I would also like to acknowledge the Centre for Doctoral Training in Sustainable Materials and Manufacturing (SMM) for giving me the opportunity to conduct such an interesting project.

In this regard, I would like to thank Sue Gibson for her support during both the exciting and more challenging times. I appreciated our coffee walks. I would also like to thank the other members of the SMM group (Marco, Tina, Cynthia, Dan, Felipe, Pete, Maryam and the others) because it was lovely to be part of such a nice research group. I would like to reserve a special thanks to Tina, Cynthia and Dan, with whom I shared laughs and tears from the first day. I am glad I had you as my colleagues and now I have you as my friends.

A special thanks goes to my flatmates, Anna, Kirsty and Sian, which were there for me every day for the past three years. You have motivated me and understood me when I needed it and have become invaluable friends.

Vorrei ringraziare la mia famiglia, che mi ha sempre supportata e spronata ad essere la versione migliore di me stessa. Grazie a mamma e a nonna, che sono sempre state le prime a fare il tifo per me. Grazie a Rebe, perché trovo ispirazione ogni giorno nel tuo modo di realizzarti; a Nico, perché anche se siamo a distanza, nei momenti importanti hai trovato il modo di esserci; a papà per l'incoraggiamento e il sostegno. Grazie a nonna Marina, perché sei sempre stata curiosa dei miei

racconti. Grazie a nonno che, anche se non ci sei più, sei il mio riferimento. Mi hai insegnato il valore dello studio e della dedizione, il rispetto e la cura per l'ambiente che mi hanno portato a scegliere questo lavoro. Spero di avervi reso tutti orgogliosi di me.

Vorrei ringraziare le mie amiche di una vita: Ila, Isa, Silvia, Tere, Totta, Vitto. Nonostante siano anni che siamo lontane, non mi avete mai fatto mancare il vostro supporto.

Lastly, but most importantly, thank you Tom. You know how much you have been supportive to me. You always believed in me, even when I thought I couldn't do it. I truly appreciated how you encouraged me when I most needed it.

Declaration

This Innovation Report has been submitted to the University of Warwick in partial fulfilment of my application for the degree of Engineering Doctorate. This work has been carried out by myself and has not been submitted in any previous applications for any other degree.

Table of Contents

List of Figures

List of Tables

Abbreviations

BET: Brunauer-Emmett-Teller method

C_t: Concentration at a time t

C_0: Initial concentration

DSC: Differential scanning calorimetry

DTG: Derivative of thermogravimetric curve

EBCT: Empty Bed Contact Time

EQS: Environmental Quality Standard

FFT: Full Flow Treatment

FTIR: Fourier Transform Infra-Red spectroscopy

ICP-OES: Inductively coupled plasma technique optical emission spectrometry

MOF: Metal-Organic Framework

PC: Process contribution of a contaminant

PDA: Polydopamine

PE: Person equivalent

PFO: Pseudo-first order kinetic model

PSO: Pseudo-second order model

Q_e: Adsorption amount at the equilibrium

Q_t: Adsorption amount at a time t

Q_{max}: Maximum adsorption capacity

RC: Release concentration of a contaminant

rCF: Recycled carbon fibres

RT: Room temperature

SEM: Scanning electron microscopy

TEM: Transmission electron microscopy

TEM-EDS: TEM coupled with Energy Dispersive X-Ray Spectroscopy

TGA: Thermogravimetric analysis

UV-vis: Ultraviolet-visible spectroscopy

WWT: Wastewater Treatment

XPS: X-Ray photoelectron spectroscopy

XRD: X-Ray powder diffraction

1 Introduction

Water pollution poses a serious threat to human health and the environment. The challenges caused by climate change that are being faced nowadays in both developing and developed countries are unprecedented. It has been estimated that the change in climate that has occurred in the past century has indirectly impacted wastewater treatment plants due to sudden temperature change, floods, droughts, storms and heavy precipitation [1]. One of the United Nations Sustainable Development Goals (UN SDG) states: "ensure access to water and sanitation for all", since it is a basic human need [2]. Effective wastewater management is therefore critical to ensure water quality and pollution control. To tackle water pollution, in recent years, regulations on the effluent limits have become stricter. This has translated in more energy and chemicals that wastewater treatment companies have to employ to remove contaminants and ensure treatments are effective and limits are met. Interestingly, the threat of climate change and consequent change in governments' policies has also pushed wastewater treatment companies towards the development of more sustainable treatment works, with focus on the reduction of the emissions and the recovery of valuable products. As a result, research in the wastewater sector has moved towards circular economy, which promotes the recovery of products at the end-of-life stage to reuse them or convert them to new products that can be put back in the economy [3]. In this regard, wastewater and sludge are a source of energy, metals and nutrients. The latter, such as phosphorous and reactive forms of nitrogen (nitrate, ammonia), must be removed as they can cause oxygen deficiency and uncontrolled growth of algae in the receiving water body, with critical consequences for aquatic life. Fortunately, both are valuable resources and find commercial applications as fertilisers. Nitrogen is an essential element for life on Earth and is largely present in the atmosphere (78 %) in its inert form N_2. However, it is indispensable for plants growth in its reactive forms which are present in soil. In the 20th century, the invention of the Haber-Bosch process changed the agricultural world. The technology was able to fixate nitrogen gas and produce ammonia

on industrial scale. The sudden wide availability of ammonia promoted the increase in the production of nitrogen-based fertilisers and enabled a surge in crops growth, which subsequently resulted in a sharp rise of the world population. However, the industrial fixation of nitrogen has also had a negative impact in the environment, by altering the nitrogen cycle and nitrogen pollution [4]. The greater use of fertilisers has indeed provoked the increase in soil contamination due to fertilisers solubility and consequent run-off of harmful chemicals to groundwater (e.g. nitrate). The rise of the population has affected wastewaters pollution due to discharges by households and offices. Nitrogen is present in domestic wastewater as ammonia due to urea, faeces, and households' chemicals. Then, energy is used to transform it into nitrogen gas, as it has been done for over 100 years via biological treatments. It is therefore a waste to produce ammonia via the Haber-Bosch process using fossil fuels and energy, when at the same time ammonia could be recovered from a waste source and regain its value.

1.1 The need for this project

Severn Trent Water is one of the major wastewater treatment companies in the UK, providing clean water for 4.3 million homes in England and part of Wales. Treating 2.6 billion litres of wastewater every day, the company has been deeply committed to building a sustainable future. Their investments are focused towards carbon neutrality and also the development of technologies which look at the recovery of resources from sewage and wastewater. In particular, the recovery of ammonia is an opportunity to simultaneously reduce nitrogen pollution and obtain a valuable product. An effective recovery technology would replace conventional nitrogen removal technologies which use bacterial activity to transform the reactive forms of nitrogen (including ammonia, NH_3, and ammonium, NH_4^+) into nitrogen gas. Biological treatments processes, despite effective, require oxygen and energy to maintain the bacterial environment, and are sensitive to shock loadings. Moreover, they are responsible for nitrous oxide emissions, a powerful greenhouse gas [5,6]. Thus, research in ammonia recovery technologies is a necessary step to move towards circular economy models in the wastewater treatment sector.

1.2 Aim and objectives

This research project, sponsored by Sever Trent Water, had to answer one high-level research question: **how can we recover ammonia from sewage and wastewater using environmentally sustainable and economically feasible technologies?**

The principal aim of this research was to improve existing processes and provide new knowledge for the development of new technologies, to facilitate Severn Trent Water in their decision-making process to develop innovative solutions for this application. Thus, the broad objectives of the project were:

1. Identify gaps in the research regarding ammonia recovery technologies from wastewater and formulate research questions;
2. Develop a methodology to assess and provide answers to the research questions;
3. Conduct experiments based on the defined methodology to fill the gaps in the research and answer the research questions.

2 Research background

Ammonia is a colourless compound with a pungent odour, composed by one atom of nitrogen and three atoms of hydrogen. This chemical is of great importance in the production of food because it is used to prepare most nitrogen-based fertilisers. It is synthesised industrially from nitrogen and hydrogen gases through a process that involves temperatures over 400 °C and pressure of 200 bar [7], and requires up to 2 % of the world energy consumption [8]. This process also uses fossil fuels such as methane or coal, which are treated to obtain the hydrogen. This technology is called Haber-Bosch after the names of its inventors and has driven the ammonia production to large scale in the early 20th century. By doing so, food production rose exponentially, and it is considered one of the main reasons of the population increase from 1.8 in 1920 to over 6 billion in 2000 (Figure 1) [9]. The current yearly demand for ammonia is over 160 million tonnes, and its value fluctuates between $ 400 and $ 550 per tonne [10].

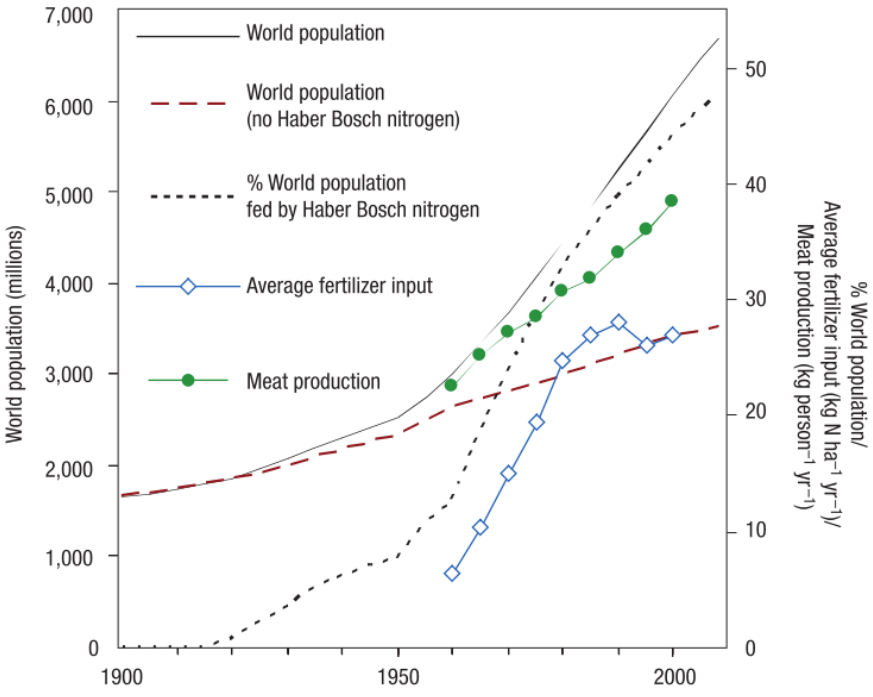

***Figure 1**: Influence of Haber-Bosch production of ammonia on population growth in the 20th century,* [9]. *Permission granted by the author.*

Despite the importance of ammonia as a resource, this chemical can also be harmful to the environment. It is found in wastewaters due to human activities (urine, pharmaceuticals or

chemicals, food), and can be a threat to aquatic life. In water it is also present in the oxidised form, ammonium (NH_4^+), according to the reaction:

$$NH_4^+ \rightleftharpoons NH_3 + H^+ \qquad \text{(Eq. 1)}$$

This equilibrium reaction is regulated by pH, in fact the two forms co-exist in equilibrium when pH is between 7 and 12 [11].

Substantial concentrations of ammonia and other nutrients, such as nitrate and phosphorous in water bodies can cause uncontrolled growth of algae, which then results in oxygen depletion, a phenomenon known as eutrophication. Eutrophication is a major threat to aquatic life and can destroy biodiversity. Thus, wastewater treatment (WWT) companies employ different technologies to reduce and control the levels of nutrients such as ammonia before discharging the treated water. An explicative approach to classify these technologies has been proposed by Mehta *et al.* and is depicted in Figure 2 [12].

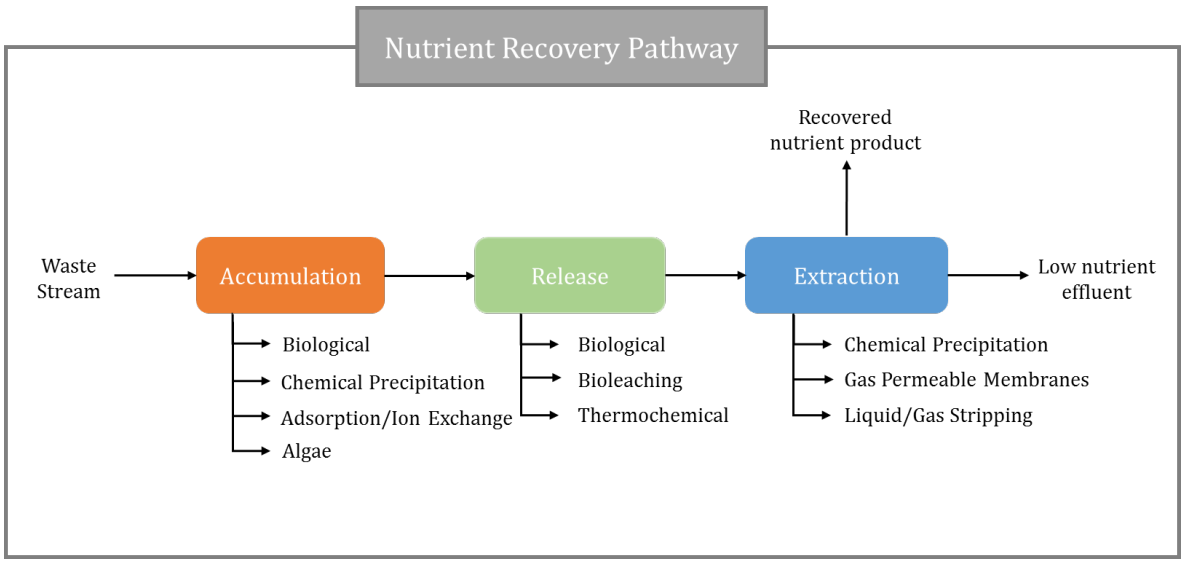

***Figure 2**: Schematic view of the nutrient recovery pathway, adapted from* [12]

The pathway is divided into three steps: accumulation, release and extraction. If recovered, nitrogen has to be accumulated before being released and extracted in the form of a final product. The most conventional pathway applied in WWT works only removes ammonia by applying only the accumulation and release steps. This is usually achieved via biological treatments that use bacterial activity in aerobic and anaerobic conditions to transform ammonia and other reactive forms of nitrogen (nitrate, nitrite) into nitrogen gas [13].

Biological treatments include activated sludge process, trickling filters, the Anammox process [14]. It has been estimated that between 70 and 320 billion euro are spent every year in the European Union to treat nitrogen and related pollution [15]. Recently, more stringent regulations were implemented on effluent limits to ensure the quality of freshwater and seawater is maintained. The Urban Wastewater Directive 91/271/EC sets the maximum concentration of the effluent based on the size of the plant. A reduction by 70 - 80 % of the total reactive nitrogen in the influent is required, where the term includes nitrate, nitrite, organic nitrogen and ammoniacal nitrogen. The maximum average of total nitrogen allowed is 10 mg L^{-1} for a plant serving more than 100,000 person equivalent (PE) and 15 mg L^{-1} for one that serves between 10,000 and 100,000 PE [16]. The Water Framework Directive 2000/60/EC focuses instead on ensuring the quality of the receiving water body [17]. The regulation is defined depending on the pollution levels of the receiving waters and can establish management plans for selected river basins or designate protected areas. As a result, many WWT plants already require effluents concentration below 5 mg L^{-1} [18]. Consequently, higher energy inputs are needed to meet the target outlet concentration limits, increasing the operational cost of the treatment plants. In addition to this, the water utilities are looking to implement more sustainable processes and interest in resource recovery from wastewater has risen significantly in the past decade. Thus, the recovery of ammonia from wastewater represents a great opportunity to concurrently reduce nitrogen pollution in liquid streams and gain a valuable and marketable product that finds applications in industry, including the production of fertilisers. Therefore, it was the primary aim of this project to investigate ammonia recovery technologies from wastewater. For the aforementioned reasons, nitrogen removal technologies that belong to the release stage will not be discussed in this report, as they do not align with the scope and objectives of this research. These conventional technologies have been extensively studied and can be found in recent review papers [19,20].

As far as the recovery technologies are concerned, the available techniques that serve this purpose are chemical precipitation, air stripping, membrane contactors, adsorption and ion-

exchange, algae or bio-electrochemical processes, such as microbial fuel cells. Table 1 provides a review summary of the different technologies with respect to existing knowledge, industrial application potential, sustainability factor, cost, and margins for improvement, ranked from low (√) to high (√√√). The table is the result of a review of the literature (Submission 1) updated with the most recent publications and the evaluation of the technologies in explained in detail in the following paragraphs.

***Table 1**: Graphic review of the technologies for ammonia recovery from wastewater*

Technology	Existing knowledge	Industrial application potential	Sustainability factor	Cost effectiveness	Margins for improvement
Air stripping	√√	√	√	√	√
Membrane contactors	√√√	√	√√	√	√√
Ion exchange	√√√	√√√	√√√	√√	√√√
Chemical precipitation	√√	√√√	√√√	√√	√√
Algae	√√	√	√√√	√√√	√√
Bio-electrochemical systems	√√	√	√√	√	√√√
√√√ high; √√ medium; √ low					

2.1 Air Stripping

The air stripping technology belongs to the "extraction" phase because it recovers gaseous ammonia, which is stripped in a packed column through the use of a stripping gas (air) that usually flows counter current to the influent [21]. Ammonium and ammonia that are present in the liquid phase are transferred to the gas phase due to a mass transfer phenomenon, which is facilitated by several parameters, including the most important pH and temperature. If the stripping column is then combined with a condenser, the ammonia is made to react with an acid to recover an ammonium salt, such as ammonium sulfate, $(NH_4)_2SO_4$. This technique

involves high costs, due to the need of chemicals like sulfuric acid, or calcium hydroxide for pH regulation and the effect of other parameters, such as air flow rate and temperature [22]. Therefore, it becomes a possible option only at very high NH_4-N concentrations in the inlet. For this reason, it has mainly been applied in industrial ammonium-rich liquid waste stream; hence, the industrial applicability for WWT works was ranked as low. The margins for improvement are also low, since the technology is well-established and work on the principles explained above, which require the control of several parameters (pH, T, air flow). Despite $(NH_4)_2SO_4$ is a marketable product, the process is not economically viable also due to significant issues: fouling caused by formation of by-products in the column; difficulty in recovering all the gaseous ammonia; production of sludge in the effluent which requires further treatment [23]. For these reasons, this technology was assigned a low sustainability factor and low cost effectiveness.

2.2 Membrane contactors

Membrane contactors work on a similar principle of mass transfer, and thus need temperature and addition of sodium hydroxide to increase the pH [24]. The membrane is usually a polymeric hollow fibre membrane with high surface area (e.g. polypropylene [25]). Also for this technology fouling represents a challenge, in addition to high operating costs due to alkali addition, [26]. Moreover, It has been estimated that more than one membrane contactor would be needed in sequence in order to achieve concentrations below the limit (10 mg L^{-1}) in the outlet [26]. This would greatly increase the capital costs (hence the lowest score as for air stripping in terms of cost effectiveness, Table 1) and would require the combination of this technology with another treatment (e.g. biological nitrogen removal). Interestingly, Sancho *et al.* coupled this process with an adsorption column that employed a natural zeolite [27]. The membrane contactor was used as an alternative process to recover the NH_4-N adsorbed from the zeolite. In particular, the ammonium-rich solution eluted from the media was fed into the membrane and reacted with phosphoric acid or nitric acid to form respectively di-ammonium

phosphate or ammonium nitrate, liquid fertilisers. According to the authors, this technique is a more sustainable alternative compared to the air stripping method [28].

The margins for improvement were considered medium since there is potential in the development of customised membranes by adjusting the hydrophobicity and modifying them to reduce fouling.

2.3 Algae

The algae technology could represent a sustainable option for nutrients accumulation. Algae are autotrophic organisms that can be unicellular or multicellular and use nutrients to grow, and produce biomass that can be exploited as an energy source [12]. Algae accumulate all the inorganic forms of nitrogen by converting them into organic nitrogen through a process called assimilation [29]. After the accumulation, ammonium can be released using thermochemical methods or the algae containing the nutrients can be directly applied as fertilisers [12]. The process is relatively simple, requiring a photobioreactor and a solid separation unit (hence, the cost was evaluated as low). However, algae need sunlight for the photosynthesis of the algal cells and a hydraulic retention time in the order of days to be effective [30,31]. Thus, this process could only be viable to treat high nutrients streams. Moreover, the lack of sunlight during wintertime negatively impacts the removal efficiency, making this technique unreliable in temperate regions. Chang *et al.* investigated the effect of artificial illumination and reported the improved removal capacity of microalgae [32]. However, this would greatly affect the cost effectiveness of the technology and the sustainability factor, which were ranked as high thank to the low use of chemicals and materials. Thus, the key challenges that are inhibitors for industrial applications are lack of light exposure, contamination, harvesting and high hydraulic retention time [29].

2.4 Bio-electrochemical systems

As far as the bio-electrochemical systems (BES) are concerned, they have recently attracted attention in the wastewater treatment sector for the production of hydrogen and energy, but also the recovery of nutrients. Currently, the state of the research is still at lab-scale because

there are major challenges that need to be addressed. There are two types of BESs: microbial fuel cells and microbial electrolysis cells. The former produces electricity from the decomposition of organic matter through microorganisms, whereas the latter is run by applying a current to produce hydrogen gas [33]. Despite these work effectively at laboratory scale [34], the process scale-up is extremely challenging. The greatest issues involve high capital costs and a drop of performance in system with greater capacity [35–37].

2.5 Adsorption and ion-exchange

On the contrary, ion exchange seems like a more promising technology for industrial scale applications. This technique is a recovery technology which accumulates the ammonium onto a sorbent by exchanging it with one of its ions. The technology presents columns packed with the adsorption media, and it can be operated in batch or continuous [38]. It has several advantages: temperature does not affect the system in any particular way and pH can be maintained at values around 7, since it is important to keep ammonia in the liquid phase. The media, usually zeolite, is used for multiple cycles, being regenerated with a brine (NaCl or KCl) once exhausted and then reused [27,39–44]. The ammonium is then extracted and recovered in the form of an ammonium salt by adding an acid solution (e.g. sulfuric acid). The cost effectiveness of this technology was evaluated as medium compared to air stripping, membrane contactors and bioelectrochemical systems. The scalability and economic feasibility of this process is strictly related to the adsorbent. This was demonstrated in a research study that carried out a Life Cycle Assessment, a comparative tool that uses mass and energy balances to model processes in order to evaluate their environmental impacts. The study conducted by Lin *et al.* confirmed that by only improving the adsorption capacity, which is maximum 50 mg g^{-1} for synthetic zeolites, the overall environmental impact could be improved by 10-200 % [45]. Very recently, researchers have started investigating the synthesis of porous materials tailored for specific applications. New materials such as Metal-Organic Frameworks could represent an opportunity for this application.

2.6 Chemical precipitation

Lastly, chemical precipitation combines the accumulation and extraction stages of the nutrient recovery pathway. This technique has been developed to overcome operational issues, such as pipe blockages that are caused by the spontaneous formation of a substance called struvite [46,47]. This phenomenon happens in the effluent of the anaerobic digester, which is rich in nutrients, because struvite is formed by ammonium, phosphate and magnesium reacting in molar ratio of 1:1:1. The controlled precipitation of struvite offers an opportunity to solve an operational problem that takes place in WWT plants and to recover simultaneously nitrogen and phosphorous. Struvite is a mineral that can be applied on land as slow-release fertiliser, and therefore is a valuable product. From a process point of view, however, a magnesium source (magnesium chloride) has to be added because it is present in lower concentrations compared to ammonium and phosphate. Furthermore, struvite usually contains heavy metals which lower the economic value of the fertiliser. In this regard, thermal decomposition of struvite has emerged as an opportunity of recovering higher valuable products and recycle the magnesium in the process, reducing the costs for the chemical [48]. Research shows struvite decomposes releasing water and ammonia gas, but the studies are not clear on the steps of the decomposition and the temperature at which ammonia is released. In some studies it is shown how the rate of evaporation is influenced by the heating rate and ammonia can evaporate with water molecules below 100 °C. Further research could explore more in detail the full recovery process through thermal decomposition of struvite, also looking at recovering phosphorous by separating it from the heavy metals.

2.7 Challenges

Currently, the key challenges related to the development and use of ammonia recovery technologies on industrial scale can be summarised as:

- Low concentration in wastewater mainstreams which makes processes not cost-effective;
- Efficient removal to below the environmental limits;

- High operational costs and use of chemicals;
- High environmental impact of the current recovery technologies.

In some stages of WWT plants the ammonium nitrogen concentration (NH_4-N), term which refers to the nitrogen content of ammonium, can increase up to 800 mg L^{-1}. The NH_4-N concentration reaches such high levels in the sludge liquors because it is first accumulated by the bacteria and then released during the anaerobic treatment of biomass. However, in the wastewater mainstream the concentration is typically up to 35 mg L^{-1} [11,13]. Thus, the concentration of NH_4-N in wastewater is one key factor that affects the cost-effectiveness of ammonia recovery technologies.

Challenges for the development of recovery technologies lie also in the efficiencies of these processes. For example, the ion exchange technique with zeolites can potentially achieve effective recovery but performance can drop in presence of competing cations, or after regeneration, and considerable amount of brine is needed to regenerate the zeolites, thus resulting in high operational costs. Regarding chemical precipitation, NH_4-N is not completely removed because the reaction takes place in equal molar ratio with the phosphate ion, but the concentration of phosphorous is typically much lower. Lastly, operational costs are largely due to the use of chemicals and maintenance operations, and this also contributes to the high environmental impact of these techniques.

2.8 Research objectives

This Engineering Doctorate (EngD) addressed the aim and scope of this research by tackling the problem from two different perspectives, highlighted in Figure 3. The diagram also shows an indicative nitrogen mass balance based on data from the literature and data provided by Severn Trent [49].

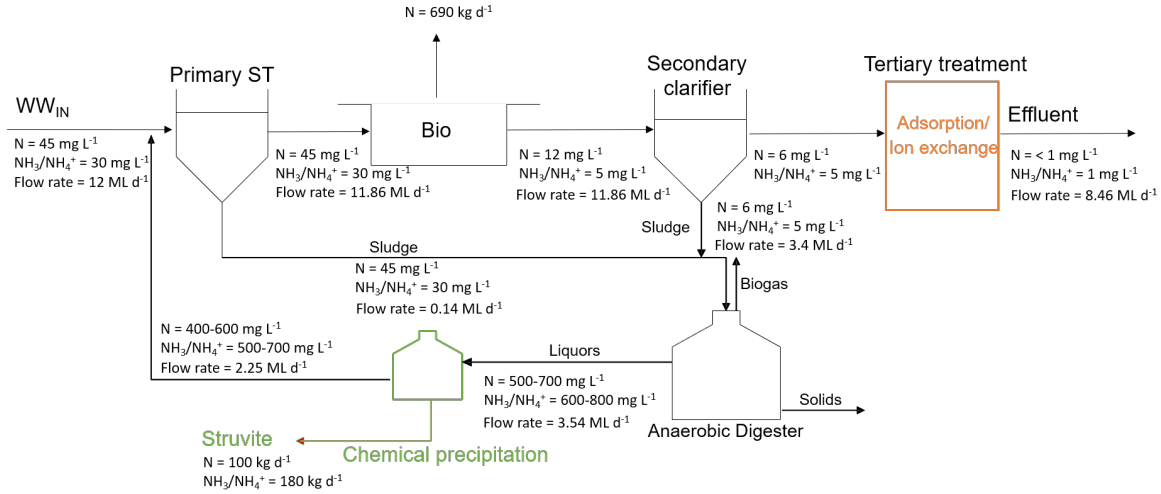

***Figure 3**: Simplified representation of a WWT plant and of the techniques investigated (in green and orange) with an indicative mass balance*

During the first two years, the research was focused on the chemical precipitation technique. As mentioned previously, this technology is typically used in ammonium-rich liquors (concentration of circa 800 mg L^{-1}), which are found after the anaerobic digestion stage, where struvite spontaneously precipitates. In this research, thermal decomposition of the precipitate was investigated to recover more valuable products (e.g. ammonia solution) and recycle the chemical used as reagent in the treatment. This would result in a more sustainable process that would reduce the use of chemicals and recover a higher quality, marketable product. The specific objectives of this research were the following:

A.1 Can struvite be decomposed at low temperature and release ammonia and water, both in a vapour form?

A.2 What is the mechanism of decomposition of struvite in the solid state and what is the energy required?

A.3 How can ammonia be recovered from the struvite decomposition and how can the magnesium compound be recyclable and put back in the process?

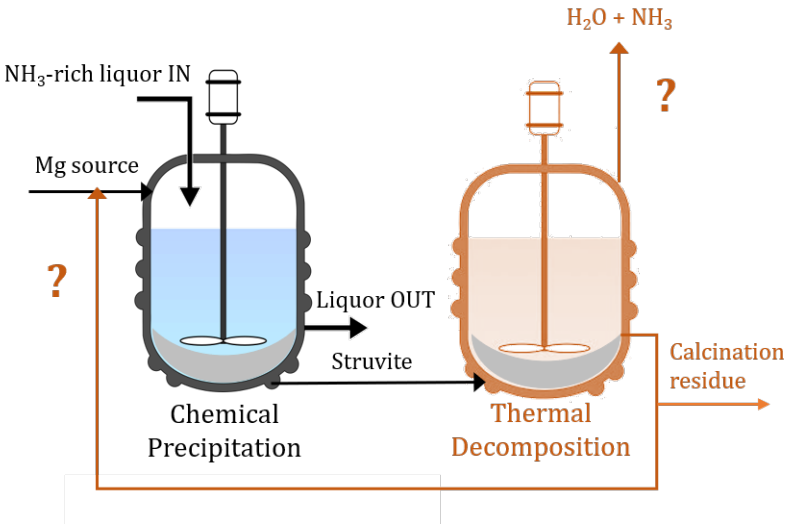

***Figure 4**: Schematic view of the research questions regarding chemical precipitation technique*

After providing answers to the questions above and evaluating the economic feasibility of the process, another opportunity for research and development was identified in the adsorption technology, a process that finds application in the tertiary treatment where concentrations are generally much lower (5 – 35 mg L^{-1}) and advanced treatments are carried out to make sure the effluent concentration meets the standard. It is important to note that this technique may follow a non-nitrifying biological secondary stage. Nitrification is in fact the aerobic process by which ammonium and ammonia are oxidised to nitrate. However, this step is also responsible for reducing organic matter, measured as Biochemical Oxygen Demand (BOD), which may not meet the discharge limit if the nitrification process did not occur. Despite this research focuses on ammonia recovery, it is important to have a holistic view of the treatment processes and note possible side effects of changes in the design.

Regarding adsorption, this work assessed the role of the adsorbent media and aimed at answering one key research question: **what new materials could potentially be applied for the adsorption of ammonium in a form that can be recovered?**

After a thorough literature review on porous materials, this work was directed towards Metal-Organic Frameworks (MOFs), a new class of nanomaterials. For this project, the principal aim was the following:

- Understanding the behaviour of several water-stable MOFs towards the adsorption in the liquid phase of ammonium and ammonia; and,
- Identifying the best characteristics of these MOFs for ammonium and ammonia recovery from wastewater.

In particular, this research had the following objectives:

B.1 Evaluate the ammonium adsorption capacity of the selected MOFs in controlled conditions;

B.2 Compare the adsorption performance with benchmark adsorption media (zeolites);

After having established and identified the best MOF for this application, the research project focused on understanding the mechanism of adsorption, with the following objectives:

B.3 Study the potential for increasing the adsorption capacity of the selected MOF;

B.4 Identify the adsorption behaviour by investigating adsorption isotherms using Freundlich and Langmuir models; and

B.5 Deepen the knowledge regarding the adsorption/desorption mechanism towards ammonium ions.

3 Research methodology

3.1 Guide to the portfolio and the submissions

The EngD portfolio is illustrated in Figure 5 and is a guideline to the Sections of this document and the related Submissions.

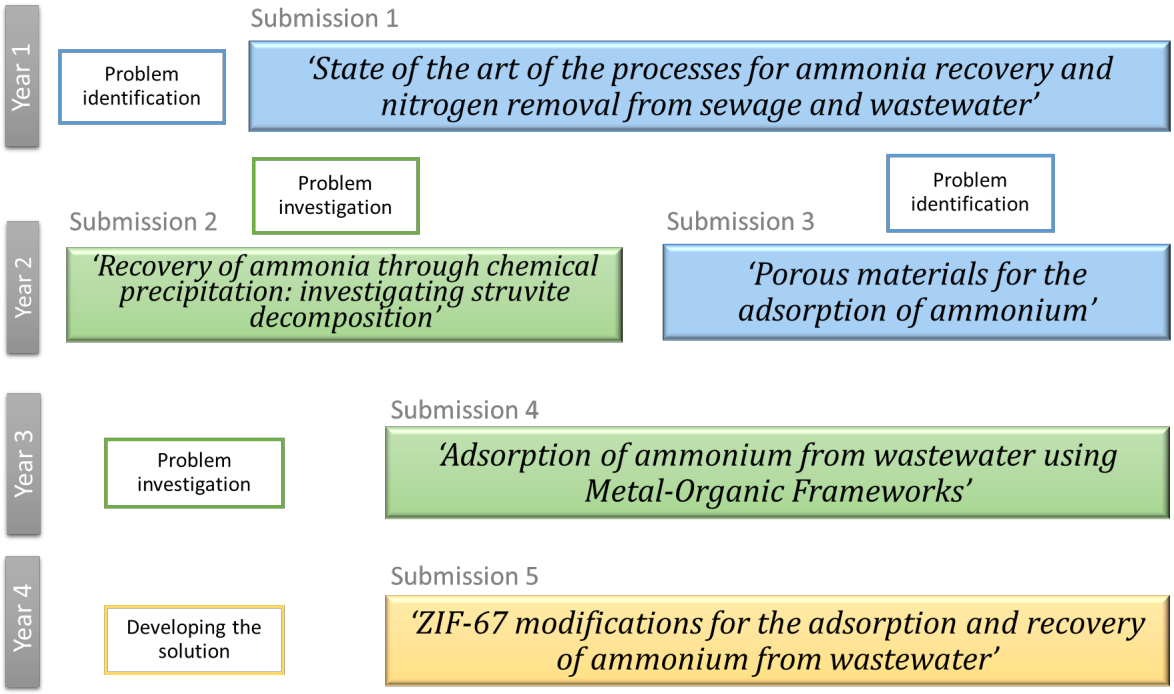

***Figure 5**: Structure of the EngD portfolio*

A first literature review that aimed at analysing all the existing technologies for the removal and recovery of ammonia from wastewater was written as Submission 1. The review reported the advantages and disadvantages of both fully developed processes and lab-scale technologies, revealing the gaps in the literature and setting the topics and the research questions that needed to be addressed. From this review, the broad aim and more detailed research objectives of the projects were defined. The project focused on two streams of work which regarded the optimisation of an existing chemical precipitation process and the development of a novel adsorption process for the tertiary treatment. This Section details the materials and methods that were used to conduct the research for both techniques.

Submission 2 reported the research and outcomes of the experimental work regarding the chemical precipitation technique, which involves the production of struvite (Section 4 of the

Innovation Report). Starting from the assessment of existing knowledge, this study answered the research questions A.1, A.2 and A.3 by providing new knowledge regarding the mechanism of decomposition of struvite, which could be used to optimise this technology.

After achieving the research objectives related to chemical precipitation, a second literature review explored research routes on the adsorption technology, with particular focus on the available porous materials that could be suitable for this application (Submission 3). In this review, several classes of materials were compared, from zeolites, resins, and hydrogels to Metal-Organic Frameworks. A gap in the knowledge was revealed regarding the use of Metal-Organic Frameworks for this application. This review led to set the objectives for the second project and is summarised in the introduction of Section 5. Section 5 reports also the experimental work carried out in Submission 4, which regarded the investigation of several Metal-Organic Frameworks for their use in ammonia adsorption in the liquid phase, fulfilling the objectives B.1 and B.2. Submission 5 is reported in Section 6 and regards the research carried out during the international placement at UNSW, Sydney (Australia). The work focused on one particular MOF, ZIF-67, which emerged as the best MOF amongst the ones tested in Submission 4. In this study, chemical modifications on the structure of the MOF were applied to answer objective B.3, and thus increase the adsorption capacity towards ammonium. Isothermal tests were conducted to understand the mechanism of adsorption, and further tests were run to understand the desorption process (objectives B.4 and B.5). In Submission 5, a section was dedicated to a preliminary cost-benefit analysis that compared the use of MOFs with the more conventional zeolites. The cost-benefit analysis is reported in Section 7 of the Innovation Report.

In summary, this research aims to provide new knowledge regarding the optimisation of an existing ammonium recovery technique through the application of thermal decomposition of struvite for the recovery of more valuable ammonium products as well as the development of a new process in the use of MOFs as adsorbents for ammonium recovery in the liquid phase. To the best of the author's knowledge, currently no research has yet focused on the use of these

materials for this application, and in particular ZIF-67. Nevertheless, growing interest in the nanomaterials field and the innovative capacity of tailoring these materials for selective applications could enhance and change the future of the adsorption technology.

3.2 Chemical precipitation: materials and methods

3.2.1 Materials

For this work, struvite (magnesium ammonium phosphate hexahydrate 98%) was purchased from VWR International Ltd, named as "struvite A". Severn Trent Water provided samples of struvite produced at one of their sites, which will be name as "struvite B".

3.2.2 Methods

This research involved thermal analysis as a first step to assess the results provided from previous literature and verify the effective release of ammonia in vapour form. Moreover, chemical characterisation techniques were used to identify the products of the decomposition. These techniques include elemental analysis to determine the concentration of the elements and also quantify the heavy metals present in the sample collected on site (Inductively Coupled Plasma and CHN); Fourier-Transform Infra-Red spectroscopy (FTIR) to understand the chemical structure; X-Ray Diffraction (XRD) to reveal the phase and crystallinity. A kinetic analysis was then carried out to establish the reaction pattern and provide useful information that is needed for the design of the technology. The methods employed for this study were the isoconversional and model-fitting methods and are explained in Section 3.2.3. Preliminary technical and economic considerations for the design of the technology were possible thank to the data and information gathered in this research.

The techniques and instrumentation used in this study are highlighted in Table 2.

***Table 2**: Summary of the methods and corresponding instruments used to investigate struvite decomposition*

Technique	Instrument	Notes
Thermogravimetric Analysis (TGA)	Mettler Toledo TGA 1 STAR^e System	Nitrogen flow 50 mL min^{-1}, Alumina crucibles (3 samples tested per condition)

Differential Scanning Calorimentry (DSC)	Mettler Toledo DSC 1 STAR^e System	Nitrogen flow 11 mL min^{-1}, Alumina crucibles (3 samples tested per condition)
Fourier Transform Infra-Red (FTIR) spectroscopy	Cary Tensor 27	Attenuated Total Reflection (ATR) method, wavenumber 500-4000 cm^{-1} (3 measurements per sample)
X-Ray Powder Diffraction (XRD)	Panalytical X'Pert Pro MPD	Cu Kα radiation
Scanning Electron Microscopy (SEM)	Benchtop SEM TM3030Plus, Hitachi	Magnification of 500
Inductively Coupled Plasma (ICP)	PE Optima 5300 Dual View ICP-OES Analyser	0.1 ppm accuracy
Elemental CHN analysis	CE 440 Elemental Analyser	N.A.

3.2.3 Kinetic analysis: isoconversional and model fitting methods

Kinetic analysis is a tool to identify the mechanism and rate law of a reaction. The rate law of a reaction expresses the dependence of the concentration of the reagents with the rate of the reaction and other reaction constants. This information is useful to gain an understanding of the reaction mechanism. By identifying the rate law of a reaction, it is possible to determine the controlling factors, important information that can be used for the design of the reactor. In this study, it was used to understand the mechanism of decomposition of struvite and its activation energy E_a, the energy required for the reaction to take place. Several approaches can be employed to determine the reaction model based on experimental data, including isoconversional and model-fitting methods [50,51]. Both are derived from the Arrhenius equation, which is the basic law of kinetics (Eq. 2):

$$k(T) = Ae^{-\frac{E_a}{RT}} \quad \text{(Eq. 2)}$$

Where *k(T)* is the rate constant, *A* is the pre-exponential factor, *R* is the universal gas constant equal to 8.314 J K^{-1} mol^{-1} , and *T* is the temperature expressed in Kelvin. For both methods, the conversion α is expressed as a function of the residual mass at a time *t*, m_t:

$$\alpha = \frac{m_i - m_\infty}{m_t - m_\infty}, \quad \text{(Eq. 3)}$$

Where the initial mass of the sample is m_i, and m_∞ is the mass at the equilibrium, at 500 °C. The conversion rate is defined as:

$$\frac{d\alpha}{dt} = k(T)f(\alpha) \quad \text{(Eq. 4)}$$

Where $f(\alpha)$ is the reaction model.

In the case of the isoconversional technique, Friedman's method was used, which required data from thermal analysis carried out at different heating rates and involved the following equation:

$$\ln\left(\beta_i \frac{\mathrm{d}\alpha}{\mathrm{d}T_i}\right) = \ln\left(A_\alpha f(\alpha)\right) - \frac{E_{a_\alpha}}{RT_i} \quad \text{(Eq. 5)}$$

The index "*i*" denotes the different non-isothermal experiments carried out at different heating rates (β_i). With this method, E_a is simply determined as the negative of the slope of the resulting curve, by plotting $\ln\left(\beta_i \frac{\mathrm{d}\alpha}{\mathrm{d}T_i}\right)$ against $1/\mathrm{T_i}$ (K^{-1}) at selected values of conversion, whilst $\ln\left(A_\alpha f(\alpha)\right)$ is the intercept.

Regarding the model-fitting method, data gathered from isothermal experiments was used. In this method the reaction model $f(\alpha)$ or $g(\alpha)$ are calculated for every reaction model with the experimental values of α. The different reaction models can be found in the literature and are shown in Table 3 [52,53].

***Table 3**: Thermal decomposition in solids expressed through reaction models*

	Reaction model	$\boldsymbol{f(\alpha)}$	$\boldsymbol{g(\alpha)}$
1	Power law	$4\alpha^{3/4}$	$\alpha^{1/4}$
2	Power law	$3\alpha^{2/3}$	$\alpha^{1/3}$

3	Power law	$2\alpha^{1/2}$	$\alpha^{1/2}$
4	Power law	$2/3\alpha^{-1/2}$	$\alpha^{3/2}$
5	One-dimensional diffusion	$1/2\alpha^{-1}$	α^{2}
6	Mampel (first-order)	$1-\alpha$	$-\ln(1-\alpha)$
7	Avrami-Erofeev	$4(1-\alpha)[-\ln(1-\alpha)]^{3/4}$	$[-\ln(1-\alpha)]^{1/4}$
8	Avrami-Erofeev	$3(1-\alpha)[-\ln(1-\alpha)]^{2/3}$	$[-\ln(1-\alpha)]^{1/3}$
9	Avrami-Erofeev	$2(1-\alpha)[-\ln(1-\alpha)]^{1/2}$	$[-\ln(1-\alpha)]^{1/2}$
10	Three-dimensional diffusion	$2(1-\alpha)^{\frac{2}{3}}(1-(1-\alpha)^{\frac{1}{3}})^{-1}$	$[1-(1-\alpha)^{\frac{1}{3}}]^2$
11	Contracting sphere	$3(1-\alpha)^{2/3}$	$1-(1-\alpha)^{1/3}$
12	Contracting cylinder	$2(1-\alpha)^{1/2}$	$1-(1-\alpha)^{1/2}$
13	Second-order	$(1-\alpha)^{2}$	$(1-\alpha)^{-1}-1$

The function $g(\alpha)$ is defined as:

$$g(\alpha)=\int_0^{\alpha}\frac{d\alpha}{f(\alpha)} \qquad \text{(Eq. 6)}$$

The function $g(\alpha)$ is thus rearranged from Eq. 4 as:

$$g_j(\alpha)=k_j(T_i)t \qquad \text{(Eq. 7)}$$

At this point, $g(\alpha)$ was calculated for each reaction model j at the temperature of the isothermal test T_i (75, 95 and 145 °C). Then, $k_j(T)$ could be derived as the slope of the curve obtained by plotting $g_j(\alpha)$ against t. At this point, $E_{a,j}$ and lnA_j were determined at the different T_i using the Arrhenius equation (Eq. 2), as done previously for the isoconversional method. This approach has a drawback compared to the isoconversional method because the activation energy E_a that results from the calculation corresponds to an average that might not detect the dependency of the variable with the conversion or temperature. Thus, the best approach that identifies E_a is the isoconversional method [53].

To determine the reaction model, the best fit could be calculated by using the residual sum of squares that defines the goodness of fit:

$$S_j{}^2=\frac{1}{n-1}\sum_{i=1}^{n}\left(\frac{t_i}{t_{0.5}}-\frac{g_j(\alpha_i)}{g_j(0.5)}\right) \qquad \text{(Eq. 8)}$$

In the equation above $t_{0.5}$ is the reduced time variable that corresponds to t/t_α with t_α being the time at which the reaction has attained a specific conversion (in this case it has been chosen $\alpha = 0.5$ as suggested in the book of solid state kinetics by Brown *et al.* [54]). Once the values of ${S_j}^2$ are found, F_j is calculated as following:

$$F_j = \frac{{S_j}^2}{{S_{min}}^2} \qquad \text{(Eq. 9)}$$

Where ${S_{min}}^2$ is the smallest of ${S_j}^2$. The best fit could be identified as the closest to the one which presents the minimum value of the residual sum of squared.

3.3 Adsorption: materials and methods

3.3.1 Materials

A cross-functional flowchart was developed to provide guidance for the design of the methodology and for the research of an innovative adsorbent (Figure 6).

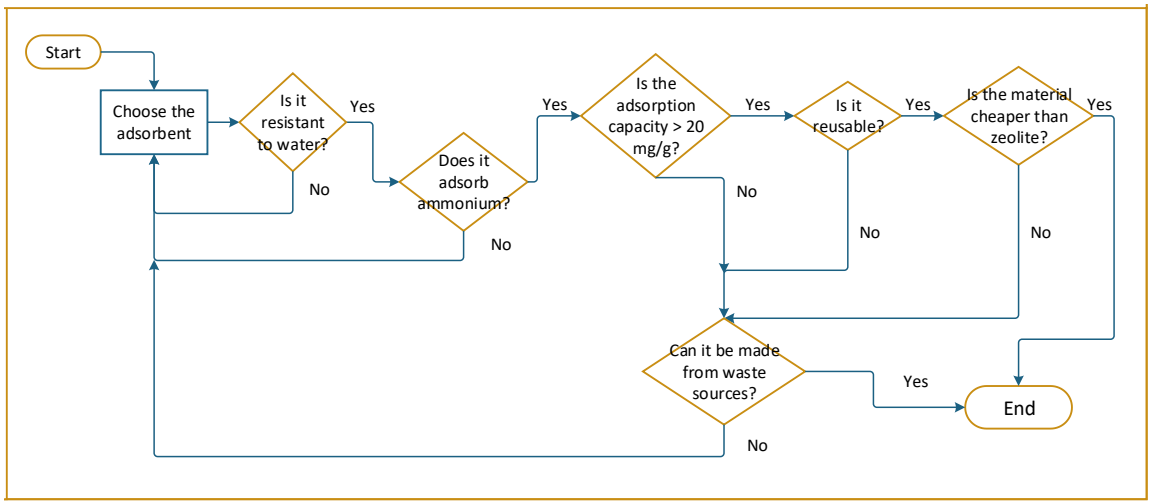

Figure 6: *Cross-functional chart of the research pathway for an innovative adsorbent*

Firstly, a selection of the most suitable MOFs was carried out. The essential criteria that would make these materials attractive for the sustainable adsorption of NH_4-N were defined as:

- Water stability
- Affinity towards ammonia/ammonium
- Reusability
- Surface area

- Green synthesis (where applicable)

The MOFs that were selected based on the aforementioned criteria are reported in Table 4.

***Table 4**: Summary of the selected MOFs with respect to the criteria*

Material	Water stability	NH_3/NH_4^+ affinity	Reusability	Surface area [$m^2\ g^{-1}$]	Green synthesis	Ref.
UiO-66 and derivatives	Yes	Yes	Yes	1000-1200	Yes	[55–59]
ZIF-8 and ZIF-67	Yes	Yes	Yes	1500	Yes	[60,61]
CPO-27 (Zn and Ni)	Yes	Yes	Yes	257-1351	Yes	[62–64]
$Ni(INA)_2$	Yes	Yes	Yes	12	Yes	[65]
HKUST-1	No	Yes	N.A.	700-1615	Yes	[66,67]
MIL-53 (Al)	Yes	Yes	Yes	945-3740	Yes	[68–71]

Out of the chosen materials, the followings could be sourced commercially: ZIF-8, ZIF-67, CPO27(Ni), CPO-27(Zn), HKUST-1(Cu) and MIL-53(Al). These materials were purchased from Promethean Particles Ltd and were used without further purification, as advised by the company. The others were made on a lab scale by the researcher or by the Department of Chemistry, at the University of Warwick. The details of those reactions can be found in Submission 4 and will not be mentioned here as they are not of interest in this report.

In Section 6, the research was focused on ZIF-67 which was selected amongst the one tested. In order to increase the adsorption capacity, structure modifications of ZIF-67 were applied with several reactions (all carried out at room temperature). To carry out modifications of the structure, ZIF-67 was synthesised in the lab on a gram scale according to the procedure by Yao *et al.* in water at room temperature (RT), and it will be called ZIF-67 lab in Section 6 [72]. The structure of ZIF-67 lab was compared to the one purchased from Promethean Particles (referred to as ZIF-67 PP in Section 6). The chemical modifications that were carried out are reported in Table 5.

***Table 5**: Chemical modifications performed on ZIF-67*

Structure Modification	Temperature	Solvent	Notes
Cu-doping	RT	CH_3OH	Method adapted from [73]
Addition of Ag NPs	RT	H_2O	Ag NPS added to cobalt solution during synthesis, reaction from [74]
Oxidised rCF/ZIF-67 composite	RT	H_2O	Oxidised rCF added to the cobalt solution during synthesys, reaction from [74]

The procedures were carried out at room temperature. The oxidation of rCF was conducted with sulfuric acid and nitric acid solutions at 60 °C, according to standard methods reported in the literature [75]. The oxidised rCF were added to one of the precursors (cobalt nitrate) during the synthesis reaction of ZIF-67 [74].

3.3.2 Methods

Firstly, a screening test was conducted to understand the suitability of the MOFs and their capacity to capture NH_4-N whilst retaining their structure (objective B.1). The techniques and instruments that were used to characterise the materials are the same as the ones reported in Section 3.2.2. The MOFs were tested in a batch system containing ammonia solution (ammonium chloride) in fixed conditions of NH_4-N concentration (100 mg L^{-1}), initial pH (neutral), volume of NH_4-N solution (100 mL) and adsorbent loading (10 g L^{-1}), as performed in other adsorption studies [76–78]. The NH_4-N concentration of 100 mg L^{-1} is a value in-between the range of realistic wastewater concentrations. However, given the cost of the materials used, the value was chosen considering the test as a proof of concept. As mentioned above, the principal aim was to assess whether these materials could uptake any NH_4-N at all in a liquid system. Therefore, it was decided that a lower concentration might not have shown any significant result. The samples and the ammonia solution were put in conical flasks and placed in a shaking incubator (SI500, Stuart). The conditions of the test are summarised in Table 6.

***Table 6**: Conditions of the adsorption screening test*

Temperature	Ambient
Pressure	Ambient
Initial pH	7
Volume of NH_4-N solution	0.1 L
NH_4-N concentration	100 mg L^{-1}
Adsorbent dosage	1 g
Agitation	200 rpm
Test duration	6 h

The residual concentration of ammonium (NH_4-N) in the solution was determined using ultraviolet-visible spectrophotometry (UV-vis, DR 2800, HACH) at absorbance of 690 cm^{-1} and the Ammonium Test Spectroquant® kit from Merck [79]. The linear correlation between absorbance intensity at 690 cm^{-1} (x) and the concentration of ammonium (y) was found as:

$$y\ [\text{mg L}^{-1}\text{NH}_4 - \text{N}] = 11.860x - 0.282 \qquad \text{(Eq. 10)}$$

$$R^2 = 99.9\ \%$$

The removal efficiency was calculated as below:

$$Removal\ \% = \frac{C_0 - C_t}{C_0} \times 100 \qquad \text{(Eq. 11)}$$

where C_0 and C_t are respectively the initial concentration in the solution and the NH_4-N concentration at a time t (mg L^{-1}). The amount of ammonia adsorbed per gram of MOF at a time t (Q_t) is found as:

$$Q_t = \frac{(C_0 - C_t)}{m} \times V \qquad \text{(Eq. 12)}$$

Where V is the volume of the NH_4-N (L) solution and m is the mass of the adsorbent (g). From Eq. 12 is also possible to calculate the adsorption amount at the equilibrium Q_e by using C_e, which is the concentration at the equilibrium.

The MOF that showed the best performance was selected and more detailed experiments were carried out, where all the aforementioned conditions were varied to assess the behaviour of

the adsorbent in different environments. The pH was varied between 2 and 8, the adsorbent loading between 1 g L^{-1} and 30 g L^{-1}, and NH_4-N concentration in the range of 25-500 mg L^{-1}. When changing one of the parameters, the others were kept constant.

When ZIF-67 was selected for further tests (Section 6) and chemical modifications were carried out, all the samples were then activated at 150 °C for 2 hours before being used, to remove the solvent from the pores. The structure of the materials was characterised with the methods reported in Section 3.2.2. Additionally, the morphology of the materials was analysed also with Transmission Electron Microscopy (TEM, FEI Tecnai G2 20) techniques. Moreover, the surface area, void volume isotherms were investigated using the Brunauer-Emmett-Teller (BET) method. Lastly, X-ray photoelectron spectroscopy was used to determine the functionalisation of rCF.

3.3.3 Kinetic analysis

A kinetic study was conducted to understand the mechanism of adsorption and compare it with conventional adsorbents, such as zeolites (objective B.2). Kinetics analysis helps to understand how the system reaches the equilibrium, the nature of the interaction between adsorbent and adsorbate, and the variables that influence the process. Typically, the two models considered for the adsorption process are the Pseudo-first order model (PFO) and the Pseudo-second order model (PSO). The former was proposed by Lagergren in 1898 to describe a liquid-solid adsorption system [80,81]. The latter was developed more recently by Ho *et al.* [82].

The models are based on the following equation:

$$\frac{dq_t}{dt} = k_n\left(q_e - q_t\right)^n \qquad \text{(Eq. 13)}$$

Where k_n is the rate constant and it is expressed in min^{-1}, and q_e and q_t are the uptake of adsorbate per mass of adsorbent respectively at the equilibrium and at the time t, expressed in mg g^{-1}. In the case of PFO, the equation is integrated for $n = 1$ and it is solved considering that at $t_0 = 0$ the amount adsorbed is zero ($q_t = 0$), whereas at $t = t_{fin}$, $q_t = q_e$, indicating the maximum adsorption capacity. The result of the integral between t_0 and t_{fin} is as follows:

$$ln(q_e - q_t) = \ln q_e - k_1 t \quad \text{(Eq. 14)}$$

This expression can be rewritten in respect to q_t:

$$q_t = q_e(1 - e^{-k_1 t}) \quad \text{(Eq. 15)}$$

Considering that q_t and q_e are available from experimental data, it is possible to use the linear correlation in Eq. 14 to calculate k_1. In fact, by plotting $ln(q_e - q_t)$ in respect to time, $-k_1$ is found as the slope of the curve and $\ln q_e$ can be determined as the intercept.

Regarding PSO, Eq. 13 is integrated for $n = 2$ with the same boundaries, and the result in respect to q_t is as follows:

$$q_t = \frac{{q_e}^2 k_2 t}{{q_e}^2 k_2 t + 1} \quad \text{(Eq. 16)}$$

Eq. 16 can also be expressed in a linear form:

$$\frac{t}{q_t} = \frac{1}{k_2 {q_e}^2} + \frac{1}{q_e} t \quad \text{(Eq. 17)}$$

From Eq. 17, k_2 and q_e can be obtained by plotting $\frac{t}{q_t}$ versus time. Once k_1, k_2, and q_e for both models are determined, the best fitting is revealed by plotting q_t in respect to time for both models and comparing it to the experimental data.

3.3.4 Adsorption isotherms

The equilibrium data in isothermal conditions was analysed with Freundlich and Langmuir models to understand the adsorption mechanism of the chosen adsorbent. This data is highly valuable to identify the interactions between adsorbate and adsorbent. The Freundlich and Langmuir models are two-parameter correlations that had been initially developed for gaseous adsorption systems [83,84]. However, they are now extensively used also to characterise liquid adsorption systems. The Langmuir model is a theoretical construct which assumes that the adsorption happens on a homogeneous surface, on a single layer where the adsorption sites are identical [85]. It also considers that the process is reversible and that once the adsorption site is occupied by the guest species, that site will not be available for further adsorption. The

model should show a plateau at high concentrations that indicates complete saturation of the sites has been reached. The Langmuir equation is shown below:

$$Q_e = \frac{Q^0{}_{max} K_L C_e}{1 + K_L C_e} \quad \text{(Eq. 18)}$$

The equation can be used in the linearised form proposed by Hanes-Woolf:

$$\frac{C_e}{Q_e} = \left(\frac{1}{Q^0{}_{max}}\right) C_e + \frac{1}{Q^0{}_{max} K_L} \quad \text{(Eq. 19)}$$

Where $Q^0{}_{max}$ is the maximum saturated adsorption capacity on the monolayer, expressed in mg g^{-1} and K_L (L mg^{-1}) is the Langmuir constant which indicates the affinity of the adsorbate towards the adsorbent. To better understand this model, the separation factor R_L (dimensionless) can be used. This parameter depends on the initial concentration C_0 and is defined as:

$$R_L = \frac{1}{1 + C_0 K_L} \quad \text{(Eq. 20)}$$

If R_L is less than 1 the adsorption is favourable, if $R_L > 1$ the adsorption is unfavourable. Lastly, if R_L is equal to 1 the process is linear.

The Freundlich model is an empirical model which states that the adsorption is heterogeneous and takes place on multilayers. Compared to Langmuir model, this correlation does not describe the saturation of the adsorbent at high concentrations. The nonlinear Freundlich equation is the following:

$$Q_e = K_F {C_e}^n \quad \text{(Eq. 21)}$$

Which is linearised as follows:

$$\log Q_e = n \log C_e + \log K_F \quad \text{(Eq. 22)}$$

In this case, the Freundlich constant is K_F (mg g^{-1})/(mg L^{-1})^n, whilst n is a parameter which expresses the intensity of the adsorption or the surface heterogeneity. The adsorption is favourable when $n < 1$, whereas it is unfavourable when $n > 1$.

4 Chemical precipitation: struvite thermal decomposition to recover ammonia solution

This section first analyses the research gaps concerning chemical precipitation, which were briefly introduced in Section 2. Afterwards, it discusses the findings of the experimental work carried out regarding this technology. The research reported in this Section has been accepted for publication by Journal of Thermal Analysis and Calorimetry.

4.1 Introduction

Chemical precipitation is one of the limited technologies that recover both phosphorous and ammonium in the form of struvite, a mineral that finds applications as a slow-release fertiliser. This technology is being already applied in one of Severn Trent WWT sites, and is also employed in other waste streams with high nutrients concentration (e.g. manure and pig slurry) [86,87]. It was initially developed to overcome pipeline blockages and inefficiencies caused by the spontaneous precipitation of struvite after the anaerobic digestion stage, where the effluent is rich in phosphorous and ammonium. The uncontrolled accumulation of struvite in the stream causes additional maintenance operations and extra costs (e.g. pump breakage) [46].

Struvite ($MgNH_4PO_4 \cdot 6H_2O$)precipitates spontaneously due to its very low solubility product (3.89 x 10^{-10} at 25 °C in wastewater, 4.330 x 10^{-14} at 25 °C in aqueous solution) [88,89]. The reaction is the following:

$$Mg^{2+}_{(aq)} + PO_4^{3-}{}_{(aq)} + NH_4^{+}{}_{(aq)} + 6H_2O_{(l)} \rightarrow MgNH_4PO_4 \cdot 6H_2O_{(s)} \quad \text{(Eq. 23)}$$

The reagents react in molar ratio of 1:1:1. Since the magnesium content in the stream is much less than the ammonium and phosphate ions, magnesium chloride ($MgCl_2$) or magnesium oxide (MgO) are dosed to initiate a controlled precipitation. Therefore, the use of this chemical significantly increases the operating cost of the technology. Another cost contribution is the dosage of sodium hydroxide needed for pH control, another parameter that affects

crystallisation [90]. Furthermore, the precipitate usually contains heavy metals that affect the crystal growth of struvite [91]. Depending on their concentration, they also negatively impact on the value of struvite, that must be treated before being sold commercially [92]. Struvite can be worth £ 60 tonne^{-1}, whereas the cost of $MgCl_2$ is £ 590 tonne^{-1} and on average 0.6 tonne are dosed to produce 1 tonne of struvite (data provided by Severn Trent Water). Therefore, without taking into account other costs (e.g. energy, labour, maintenance operations) the process is not cost-effective, and optimisation is needed to improve the value of the product.

Recently, researchers have highlighted the possibility of thermally decomposing struvite to recycle the magnesium. Consequently, research studies have demonstrated struvite can be decomposed upon heating, losing ammonia and water molecules which make over 50 % of the solid [93–95]. Currently, the mechanism of decomposition has not yet been established. From an industrial perspective, it is important to identify the way struvite decomposes and what the decomposition product is, to understand what the optimal process conditions are and whether the final product can be reused as magnesium source. Sugiyama *et al.* [96] used solid state NMR and X-Ray diffraction techniques to affirm that struvite first transforms to magnesium hydrogen phosphate ($MgHPO_4$) and then into magnesium pyrophosphate ($Mg_2P_2O_7$). The mechanism in which the intermediate compounds are formed was not explained in this study. At temperatures higher than 200 °C the calcination product was amorphous. Contrarily, Bhuiyan *et al.* [94] indicated $MgHPO_4$ as the final calcination product (equal to 51 % of mass loss). Moreover, they stated that the compound loses crystallinity when the water molecules start evaporating. Chen *et al.* proposed several intermediate steps, but the chemical reaction were incorrectly balanced and the theory was only supported by Fourier Transform Infra-Red spectroscopy [95]. It has been reported in several studies that the decomposition is affected by the heating rate [93,94]. Frost *et al.* confirmed that with a heating rate of 2 °C min^{-1} struvite began to degrade at 85 °C, whereat at 1 °C min^{-1} the decomposition began at circa 40 °C [93]. This research concluded ammonia is released before water at 1 °C min^{-1}. This was confirmed with mass spectrometry that analysed the gases. However, the results could be incorrect as the

molecular weight of water and ammonia is similar (respectively 18 and 17 g $mole^{-1}$). Therefore integration of this data with quantitative analysis would have been beneficial. In this regard, Bhuiyan described the mechanism as the simultaneous release ammonia and water in one stage, which was faster with slower heating rates [94]. This was concluded from the thermogravimetric analysis and the shape of the derivative curves.

Thus, due to the contradictory information present in the literature the reaction mechanism of struvite calcination and the opportunity to recover valuable products have not yet been discerned. Therefore, this research investigated struvite decomposition in the solid state and carried out a kinetic analysis to investigate the mechanisms of the reactions involved.

4.2 Results and discussion

4.2.1 Material characterisation

Firstly, struvite A (purchased) and B (sample collected from Severn Trent) were compared to investigate any relevant differences. Struvite B appeared as a light brown powder, different from the white fine powder of struvite A. The FTIR spectra of struvite A and B are reported in Figure 7 and no significant difference was detected between the two samples, showing the same important peaks that characterise struvite, as reported in the literature [97,98]. In particular, the ammonium bond H-N-H corresponds to the band at 1431 cm^{-1} wavenumber [93].

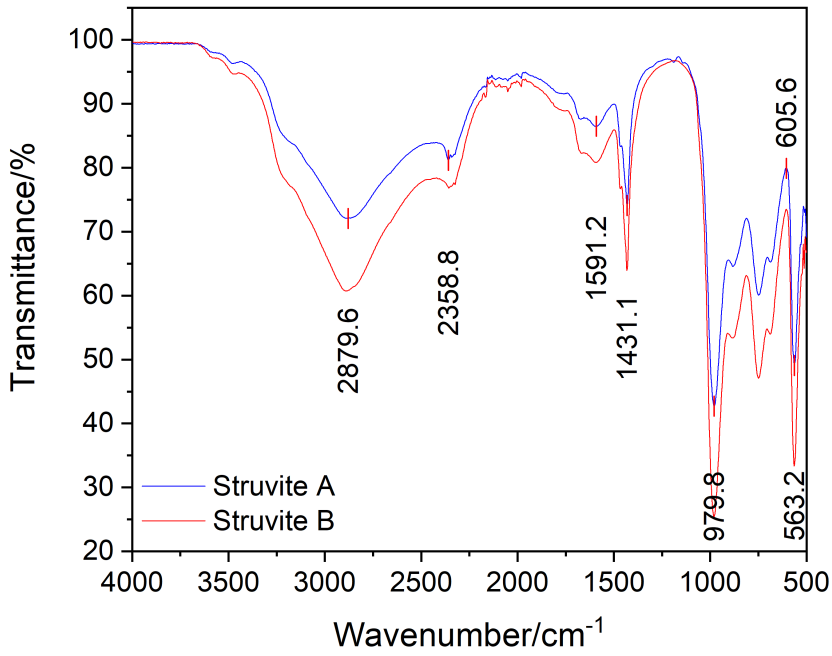

***Figure 7**: FTIR of struvite A and B from 4000 to 500 cm-1 in transmittance mode*

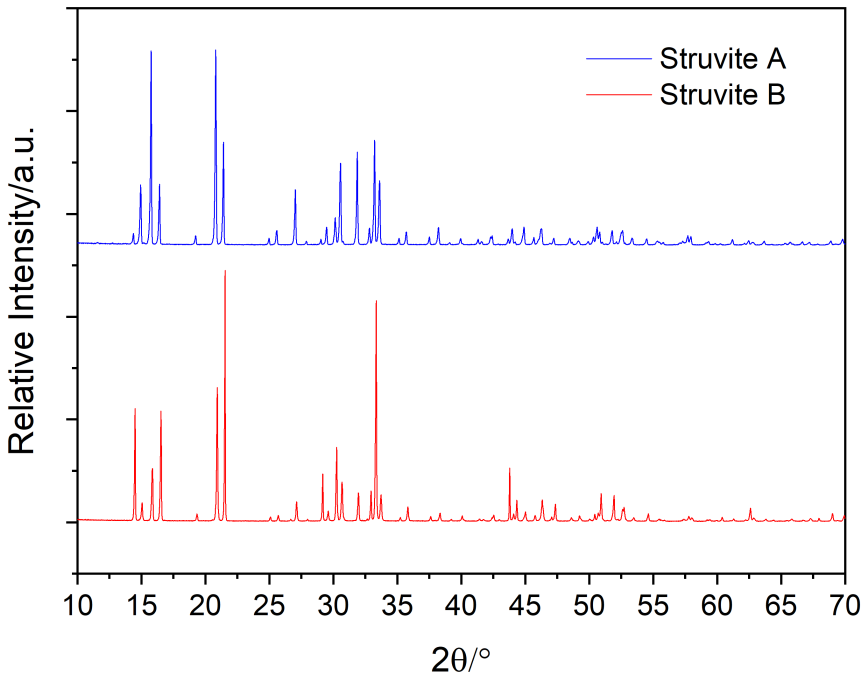

***Figure 8**: XRD pattern of struvite A and B*

The XRD results (Figure 8) provided two very similar spectra, despite differences were detected regarding the intensity of some peaks. This could be due to several reasons, including different grain size of the two materials, crystallite size or sample preparation. Overall, the

identical mineral phase of the two samples could be confirmed. These results mean that the impurities that might be present in struvite B did not alter the chemical structure of the sample, which is an important requirement for the value of the product.

Nevertheless, it was in fact confirmed that the two materials differed substantially from a morphological point of view (Figure 9). Struvite A has a neat crystal-like structure with crystals of circa 100 μm width, whereas struvite B has grains of various shape, and the size that ranges from 10 to over 100 μm.

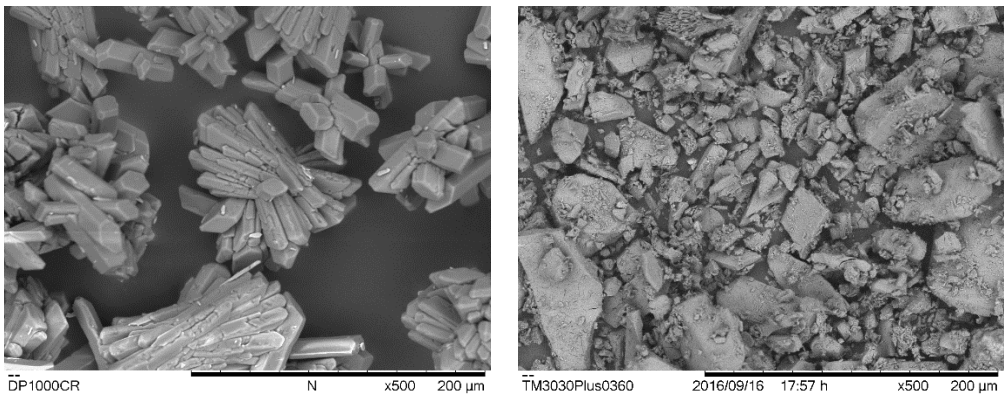

***Figure 9**: SEM images of struvite A (left) and struvite B (right)*

This difference may already denote an uncontrolled precipitation reaction for struvite B that could be due for example to a lack of pH control; whilst struvite A has been synthesised industrially in specific conditions to obtain the optimal product specifications. In this regard, it has been reported how for example the presence of calcium can influence the precipitation of struvite, by affecting the crystal growth rate [99]. Other images of struvite precipitate from wastewater similar to the image of Struvite B shown in Figure 9 can be found in the literature [100–102]. The different shape and size of the crystals should not affect their quality which is guaranteed by matching mineral phases shown in the XRD analysis (Figure 8) [103].

From ICP elemental analysis, it also resulted that the content of magnesium in both struvite A and B was higher than the theoretical value, 9.90 % (Table 7). For struvite A this was also coupled with a higher phosphorous content. Considering that Mg, P and N react with a molar ratio of 1:1:1, these results could suggest the presence of a fraction of the unreacted precursor,

magnesium chloride. Table 7 also shows how the values of commercial struvite Crystal Green® synthesised by the Ostara technology are almost equal to the theoretical concentrations [104].

***Table 7**: ICP-OES on struvite B, Mg and P concentrations expressed in % wt/wt*

Element	Unit	Struvite (Theoretical values)	Struvite A	Struvite B	Commercial struvite (Crystal Green®), [104]
Mg	%	9.90	11.34	10.57	10.00
P	%	12.60	17.42	12.41	12.60

The elemental analysis identified the presence of impurities in the samples, which were analysed for several elements, including heavy metals like arsenic, cadmium, chromium, lead, nickel and mercury that must be within limits set by the EU fertilisers regulation (EC 2003/2003) [105]. For clarity, the value of cadmium had to be expressed in mg kg^{-1} P_2O_5, as it is referred to in the regulation. Struvite A resulted to be highly pure, as expected, with the concentration of most elements being below 0.1 ppm (Table 8).

***Table 8**: ICP-OES on struvite B, metals concentrations expressed in ppm (* Cd concentration has been converted to mg kg^{-1} P_2O_5 to compare it with Crystal Green and EU regulations)*

Element	Unit	Struvite A	Struvite B	EU current Fertiliser Regulation, EC 2003/2003
As	ppm	0.00	30	60
Ca	ppm	1.83	5303	N.A.
Cd	ppm	0.00	15.8 (= 55.5 mg kg^{-1} $P_2O_{5*)}$	60 mg kg^{-1} P_2O_5
Cr	ppm	0.00	11	2
Cu	ppm	0.01	12	N/A
Hg	ppm	0.00	< 5	2
Ni	ppm	0.07	24	120
Pb	ppm	0.00	19	150
Zn	ppm	0.06	28.2	N/A

More importantly, Struvite B resulted to contain several impurities. Calcium was determined as the most abundant with 5303 ppm, and this may confirm the hypothesis mentioned above that indicated the influence of the metal on the morphology of struvite. Regarding the metals that are considered hazardous, most of them were found to be below the EU limits. Nevertheless, cadmium was just under the threshold value of 60 kg^{-1} P_2O_5, and chromium and mercury exceeded the limits. Chromium resulted to be more than 5 times above the maximum concentration, and mercury was over two times the limit of 2 ppm. These metals are highly pollutant and can be a threat for soil contamination. Thus, from this test it emerged that the wastewater-based struvite could potentially be unsuitable as a commercial fertiliser. However, it is important to consider that this is the result of a single test, thus further analysis would be required to confirm this preliminary data. Nevertheless, if the results were confirmed, it would implicate the need to pre-treat the solid to reduce the concentration of the heavy metals, before being able to sell it as fertiliser. In fact, the presence of these contaminants in the product lowers its economic value. In recent studies, the possibility of using a hydrothermal treatment was discussed as pre-treatment before struvite precipitation to remove heavy metals and other contaminants [91,106]. The process conditions were a temperature range between 180 and 220 °C, respectively in nitrogen or oxygen atmosphere (thermal hydrolysis and wet oxidation processes), and 30 bar of pressure. The study claims that this would allow a reduction in the sludge and heavy metals content, with a higher recovery of phosphorous [106]. However, high costs and energy would be involved in adding this process to a WWT plant. The cost analysis revealed a positive economic return with the wet oxidation technique, nevertheless the study considered MgO as precursor of the struvite precipitation (cheaper but less effective than $MgCl_2$) and did not account for the energy required. Ultimately, the elemental analysis further confirmed that due to the heavy metals content present in struvite B, it is important to find an optimisation of this process to obtain a higher-quality product.

4.2.2 Heating rate influence on struvite degradation

The thermal analysis confirmed some knowledge that was already present in the literature, but also revealed new important information that will be useful for the design of the struvite decomposition technology.

Thermogravimetric analysis (TG) involved calcination of the samples from 25 to 500 °C. The samples showed structured decomposition curves and their derivatives with respect to time (DTG) at different heating rates, with a maximum mass loss of 54.5 %, that corresponds to the evaporation of water and ammonia (Figure 10). The plotted lines are the mean of three tests carried out for the two samples in each condition and the standard deviation was found to be less than 1 %. The curves of struvite A and B almost overlapped during the major mass loss, confirming a similar behaviour of the two samples.

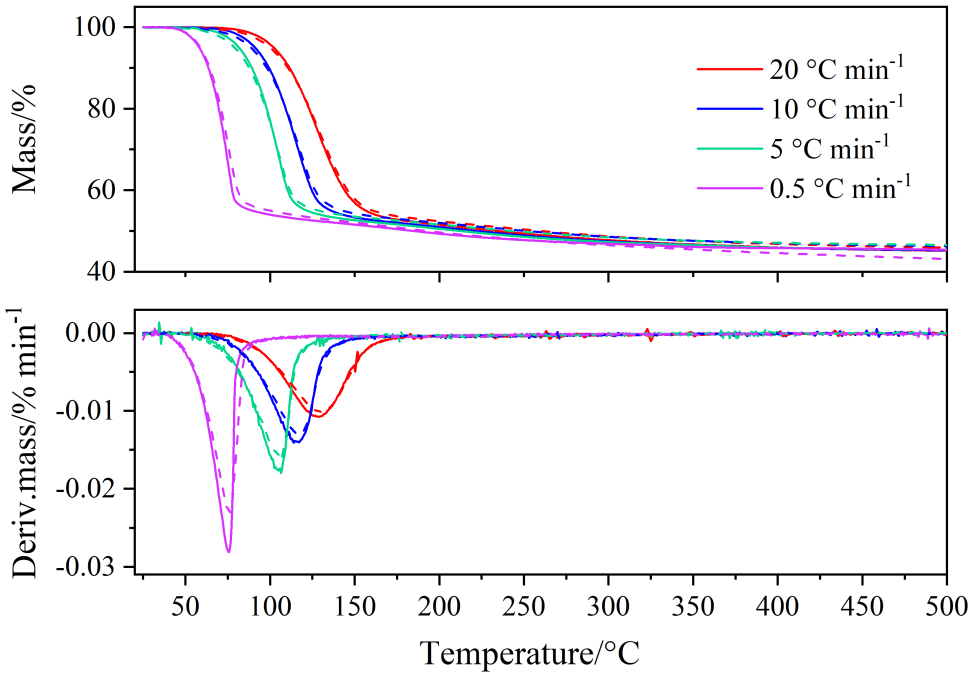

***Figure 10**: TG and DTG curves of struvite A (continuous line) and B (dash) at heating rates of 20, 10, 5, 0.5 °C min-1, curves are the mean of three samples, average standard deviation below 0.3 % apart from 0.5 °C min-1 (< 1 %)*

A slight difference was noted in the residual mass, where the residual mass of struvite B at 500 °C was 46.3 %, whereas struvite A had 45.3 %. The difference of 1 % could be associated to the

excess of magnesium and non-volatile heavy metals. However, it could mostly be due to the presence of calcium which was detected in higher concentration with the elemental analysis, or iron, commonly present in wastewater, especially if added as treatment to remove phosphorous. Overall, the rate of mass loss was not influenced by the contaminants. In fact, a statistical analysis (T test) was carried out on the comparison of the mean of the tests between struvite A and B. It was found that there was a statistically significant difference between the struvite A samples and the struvite B samples, even though the average mean difference was 0.14 %. This test also confirmed how the degradation of struvite is affected by the heating rate (Figure 10). Indeed, the calcination onset temperature decreased when the heating rate diminished, as previously reported in the literature [94,107]. At 0.5 °C min^{-1} struvite A started losing mass at 31.8 °C, and the temperature at which the rate of decomposition was the greatest was 76.8 °C. On the contrary, at 20 °C min^{-1} the decomposition began at 68.3 °C and achieved its maximum rate only at 129 °C. This might indicate that in an industrial process, where the temperature of the reactor would be kept isothermal, most of the degradation could be achieved at a temperature below 80 °C. This result would positively achieve objective A.1, by confirming that both NH_3 and H_2O can be released at relatively low temperature. However, the greatest mass loss is due to the evaporation of the six molecules of water, which make 44 % wt/wt of the sample. Therefore, it was necessary to conduct further analysis understand the maximum temperature required to evaporate all the ammonia.

4.2.3 Evidence of multi-stage degradation

Further experiments were carried out based on the results of the previous analysis. The conditions in this case were isothermal to investigate the behaviour of struvite in a more realistic environment and understand the minimum temperature required to decompose the material and release the ammonia. This test was only performed on struvite B, having previously established its identical behaviour with struvite A. The isothermal conditions were 40, 50, 60 and 75 °C, which were the temperatures at which the biggest mass loss occurred at 0.1 °C min^{-1}.

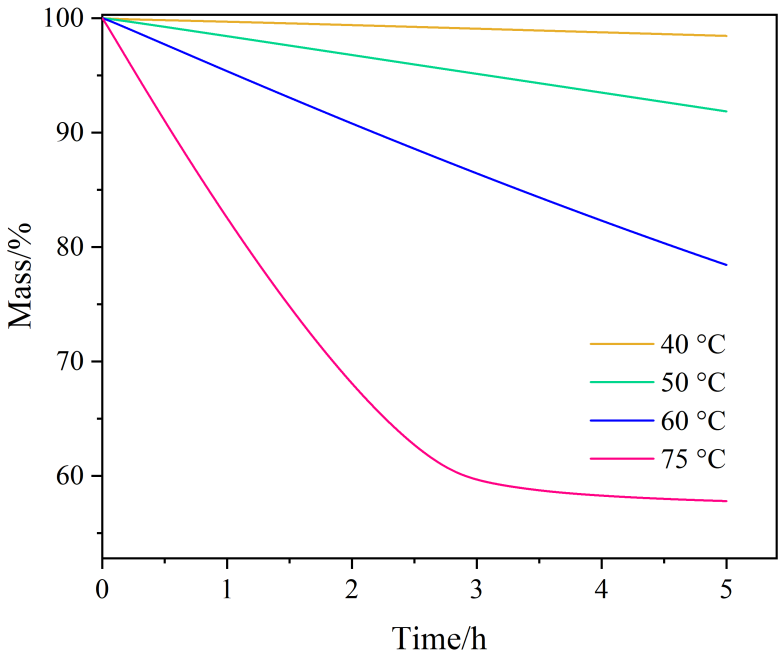

***Figure 11**: TG curve of isothermal tests on struvite B at temperatures of 40, 50, 60, 75 °C for 5 hours*

The evaporation at 40 and 50 °C was less than 10 % (Figure 11). At 60 °C, a mass loss of 21.5 % was noted over 5 hours, whilst at 75 °C there was a decrease of 42.2 %. Still, this percentage is lower compared to the 54.5 % obtained with a complete decomposition, indicating that 12.3 % of the mass could not be released at that temperature. These samples kept at 60 and 75 °C were analysed with CHN and the nitrogen content was respectively 4.27 % and 2.61 %, compared to the original sample which had 5.47 %. This data proved that there is simultaneous evaporation of ammonia and water, as reported by Frost *et al.* [93]. Moreover, from an industrial point of view it emerged that the temperatures of interest for the evaporation of all the ammonia are above 75 °C. Thus, a multi-stage isothermal experiment was carried out with the following steps: 75 °C, 145 °C, 250 °C and 500 °C. The temperatures were chosen as intervals between 75 °C and 500 °C. In Figure 12 (left), the TG and DTG curves are shown. For clarity, the coloured bars correspond to isothermal conditions, whereas the white bars indicate when the temperature is being increased.

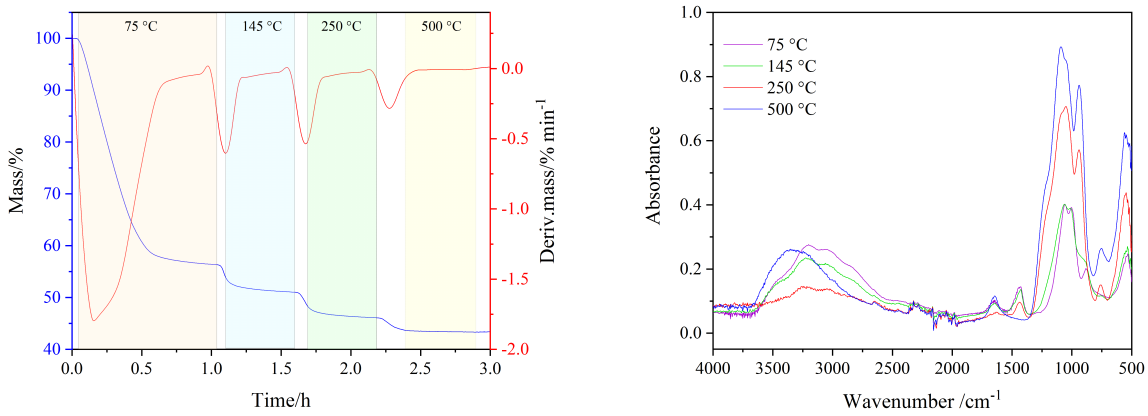

***Figure 12**: Multi-stage isothermal test on struvite A (left), and corresponding ATR-FTIR of the samples decomposed at the following temperatures: 75, 145, 250, and 500 °C (right)*

The TG graph reveals that at 250 °C struvite is not fully decomposed, and this is further confirmed by the FTIR which shows the ammonium peak (ν_4 bending mode vibration at 1431 cm^{-1}) is still present at this temperature (Figure 12, right).

Another important consideration that can be drown from the FTIR spectra is that two different compounds can be distinguished. In fact, the spectra have similar patterns until 145 °C, with the antisymmetric stretching ν_3 of HPO_4^{2-} and PO_4^{3-} at 880 cm^{-1} 1000 and 1062 cm^{-1}, whereas from 250 °C up to 500 °C the spectra changed in the fingerprint region, with a shift of these three peaks and the formation of a peak at circa 750 cm^{-1}, which can be attributed to the bending vibrations of O-P-O. This may indicate that struvite decomposes to $MgHPO_4$, and then into $Mg_2P_2O_7$, as suggested in the literature [94,95]. However, from this study it can be concluded that even though this transformation happens between 145 and 250 °C, nitrogen is still present even though in a small fraction. CHN analysis confirmed that all ammonia is removed at 500 °C, with 0.15 % left in the sample. Several compounds have been suggested in the literature as possible calcination products, including magnesium pyrophosphate ($Mg_2P_2O_7$), magnesium phosphate ($Mg_3(PO_4)_2$), and magnesium hydrogen phosphate ($MgHPO_4$) [93,94,96]. The FTIR in Figure 13 (left) is consistent with previous findings, which report the peaks at 1105 and 929 cm^{-1} as indication of the formation of $Mg_2P_2O_7$ [48,108]. The

XRD in Figure 13 (right) indicates that loss of crystallinity occurred during calcination and it did not allow the identification of the mineral phase.

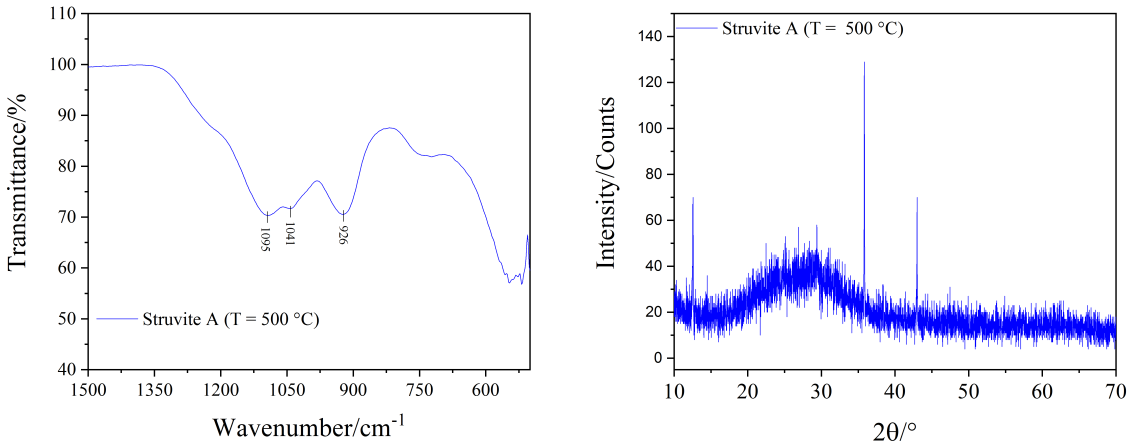

***Figure 13**: FT-IR in transmittance mode (left) and XRD (right) of the calcination product of struvite A obtained from TG tests conducted up to 500 °C*

4.2.4 Energy required for the degradation

After having identified the final decomposition product, differential scanning calorimetry technique (DSC) was used to identify the energy required to release completely the ammonia present in the compound. The curve has two peaks, confirming a two-step decomposition mechanism (Figure 14). The first peak was also observed previously in the TGA graph and regards the greatest mass loss. The second peak was not detected in the DTG curve and is at circa 250 °C. This is highly important because it has not been reported previously and indicates the presence of two distinct reactions. It is also possible to determine the temperature required for each reaction to take place at the heating rate of 10 °C min. In this condition it seems possible to decompose struvite to $MgHPO_4$ at a temperature of circa 150 °C and remove most of the ammonia. $MgHPO_4$ could be then recycled as feed for the chemical precipitation, reducing the use of $MgCl_2$.

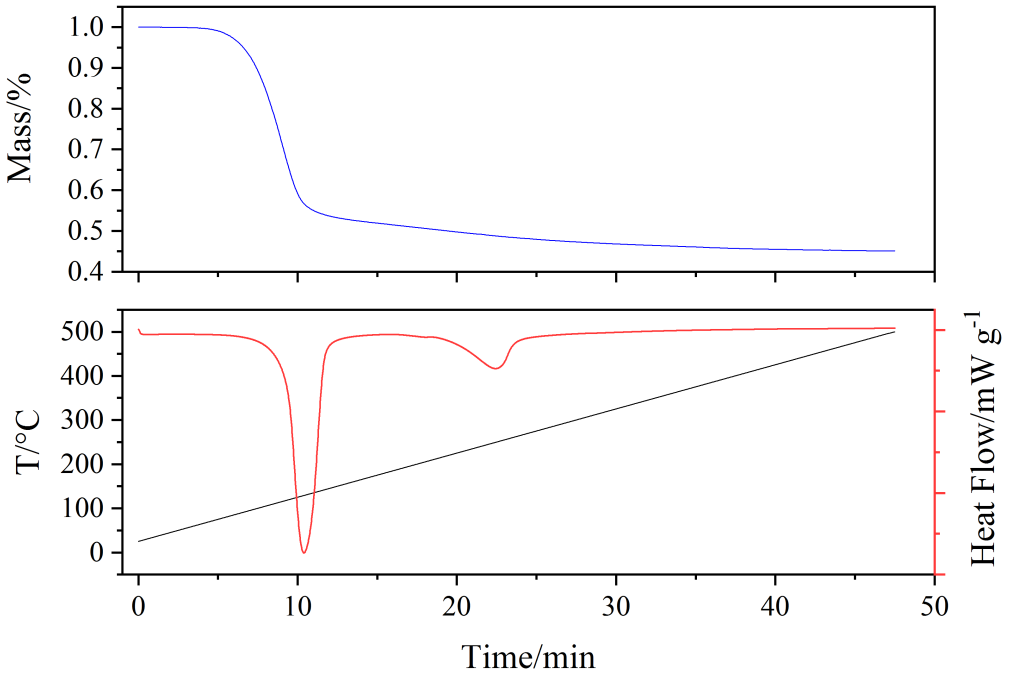

***Figure 14**: TG-DSC curves of struvite A at 10 °C min-1*

From the graph it was revealed how the decomposition was completed within 30 minutes at the heating rate of 10 °C min^{-1}. The energy was determined from the integration of the DSC curve to achieve objective A.2 of this research. It was found to be 1.87 kJ g^{-1} (1.371 kJ g^{-1} for the first peak, 0.497 kJ g^{-1} for the second peak). This includes the energy required for the transformation of the compound, but also the latent heat of vaporisation of both ammonia and water. This heat is embedded in the energy of the first peak, since all the water and most ammonia evaporate within that temperature range. The latent heat of vaporisation of ammonia was calculated as 0.029 kJ g^{-1}, whilst the one for water was 0.970 kJ g^{-1}. The activation energy, which is the energy necessary for the chemical reaction, is calculated by subtracting these values from the energy found for the first peak and is 0.37 kJ g^{-1}. The activation energy value will be derived from the models in the next paragraph and compared to this data.

Considering a plant that serves 800,000 person equivalent (PE), requires 7200 kWh day^{-1} of energy supply and produces 1000 kg of struvite per day, the energy value to completely decompose struvite at 500 °C found in this study represents 7.2 % of the total energy needed for the plant (7200 kWh day^{-1}). If considering only the first step of the decomposition, the

energy value would be 5 % of the overall energy of the plant. Thus, despite for a typical WWT plant the temperatures required are very high, actually the energy requirement and quantity of material being heated is very low. Furthermore, the decomposition could take place within minutes (less than 30 minutes were necessary to complete the degradation when heating from 25 °C at 10 °C min^{-1}), and the energy value calculated through these experiments does not take into account the energy that could be recovered associated with the condensation and recovery of ammonia solution from the gas phase.

4.2.5 Determining the reaction mechanism of struvite decomposition

As mentioned in the methodology (Section 3.2.3) kinetic analysis is essential to determine the controlling factors of the reactions and the parameters that are necessary to design the reactor for the thermal decomposition process. A first graphic determination of the mechanism of decomposition of struvite is obtained with the plot of the conversion (α) against temperature (Figure 15, left) and the derivative of α with respect to temperature against α (Figure 15, right).

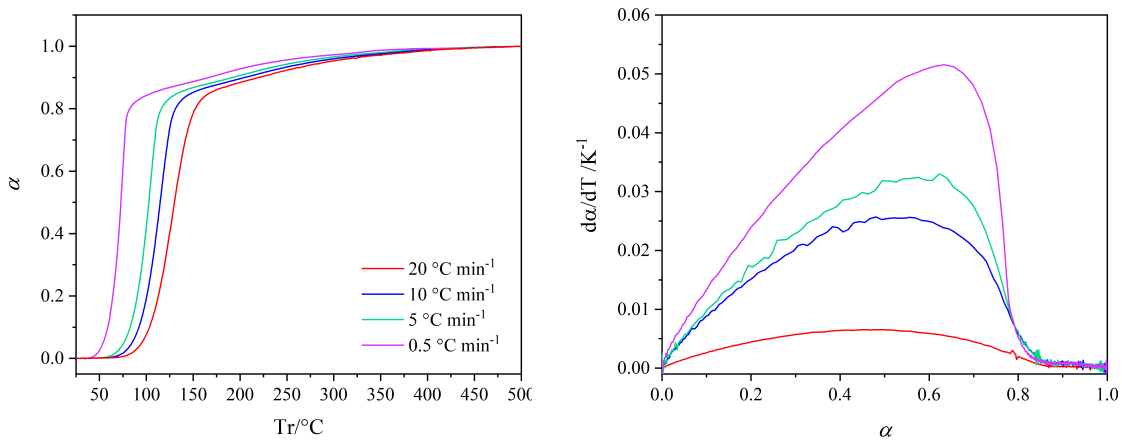

***Figure 15**: Rate of conversion α of struvite decomposition (left), and plot of the derivative dα/dT against conversion (right) at different heating rates*

The curves were compared with the ones from Khawan and Flanagan and for α < 80 % the curve resulted to be similar to an order-based model or diffusion model [109]. For α above 80 % the trend changed significantly, and this behaviour could correspond to a deceleratory region where the model is difficult to determine [51]. In this regard, the Friedman's method provided more insights of the decomposition process. From the graph in Figure 16 (left) it

emerged that the curves had different slopes, indicating that the activation energy E_a (found as the slope of the curves) depends on conversion. This information is quite important, because it indicates that the decomposition of struvite follows a multi-step process.

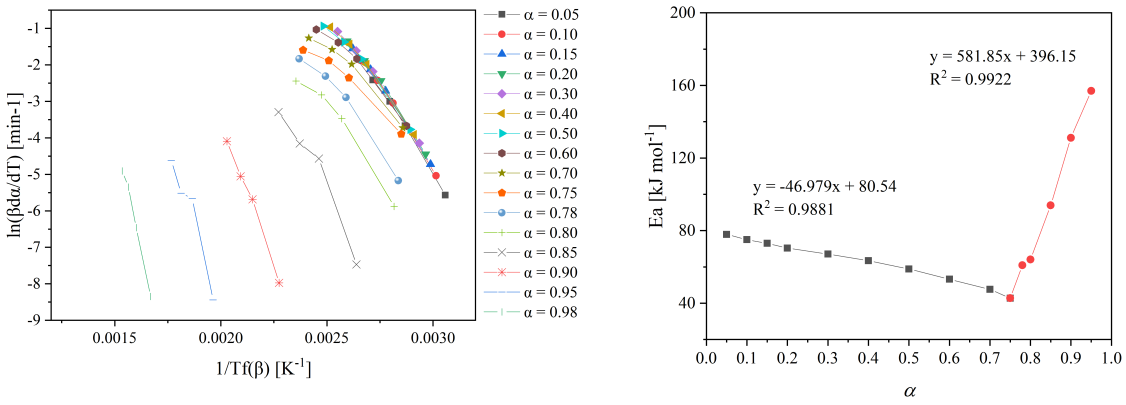

***Figure 16**: Plot of ln(βdα /dT) versus 1/T of struvite for different values of α (left); Activation energy (right) of struvite degradation derived with the Friedman's method*

Indeed, the activation energy should be constant at every value of conversion if the decomposition happened as a single-stage reaction. This result can be also understood by looking at the graph in Figure 16 (right), where two clear trends are depicted: with α is between 0 and 0.75 the activation energy drops when the temperature increases; with α between 0.75 and 1 E_α diminishes when T increases (Figure 16, right). Therefore, it was revealed that two main reaction steps occur from heating struvite between room temperature and 500 °C. This graph further confirms the second region as a deceleratory phase of the degradation. Therefore, the model-fitting approach was conducted only to the first reaction ($0 < \alpha < 0.75$). From Table 9, where the F function is reported (Eq. 9, Section 3.2.3) it can be seen that the closest reaction models to the experimental data are models' number 5 and 6 which correspond to a one-dimension diffusion model and a first-order model.

***Table 9**: Arrhenius parameters for struvite decomposition calculated with the model-fitting method*

Reaction Model	$F = S_j^2/S^2_{min}$	E/kJ mol^{-1}	log(A)/min^{-1}
1	7.573	85.97	23.43
2	7.183	82.71	22.51
3	6.415	78.30	21.24

4	2.177	65.21	17.12
5	**1**	60.72	15.59
6	1.148	61.49	16.72
7	6.651	80.06	21.88
8	5.945	76.52	20.91
9	4.552	71.46	19.53
10	5.583	52.04	11.46
11	2.112	64.75	16.40
12	2.645	66.29	17.17
13	5.243	50.47	14.08

The activation energy determined for this model is 60.72 kJ mol^{-1} (0.24 kJ g^{-1}), in accordance with the average value found for the first reaction with the Friedman's method (Figure 16, right), and comparable to the value calculated from the DSC (0.37 kJ g^{-1}). The conversion could be determined using Eq. 7. In order to do so, $\bar{k}_j(T)$ was calculated as the average rate constant of the three temperatures for each reaction model. Thus, for example, in case of reaction model one:

$$g_1(\alpha) = {\alpha_1}^{1/4} = \bar{k}(T)t \qquad \text{(Eq. 24)}$$

$$\alpha_1 = (\bar{k}(T)t)^4 \qquad \text{(Eq. 25)}$$

Figure 17 reports the plot of the conversion against the reduced time at 75 °C. The experimental values of conversion in red resulted to have better match with the one-dimension diffusion model.

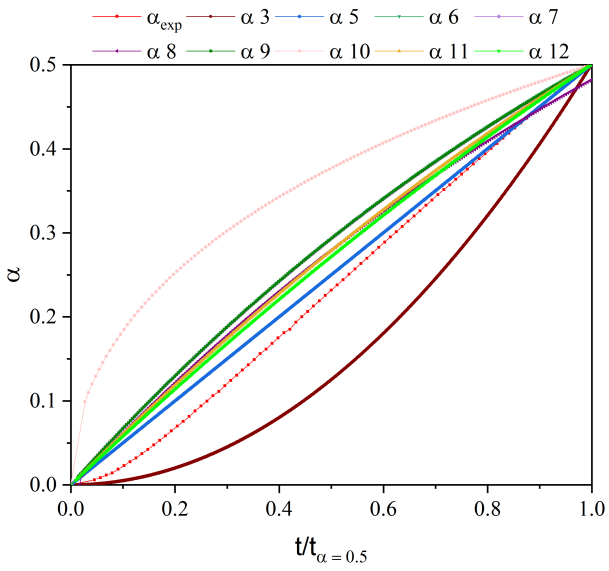

***Figure 17**: Plot of conversion of the different reaction models against reduced time at 75 °C.*

The experimental conversion is marked in red; the other curves refer to the reaction models defined in Table 3 (Section 3.2.3).

This suggests that the controlling factor for the first reaction occurring during the decomposition is likely to be the diffusion of ammonia and water molecules. The fact that one-dimension diffusion matched the experimental data much more closely than the three-dimensional one can be due to the fact that the data used in this analysis was gathered from the thermogravimetric experiments, which were conducted in small crucibles with small amounts of samples. Therefore, it is fair to assume that the release of ammonia and water is likely to have happened only in the vertical dimension. From an industrial perspective, this information can provide guidance in the design of the technology, since a reaction controlled by diffusion could be accelerated under stirring. In fact, agitation allows to maintain a concentration gradient at the reaction interface, thus endorsing convective transfer.

Thus, by combining the kinetic analysis with the thermal analysis and the characterisation analysis it can be concluded that the first reaction transformed struvite into $MgHPO_4$ (Eq. 26), as can be confirmed by the FTIR spectra, even though not all ammonia is removed.

$$MgNH_4PO_4 \cdot 6H_2O_{(s)} \rightarrow MgHPO_{4\,(s)} + NH_{3(g)} \uparrow + 6H_2O_{(g)} \uparrow \qquad \text{(Eq. 26)}$$

The reaction is regulated by diffusion of water and ammonia molecules from the solid to the gas phase. From 250 °C to 500 °C the decomposition undergoes a second step, as also highlighted in the DSC experiment, from which $MgHPO_4$ is transformed into $Mg_2P_2O_7$ (Eq. 27).

$$2MgHPO_{4\,(g)} \rightarrow Mg_2P_2O_{7(s)} + H_2O_{(g)} \uparrow \qquad \text{(Eq. 27)}$$

4.3 Considerations on the design of a struvite decomposition technology

The determination of the struvite decomposition mechanism achieved in this study provided the opportunity for considerations regarding the reuse of the struvite decomposition products. This allowed for a preliminary design of the technology that answered research question A.3. First of all, this research revealed the presence of two distinct steps of decomposition. The two products are magnesium hydrogen phosphate ($MgHPO_4$) and magnesium pyrophosphate ($Mg_2P_2O_7$). The latter compound is insoluble in water [110], whereas the former has a solubility

of 0.25 g L^{-1} (from safety data sheet, Merck). Therefore, in order to reuse the decomposition product, it is necessary to use $MgHPO_4$, since the insolubility of $Mg_2P_2O_7$ would prevent the compound from reacting again with the NH_4-N present in the stream. Recently, research has shown that $MgHPO_4$ can be effectively reused for several cycles without further addition of chemicals [111]. Moreover, from the thermal analysis it was highlighted that 42.2 % of mass loss of struvite could be reached at 75 °C. Therefore, one option could consider the use of low-grade heat to evaporate large part of the water and a small fraction of ammonia. Then, a second step could look at completing the first reaction to obtain $MgHPO_4$ by heating the solid at 250 °C (Figure 18).

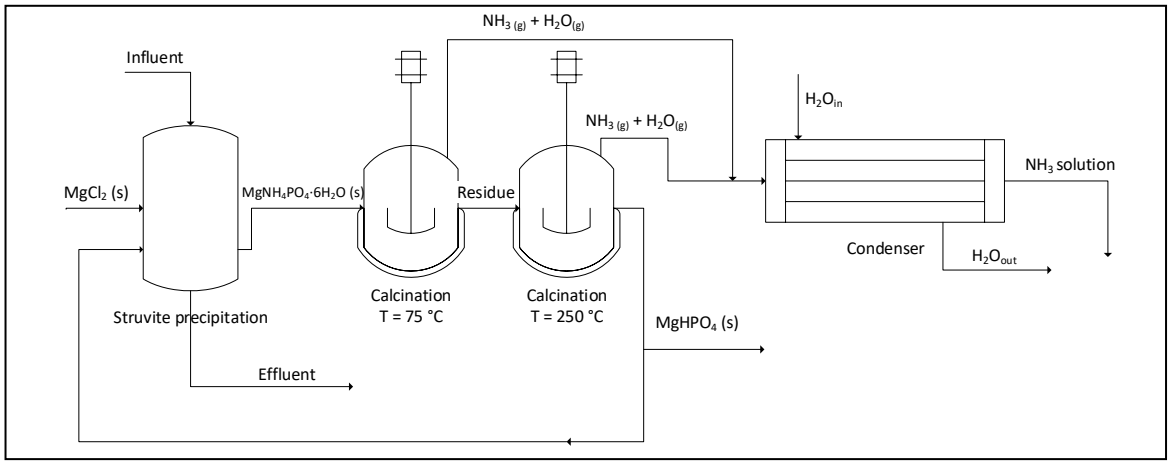

***Figure 18**: Conceptual Process-flow of one option for a struvite decomposition technology*

Another important consideration is that reusing $MgHPO_4$ could help recovering more of the NH_4-N present in the stream, which is much higher than the phosphate content at this stage of the plant. As mentioned in the introduction, the struvite precipitation is usually applied after the anaerobic digester, where due to bacterial activity the concentration of NH_4-N in the liquors can reach 800 mg L^{-1}. The concentration of the phosphate ion at this stage is within 60-100 mg L^{-1}, making it the limiting reagent of the struvite precipitation reaction. Usually, the effluent is recycled at the head of the works, keeping the nitrogen in a closed loop. Thus, having $MgHPO_4$ recycled in the feed would be beneficial to recover more NH_4-N and reduce the use of $MgCl_2$ needed for the precipitation. Despite it could be argued that the phosphorous would then be

left in a closed system, $MgHPO_4$ would be retained for longer in order to maximise the NH_4-N recovery, before being recovered from the system.

4.4 Summary

Struvite decomposition in solid state was investigated to understand if ammonia could be released and recovered as a more valuable product, and the magnesium source could be recycled in the system, saving part of the costs of the expensive chemical used. Thermogravimetric analysis showed the influence of the heating rate in the decomposition of struvite: the calcination onset temperature decreased at lower heating rates, confirming results from previous studies. At 0.5 °C min^{-1} the decomposition started at circa 31 °C. Isothermal tests highlighted the possibility of degrading struvite at low temperature. Indeed, 42 % of the total mass could be evaporated by heating struvite at 75 °C. Furthermore, elemental analysis on the samples proved that ammonia and water are released simultaneously from the sample contradicting previous studies. The analysis confirmed that nitrogen (2.5 % of the sample) is left in struvite at that temperature. Ammonia could not be completely released below 250 °C, as shown from the infra-red spectra. The final calcination product was found to be magnesium pyrophosphate. Although thermogravimetric analysis and the first derivative displayed one main peak, the differential scanning calorimetry technique highlighted the presence of two major events that represent a change in the phase or in the structure of the sample. This result was also confirmed by the kinetic analysis that revealed the presence of two different reactions. The kinetic analysis highlighted that the first one is likely to be an order-based or diffusion model, meaning diffusion is the main phenomenon controlling the decomposition. From an industrial point of view, a diffusion-controlled reaction means that the decomposition will be sped up under agitation. The decomposition reactions proposed in this study were the following:

$$MgNH_4PO_4 \cdot 6H_2O_{(s)} \rightarrow MgHPO_{4\,(s)} + NH_{3(g)} \uparrow + 6H_2O_{(g)} \uparrow$$

$$2MgHPO_{4\,(g)} \rightarrow Mg_2P_2O_{7(s)} + H_2O_{(g)} \uparrow$$

The first reaction transforms struvite into $MgHPO_4$ and is completed at circa 250 °C, whereas the second reaction converts $MgHPO_4$ into $Mg_2P_2O_7$. The energy required to complete the degradation, calculated from the DSC curves, was found to be 1.87 kJ g^{-1} at 10 °C min^{-1} (1.37 kJ g^{-1} for the first reaction). These values correspond respectively to 7.2 and 5 % of the total energy required for a WWT plant serving 800,000 PE and producing 1 tonne of struvite per day. Moreover, the decomposition would require minutes (less than 30 minutes were necessary to complete the degradation when heating from 25 °C at 10 °C min^{-1}). In this study, a prospect of the design of the technology was suggested, which involved the use of low-grade heat to evaporate most of the water and small part of the ammonia at 75 °C. Afterwards, a second unit would heat the compound up to 250 °C to complete the transformation to $MgHPO_4$. This product could potentially be reused for several times to reduce the use of $MgCl_2$ in the feed. Moreover, it would allow the recovery of larger amounts of NH_4-N, which is usually left in the stream due to the limiting concentration of phosphate ions.

These findings provided new insights regarding the thermal decomposition of struvite, since understanding the kinetic mechanism and the energy required will help in the optimisation of the design of the recovery technology. However, the economics of this process are not yet industrially viable due to the high temperatures required and the extra equipment needed for the decomposition technology. Furthermore, this technology has limited applicability since it can only be employed on sites where biological nutrient removal and anaerobic digestion of the sludge are carried out. As such, this is not a solution that could be widely applicable. Therefore, alternative solutions are needed, and the next Section explores the potential of more novel technologies for low NH_4-N concentration streams.

5 Adsorption technology: use of the Metal-Organic Framework ZIF-67 to adsorb and store ammonium

Section 4 focused on the chemical precipitation technique and investigated the optimisation of the technology by exploring the thermal decomposition of the precipitate and the recovery of higher-quality products. After having answered the research questions concerning this technique, this Section reports on the investigation of the adsorption technology. In particular, to answer research question number 2 of this project, a literature review was carried out which is briefly reported in Section 5.1. Then, Metal-Organic Frameworks were identified as a potential alternative to conventional zeolites. This hypothesis was elaborated based on the lack of knowledge regarding these materials for this application, but also for their excellent porosity, demonstrated chemical and physical properties as adsorbents, and numerous possibilities of synthesis and modifications.

5.1 Introduction

Adsorption is a technique which employs porous materials and is used in water remediation for the removal of contaminants and other filtration processes. Porous materials are materials characterised by low density and high surface area, and the presence of pores. Due to these properties, they have been employed as effective adsorbents to remove gaseous contaminants but also as catalysts, drugs delivery in the human body, or to capture pollutants from water systems [112]. Zeolites, resins and hydrogels belong to this class of materials and have been extensively investigated also as adsorbents and ion-exchangers for the recovery of ammonia from wastewater [77,78,113–120]. However, after decades of research and publications these materials have not reached industrial applicability due to the operational costs of the technology [121]. In particular, the cost of the chemicals involved in the regeneration of these media, in addition to the lower removal performance compared to biological treatments, has limited wastewater treatment companies in choosing this technology for use at industrial scale. Thus, there is the need of developing new and more effective adsorbents that can facilitate the

scale up of this technology. An innovative adsorbent should possess high adsorption capacity and reusability, lower use of chemicals needed for the adsorption process, sustainable synthesis. In this regard, a new class of porous materials named Metal-Organic Frameworks (MOFs), developed almost twenty years ago has been attracting attention due to their structure versatility. MOFs have been reported to have large surface area and porosity which make them suitable for adsorption, catalysis, and separation technologies [6–10]. These materials are also more attractive from a sustainability point of view because research has shown that it is possible to synthesise them in mild conditions, including using water as solvent, solvent-free methods, room-temperature reactions, ball milling technique [122–126]. This can be achieved because MOFs are constituted by a metal cluster which binds to organic linkers via coordination bonds, as opposed to intermolecular bonds [127]. MOFs have so far been tested mostly for gas-phase applications, including the capture of ammonia gas. In particular, they have been recently investigated for the capture of gaseous ammonia under dry and humid conditions, proving better adsorption capacity compared to other classical adsorbents such as zeolites, activated charcoal, carbon nanotubes [56,62,65,128–131]. The performance of these adsorbents for applications in the gas phase has proven to be remarkable. For example, the MOFs M-2(INA) formed with isonicotinic acid (INA) and different metal sources (M = Co, Cu, Ni, Cd) showed up to 6.6 mmol g^{-1} adsorption capacity [65]. The MOFs could release ammonia upon heating at maximum 150 °C and be reused with no decrease in performance. Katz *et al.* reported that Cu-MOF-74 in presence of 80 % humidity showed a volumetric uptake of 7.6 mmol g^{-1}, exceeding HKUST-1, another copper-based MOF [62]. However, the loss of crystallinity upon adsorption in presence of humidity was also reported, indicating the lack of structure stability of this MOF in this condition. Generally, Cu-based MOFs have high affinity towards ammonia because of the interactions between copper and nitrogen. If the metal has a square planar Cu(II) configuration in the MOF, it will prefer hard bases such as nitrogen donors. Still, for the same reason ammonia tends to bind to the metal cluster with the consequent collapse of the structure [132,133]. Hereby, copper-based MOFs apart from HKUST-1 were not

of interest in this study for their inability to be used for multiple cycles but HKUST-1 was tested to understand the copper-ammonia behaviour in presence of liquid water. Recently, MOFs have been receiving increasing interest also in the wastewater treatment sector due to their versatile structure and numerous possibilities for modifications [134–137]. With regards to water remediation, several water-stable MOFs including UiO-66, ZIF-8, MOF-74 (also called CPO-27) have been investigated for the removal of heavy metals, such as lead, chromium, cadmium, mercury [138–140]. In addition, UiO-66 has shown promising green synthesis routes, as it has been successfully synthesised from common plastic waste, polyethylene terephthalate (PET) [57]. Amongst the aforementioned MOFs, ZIF-8 belongs to the Zeolitic-Imidazolate Framework group, which is a class of MOFs with a zeolite-like structure. ZIF-8 is constituted by a zinc cluster and the methylimidazolate organic ligand, and has also been tested in water systems to adsorb arsenate in very low concentrations [60]; but also as a thin layer on a polyvinylidene fluoride membrane to enhance ultrafiltration [141]. Zinc (Zn^{2+}) can also be replaced by cobalt (Co^{2+}) to obtain ZIF-67. Despite their identical structures, the two ZIFs are suitable for different applications, due to the different Lewis acidity and lability of the two metals [142].

Despite research is increasingly focusing on water-stable MOFs, there is little or no research available regarding the recovery of ammonia in the liquid phase. Thus, the aim of this work was to explore the properties of different MOFs and to investigate whether they could be an innovative alternative for the adsorption of ammonium nitrogen (NH_4-N) in liquid systems.

5.2 Results

5.2.1 Screening test

The results of the screening tests of the MOFs that were selected are depicted in Figure 19.

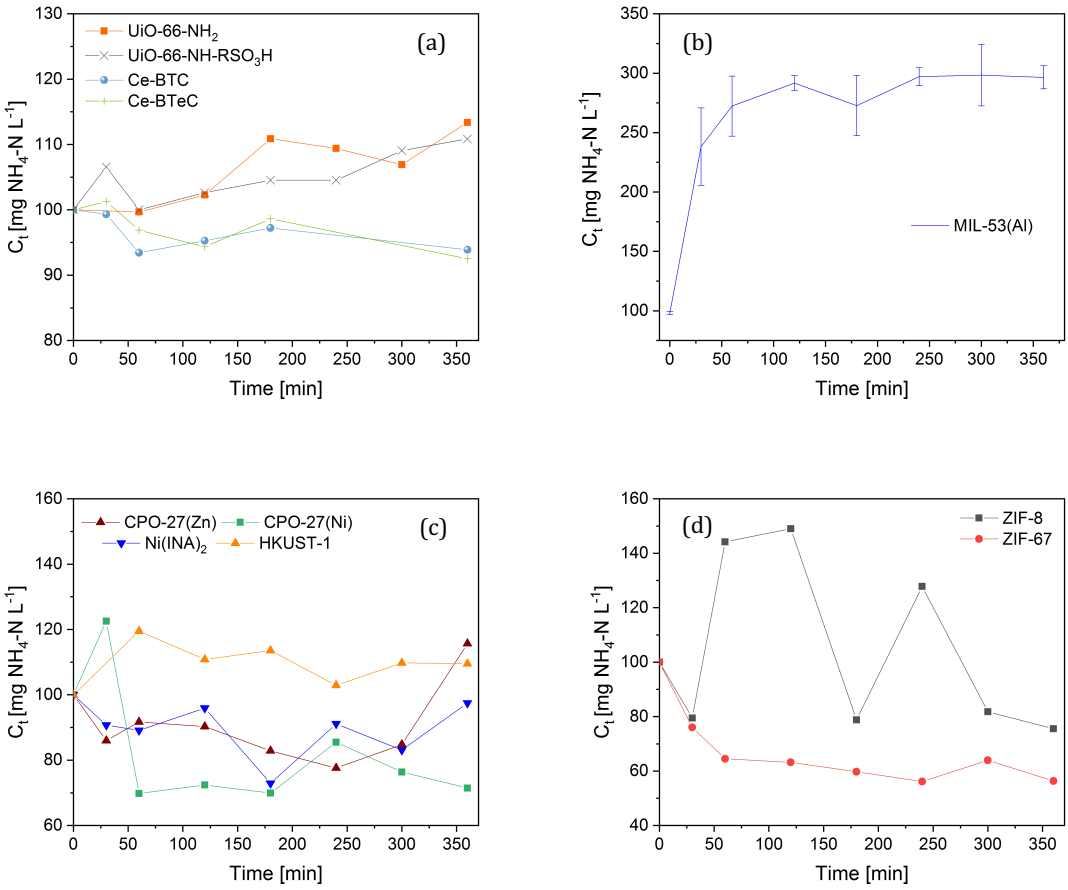

***Figure 19**: Residual NH_4-N concentration over time using UiO-66 and derivatives (a), MIL-53(Al) (b), CPO-27(Zn and Ni), $Ni(INA)_2$ and HKUST-1 (c), ZIF-8 and ZIF-67 (d)*

Several MOFs that are effective in the removal of gaseous ammonia, were not capable of uptake NH_4-N in this system. For example, UiO-66 and $Ni(INA)_2$ retained their structure they did not uptake any ammonia (Appendix A, Figure A 1). MIL-53(Al) had an unusual behaviour, causing an apparent increase of NH_4-N concentration which was attributed to an interference of the compound with the chemicals used for the UV-vis measurement. FTIR proved that its structure degraded after the test (Appendix A, Figure A 2). CPO-27(Ni) had a better performance compared to CPO-27(Zn) and was tested again (Appendix A, Figure A 3). However, the overall removal efficiency was 17 % and evaluated as unsatisfactory; in addition to this, the material

degraded after the test (Appendix A, Figure A 4). Interestingly, ZIF-67 reached 40 % removal efficiency. The uptake was lower compared to the conventional clinoptilolite, which achieved 48 % removal over six hours (Appendix A. Figure A 5). This data was considered remarkable and promising, given that no other MOF had been documented as capable of functioning in a liquid system and adsorbing ammonium. Thus, this positive result opened up to a wide range of possibilities and questions. How did the MOF adsorb the ammonium? Was the MOF structure preserved after the adsorption test? Can the performance be improved? Can the ammonium be released? To assess whether ZIF-67 could be an innovative material, further tests were carried out.

FTIR confirmed that the structure did not degrade during the test, maintaining all the peaks (Figure 20).

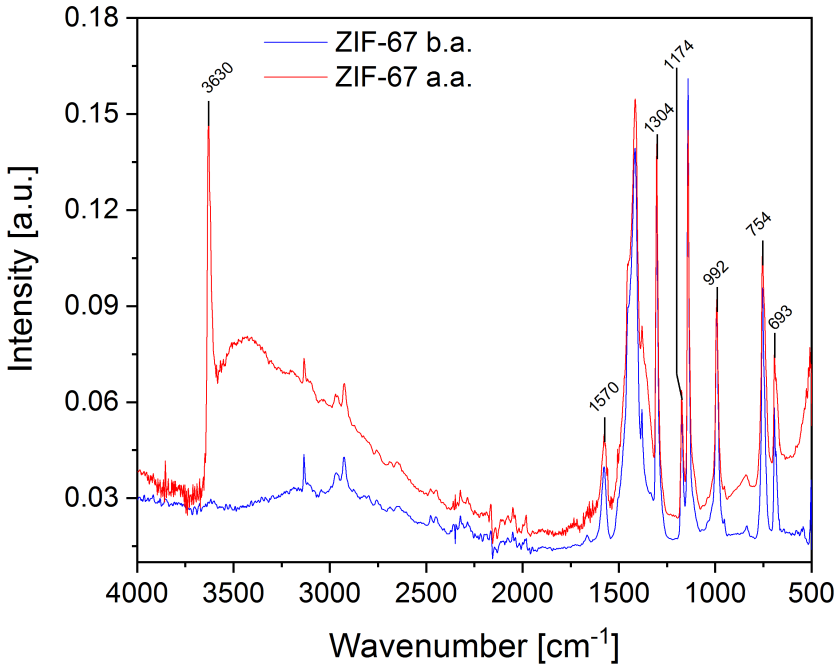

***Figure 20**: FTIR patterns of ZIF-67 before (b.a.) and after (a.a.) adsorption*

Interestingly, a new sharp peak was detected at 3630 cm^{-1}. This peak could be attributed to the formation of a N-H stretching band [143], confirming the chemical adsorption of ammonium on ZIF-67. Furthermore, XRD analysis of ZIF-67 showed how the product provided by Promethean Particles was very noisy, indicating a powdery or amorphous compound with only

few peaks visible in the spectrum. However, the XRD performed after the test confirmed the structural integrity of the MOF, as the peaks appeared that were aligned with the ones of ZIF-67 reported in the literature (Figure 21) [144].

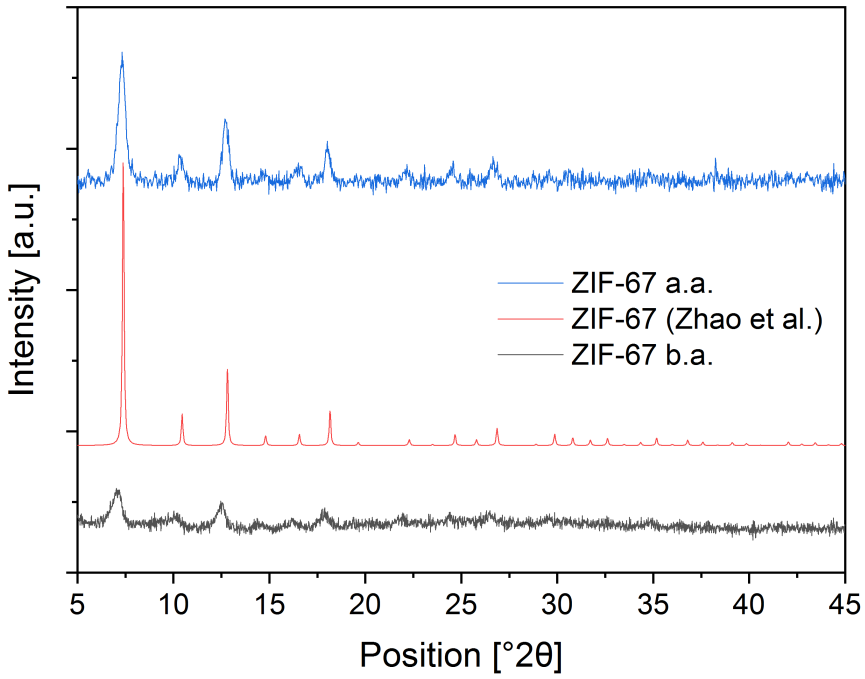

***Figure 21**: XRD pattern of ZIF-67 from Promethean Particles before and after the test, compared with the literature [48]*

5.2.2 Investigating the effect of adsorbent loading

Considering the results of the screening tests, the focus of this research was directed towards the use of ZIF-67 as a potential innovative material to recover ammonium from wastewater. This paragraph looks at the performance of ZIF-67 with different loadings. In these tests, the dosage of ZIF-67 was increased, whilst the volume of solution was kept constant. The loading is expressed in g of ZIF-67 per L of NH_4-N solution, the system was kept at room temperature, the initial pH was neutral, and the NH_4-N concentration was 100 mg L^{-1}. Interestingly, the maximum adsorption amount at the equilibrium was obtained with a loading of 1 g L^{-1} with 7.5 mg g^{-1} (Figure 22). These values are comparable and in some cases higher than the ones of natural zeolites [40,44,145].

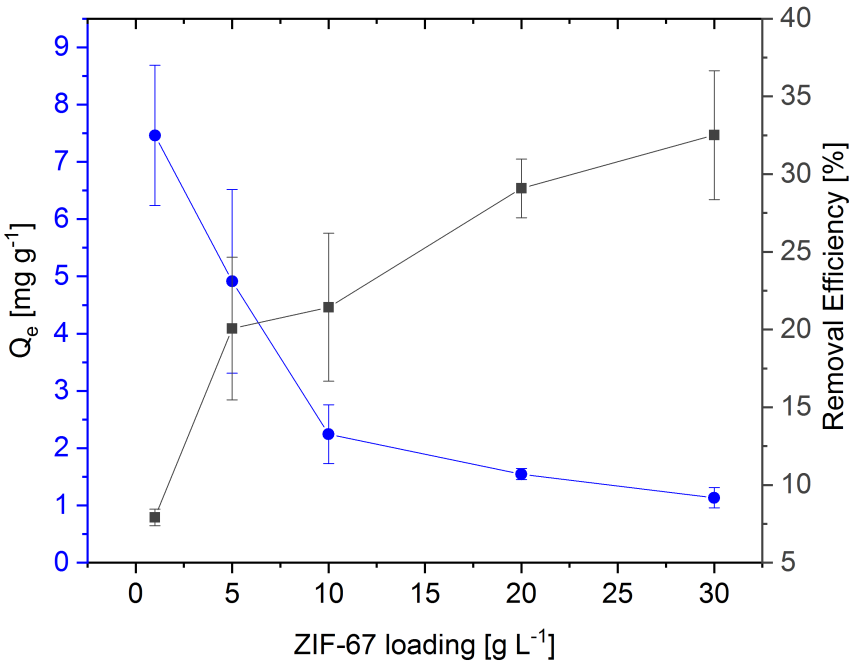

***Figure 22**: Adsorption amount at the equilibrium (Q_e) and removal efficiency with ZIF-67 loading (g L^{-1}) at initial concentration of 100 mg NH_4-N L^{-1}*

A drop in the adsorption capacity was noticed with an increase in the dosage of ZIF-67. Nonetheless, the removal efficiency was enhanced but did not achieve 50 %. When the loading was boosted from 1 to 10 g L^{-1} the amount of NH_4-N adsorbed was reduced by almost 4 times. The minimum value recorded was 1.2 mg of NH_4-N g^{-1}, reached at 30 g L^{-1}. This behaviour has been previously reported in adsorption systems elsewhere [146]. This might be because the adsorptive capacity of adsorbent available is not fully utilised at higher adsorbent dosages in comparison to lower adsorbent dosages. Possibly, the increase in the adsorbent loading might cause aggregation of the adsorbent particles, as suggested in another adsorption study [147]. As such, the availability of the adsorption sites decreases. By looking at the graph, the best condition seems to be when the loading is between 5 and 10 g L^{-1} where the removal efficiency in these conditions (C_0 = 100 mg L^{-1}) is circa 20 %, before the adsorption capacity drops considerably.

5.2.3 Investigating the effect of initial ammonium concentration

In this test, the system was kept at initial neutral pH and room temperature, while varying the initial NH_4-N concentration from 25 to 500 mg L^{-1}. Different ZIF-67 loadings were tested: 1, 5 and 10 g L^{-1}. In these conditions, the increase of initial NH_4-N concentration caused a drop in the removal efficiency for both ZIF-67 loadings, as shown in Figure 23.

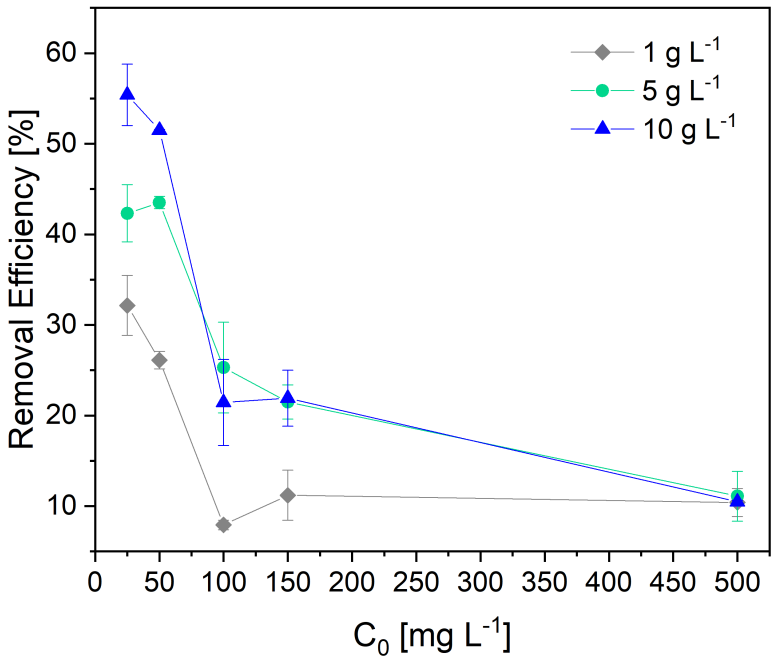

***Figure 23**: Removal efficiency (%) with different initial NH_4-N concentrations C_0 at different ZIF-67 loadings*

This may be explained by a surface saturation effect. Following an acceleration during short time due to a gradient of ammonium concentration between the solution and the adsorbent pores, mass transfer may be then reduced due to a saturation of the surface adsorption sites. The saturation of the sites can be also attributed to the water entering the pores. The maximum removal efficiency was 56 % and it was achieved when the NH_4-N concentration was 25 mg L^{-1} and the loading was 10 g of ZIF-67 L^{-1}. From an industrial point of view, in these conditions the material could reduce the NH_4-N to 11 mg L^{-1}. This value could be close to the threshold if the discharge limit was 10 mg L^{-1}. However, depending on the dilution factor the allowed maximum concentration in the effluent could vary and be in the range of 1-10 mg L^{-1}.

Interestingly, the graph below highlights how the adsorption capacity increases with an increase of the NH_4-N concentration (Figure 24).

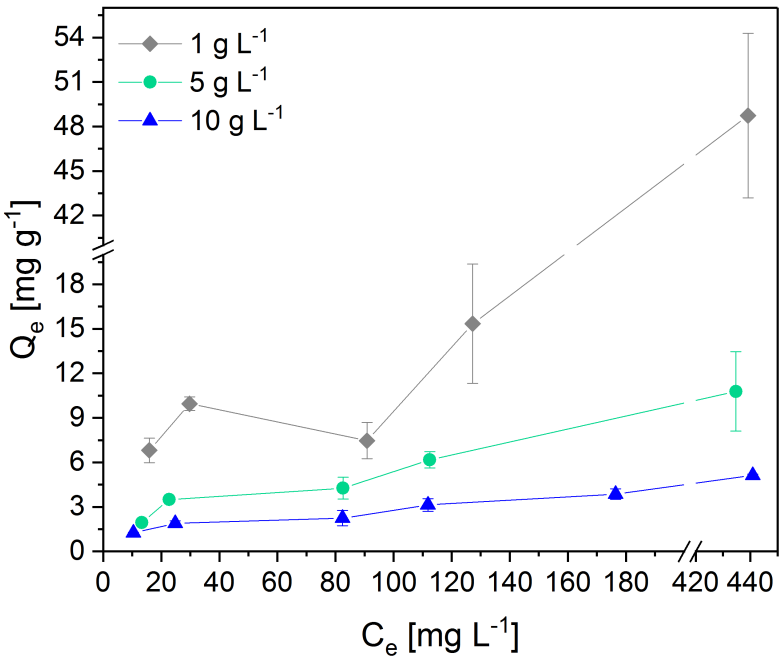

***Figure 24**: Amount of NH_4-N adsorbed at equilibrium Q_e in respect to equilibrium NH_4-N concentrations C_e with different ZIF-67 loadings*

The uptake of NH_4-N rose steadily with different initial NH_4-N concentrations at different adsorbent loadings. In particular, at 10 g of ZIF-67 L^{-1} the maximum uptake was 5.1 mg g^{-1} when the initial concentration was 500 mg NH_4-N L^{-1}. Therefore, even though the removal efficiency was lower in this condition (12 %), more ammonium is removed compared to lower concentrations. Moreover, higher adsorption capacities were always achieved with a loading of 5 g L^{-1}, and the maximum equilibrium uptake was of 10.8 mg g^{-1}. Interestingly, with a loading of 1 g L^{-1} the equilibrium uptake was much higher at every point of the curve compared to higher loadings (up to 10 times greater when C_0 was 500 mg NH_4-N L^{-1}). Moreover, it did not reach a plateau that would have indicated the saturation of the adsorption sites. This data was accompanied with a change of colour in the solid residue of ZIF-67 from purple to blue possibly indicating degradation to cobalt hydroxide (Figure 25).

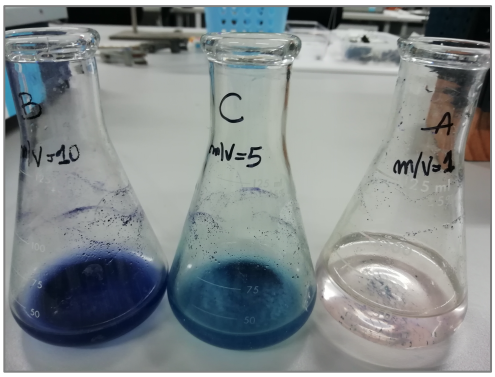

***Figure 25**: Image of flasks containing NH_4-N solution and ZIF-67 at the end of the adsorption test with adsorbent loadings of 10, 5 and 1 g L^{-1}*

In the case of ZIF-67 loading of 1 g L^{-1} a pink coloration in the liquid phase suggested a possible degradation of ZIF-67 to cobalt chloride, soluble in water. This aspect will be investigated further in Section 6.2.3.

5.2.4 Investigating the effect of initial pH

ZIF-67 demonstrated a good stability with respect to different initial pH conditions between 4 and 7. The adsorption amount was highest with an initial pH of 6 (Figure 26). A decrease of 30 % in the adsorption capacity was noted when initial pH was 2.

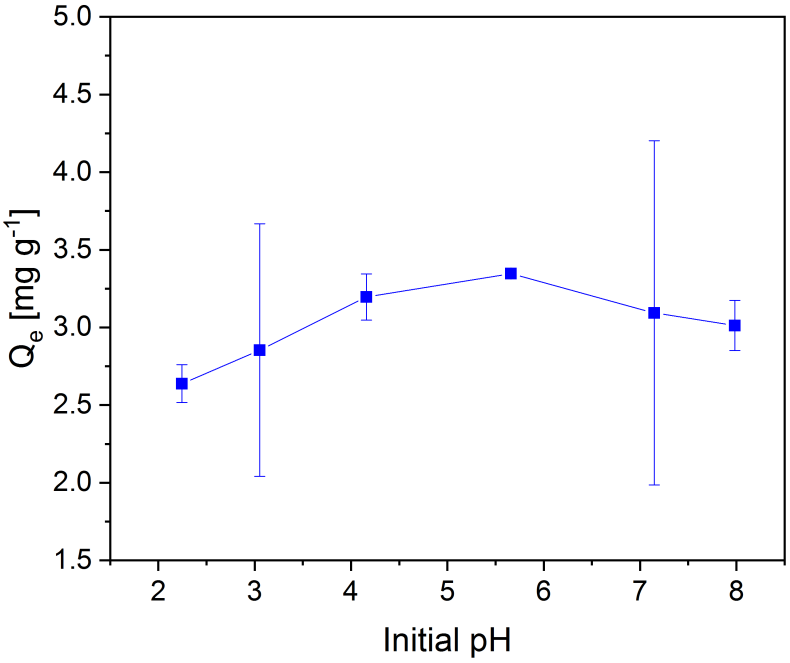

***Figure 26**: Adsorption capacity (mg NH_4-N g^{-1}) with different initial pH*

Nonetheless, two points of the graph resulted to have large error bars. A standard deviation of 81.3 % was obtained with an initial pH of 3 and a standard deviation of over 110 % with an initial pH of 7. This may be explained by the temperature setting of the test. The experiments were indeed carried out at room temperature which varied between 18-20 °C in winter and 28-33 °C in summer (for pH equal to 3 and 7 two tests were carried out in February and one in July). The temperature difference may have affected the adsorption reaction process, as it is reasonable to think that it may favour the kinetics in a chemical process. Interestingly, a change in colour was observed during these tests, both in the solid samples and in the liquid solution. In some cases, after filtering the solid from the NH_4-N solution, the liquid sample would turn to different shades of pink, as it can be seen in Figure 27.

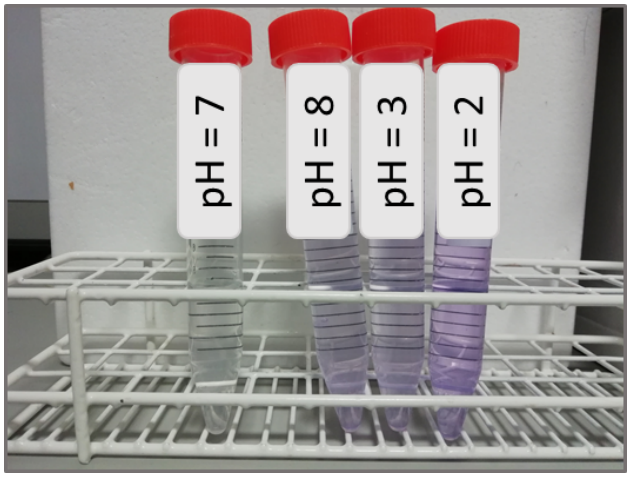

***Figure 27**: Liquid samples filtered at the end of the test of NH_4-N solution at different initial pHs*

This could be due to a degradation of ZIF-67 with consequent leaching of cobalt, due to the formation of the soluble compound cobalt chloride, $CoCl_2$. Indeed, analysis of the water samples by ICP highlighted a release of cobalt in the solution with the highest concentrations of 8.2 mg L^{-1} and 4.4 mg L^{-1} of cobalt in solution obtained respectively at initial pHs of 2 and 8 (Figure 28). The lowest cobalt concentration was detected with initial neutral pH, as it also appears from the transparent colour of the centrifuge tube (Figure 27). This indicates that ZIF-67 is highly stable in this condition and can be used without degrading.

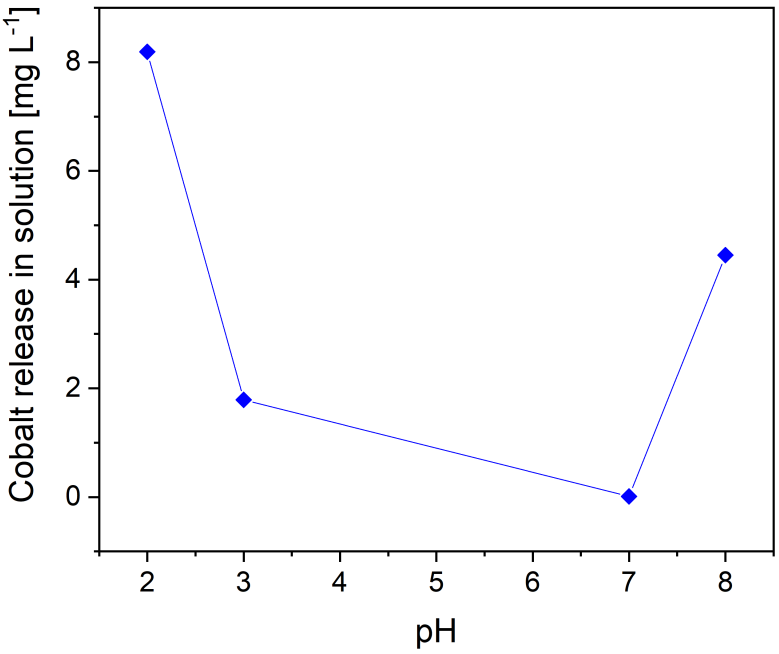

***Figure 28**: Cobalt release in solution (mg L^{-1}) versus initial pH*

To further prove this, CHN analysis that was conducted on the solid samples shows how there is also a decrease in the amount of carbon and nitrogen present in the solid samples (Table 10).

***Table 10**: CHN analysis of ZIF-67 before adsorption (b.a.) and after adsorption (a.a.) with different initial pH*

Sample	Initial pH	$Nitrogen_{total}$ (%)	$Carbon_{total}$ (%)	$Hydrogen_{total}$ (%)
ZIF-67 b.a.	N.A.	24.73	42.62	4.74
ZIF-67 a.a.	2	13.64	25.02	3.62
ZIF-67 a.a.	3	17.03	30.61	3.93
ZIF-67 a.a.	7	22.17	38.75	4.43
ZIF-67 a.a.	8	16.99	30.65	3.95

This decrease corresponds to the degradation of the organic ligand 2-methylimidazole, whose molecule contains both nitrogen and carbon. In this regard, the worst condition is to have an initial pH of 2, where the carbon content is reduced from 42.62 % in the sample before adsorption (ZIF-67 b.a.) to 25.02 % and the nitrogen from 24.73 % to 13.64 %. No significant change in the structure was detected from FTIR (Appendix A, Figure A 6). Thus, it is reasonable to conclude that ZIF-67 is more stable in neutral and basic conditions than in acidic conditions,

as reported also in other studies [148]. However, it also seems that a fraction of the organic linkers dissociates from the metal centre and dissolves in the solution. This can be confirmed by the measurement of the pH at the end of each test, which was always above 9. This test further proved the overall structural integrity of ZIF-67 in pH range that resembles realistic conditions in wastewater. However, for industrial applicability further analysis is needed to understand whether the cobalt leakage can be harmful for the environment.

5.2.5 Adsorption kinetics

Table 11 highlights the kinetic parameters that were calculated through the experimental data for the pseudo-first order and pseudo-second order kinetic models.

***Table 11**: Kinetic parameters of Pseudo-First Order and Pseudo-Second Order calculated at 50 mg L^{-1}; adsorbent loading of 10 g L^{-1} and initial neutral pH*

50 mg NH_4-N L^{-1}				
Model/ Parameters	$Q_{e,\,exp}$ [mg g^{-1}]	k_1 [min^{-1}]	$Q_{e,\,cal}$ [mg g^{-1}]	R^2
Pseudo-First Order	1.671	0.0108	1.340	0.933
Model/Parameters	$Q_{e,\,exp}$ [mg g^{-1}]	k_2 [g mg^{-1} min^{-1}]	$Q_{e,\,cal}$ [mg g^{-1}]	R^2
Pseudo-Second Order	1.671	0.0528	1.563	0.994

From the data, the pseudo-second order model seems to better fit the experimental data, with a coefficient of determination of 99.4 % and a calculated adsorption capacity of 1.563 mg g^{-1}. This suggests that chemical adsorption is the mechanism regulating the uptake of NH_4-N with ZIF-67. The fitting curves are shown in Figure 29 and clearly demonstrate the similarity between the experimental Q_e and the calculated points for the pseudo-second order.

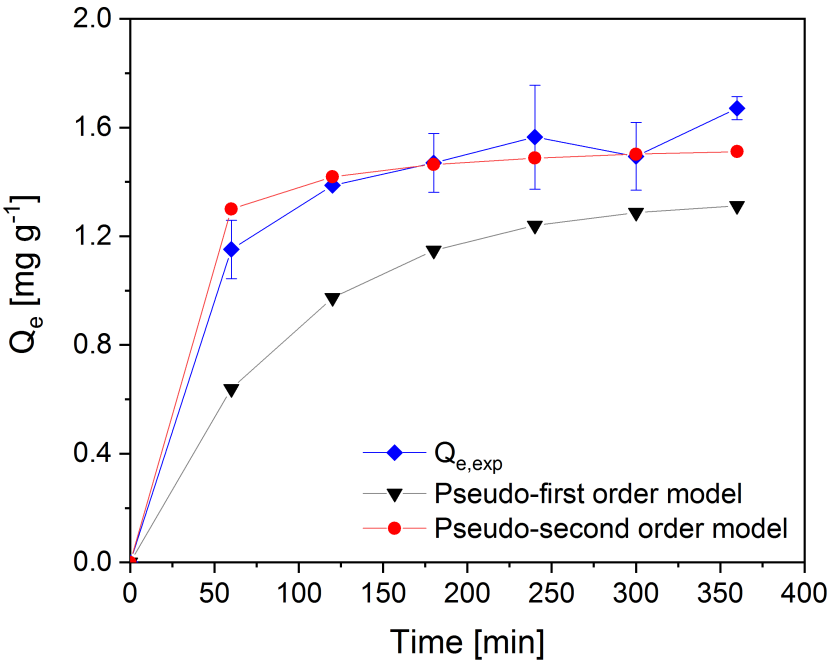

***Figure 29**: Pseudo-first order and pseudo-second-order kinetic model fitting for ZIF-67 with C_0 of 50 mg NH_4-N L^{-1}*

The chemisorption mechanism involves an exchange of electrons between the guest species and the adsorbent [82]. Moreover, it also means that the process is influenced by the number of active sites [82]. The pseudo-second order has been found as the best fit for adsorption kinetic model also for zeolites [40].

5.3 Summary

This work explored the potential of several water-stable MOFs in liquid systems, in the research of innovative materials that could be used for the adsorption of ammonium from wastewater. The characteristics of an innovative adsorbent would include high adsorption capacity, reusability, low use of chemicals needed for the process, sustainable synthesis. The aim of this study was to understand the capacity of MOFs to uptake ammonium and provide a proof of concept that these materials could represent an alternative option to conventional zeolites. After a materials selection carried out based on the aforementioned criteria for this application (water stability, ammonia affinity, reusability, green synthesis) the following MOFs were selected: UiO-66 and derivatives, ZIF-8 and ZIF-67, CPO-27, MIL-53, $Ni(INA)_2$, and HKUST-1. The MOFs were tested in a batch system with ammonia solution (ammonium

chloride). In this work, a screening test was carried out in fixed conditions of temperature, initial pH (neutral), adsorbent loading of 10 g L^{-1}, and initial NH_4-N concentration (100 mg L^{-1}). From this test, it emerged that several water-stable MOFs which had been reported to adsorb gaseous ammonia also in humid conditions, did not work in this context. For example, the UiO-66 MOFs and $Ni(INA)_2$ retained their structure but did not adsorb any NH_4-N. ZIF-8(Zn) and ZIF-67(Co) gave different outcomes during the screening test. ZIF-8 did not uptake any NH_4-N, whilst ZIF-67 was the best amongst all the MOFs tested with 40 % removal efficiency. The uptake was lower when compared to the conventional clinoptilolite, which achieved 48 % removal over six hours.

This screening test provided important preliminary considerations that could be taken into account in the design of a MOF for the capture of NH_4-N from a liquid system. Amongst all, the role of the metal cluster seems to be key in facilitating the capture of the contaminant. ZIF-8 and CPO-27(Zn) had an unstable behaviour, indicating that zinc might be inert and incapable of retaining ammonium in the structure.

Following the screening test, ZIF-67 was chosen for more detailed analyses. The main objective was to understand the capacity of the MOF in variable conditions of pH, adsorbent loading, NH_4-N concentration, and to identify the kinetic model that regulated the adsorption process. From these experiments it emerged how the adsorbent loading influences ZIF-67 adsorption capacity and removal efficiency. The optimal value was found to be at 5 g of ZIF-67 L^{-1}, before the adsorption capacity drops considerably at higher loadings. When studying the effect of the initial NH_4-N concentration, it emerged that 56 % removal efficiency could be achieved when the NH_4-N was 25 mg L^{-1}, average value found in wastewater mainstreams. This means that in these conditions the material could reduce the NH_4-N to 11 mg L^{-1}, unfortunately still above the wastewater effluent discharge standard. Moreover, the adsorption capacity had an increase towards high NH_4-N concentrations, reaching 6.4 mg g^{-1} with a loading of 5 g ZIF-67 L^{-1}. These values were found to be comparable and, in some cases, higher than the ones of natural zeolites.

As far as the initial pH condition is concerned, the MOF appeared stable within a range 4-6. The adsorption capacity decreased of 30 % when initial pH was 2.

Acidic pHs of 3 and 2, and basic pH of 8 provoked a leakage of cobalt in the solution, which was confirmed both visually (the solution at the end of the test turned to different shades of pink) and with the ICP technique. CHN analysis on the residual solid samples confirmed a decrease also in the carbon and nitrogen. However, FTIR showed that the chemical bonds were maintained. This confirmed the structural integrity of the material, suggesting a dissociation of some of the organic molecules from the metal cluster.

Lastly, the kinetics of the adsorption process with ZIF-67 were investigated, by using the pseudo-first order and pseudo-second order kinetic models. The experimental data fitted well the pseudo-second order model, as reported for zeolites. This indicates, as hypothesised during the screening test, that chemisorption is the mechanism governing the process. This means that the uptake of NH_4-N depends on the number of active sites, and on the exchange of electrons between ZIF-67 and the guest specie. This suggests that by modifying the structure and increasing the number of sites available, the adsorption capacity could be enhanced. Thus, the next Section will thoroughly investigate this material and the opportunities for improvement, to assess its suitability for industrial application.

To the authors' knowledge, this is the first study regarding the use of ZIF-67 for the capture of ammonium in the liquid phase. As the first study of MOF for ammonia removal from water, this not only provides a proof of concept for the process but has also developed some understanding of the mechanisms involved.

6 ZIF-67 as ammonium adsorbent: structure modifications, isothermal tests and ammonia release

In Section 5 the performance of several MOFs for NH_4-N removal from water was assessed and the capacity of ZIF-67 of capturing NH_4-N was validated for the first time (research objectives B.1 and B.2). Thus, further study was required to thoroughly understand the industrial potential of this material. For example, considering that the maximum removal efficiency was found to be 56 %, one research question was: can the MOF performance be improved to make the material more industrially attractive?

Thus, the work reported in this Section was carried out specifically on ZIF-67 and had the objectives of:

- Increasing the adsorption capacity of ZIF-67;
- Identifying the adsorption behaviour by investigating adsorption isotherms using Freundlich and Langmuir models; and
- Establishing the adsorption/desorption mechanism of ZIF-67 towards ammonium ions.

6.1 Introduction

ZIF-67 appears as a dark purple powder and is composed by a cobalt cluster and methylimidazolate groups as ligands. The precursors, cobalt nitrate and 2-methylimidazole, react in solution forming strong coordination bonds that generate a rhombic dodecahedron structure (Figure 30). Generally, ZIF-67 has a particle size that ranges from 100 nm to 1 μm, with pore volume of 0.70 $cm^3\ g^{-1}$ [149,150].

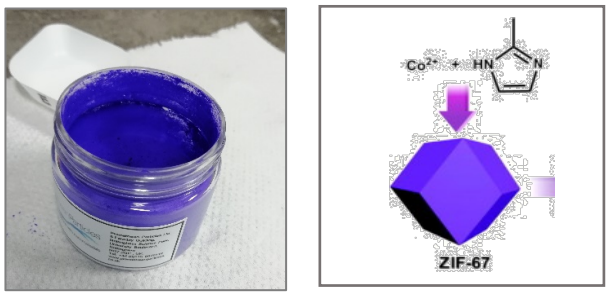

***Figure 30**: Image of ZIF-67 (left), and its structure and precursors (right)*

The nanoscale of the material can be a potential challenge in the WWT industry, especially with regard to filtration. Filters that can retain such small particles are very expensive and could substantially increase the cost of the technology. However, research has shown that MOFs can be synthesised also in tablet form, thin film or composite configuration [125,151–153].

ZIF-67 belongs to the class of Zeolitic Imidazolate Frameworks, it has a zeolite-like structure, high water stability (i.e. structural integrity) at different temperatures and pH, thermal stability and reusability [150,154–157]. These properties have been reported previously for various applications [61,149,150,158–160] . ZIF-67 has been synthesised effectively on a kilogram scale at room temperature and with a solvent-free method by Pan *et al.* [161]. This is important because it shows high potential for future sustainable synthesis, compared to solvothermal treatments. Currently, it is industrially produced in the UK via solvothermal methods by several companies, including Promethean Particles Ltd., a company specialised in nanomaterials production and technology.

ZIF-67 has been considered in water applications to: i) recover benzotriazole [162], ii) as catalyst for degradation of rhodamine B [144,149], iii) in composite configuration to remove cationic and anionic dyes [158]. Its great capacity for reusability has been demonstrated by Zhang *et al.* in the removal of boron from water (i.e. 5 cycles) [163]. All the aforementioned research studies attributed the adsorption mechanism to electrostatic interaction and the weaker π-π interaction. These forces could potentially attract also ammonium (NH_4^+) and ammonia (NH_3).

In the literature, researchers have already investigated several techniques to modify ZIF-67 with the objective of improving its properties towards certain applications. This Section reviews the state of the art regarding modifications of this MOF with the aim of identifying the most suitable and economically feasible ones for the adsorption of ammonium and ammonia in the liquid phase. Generally, the modifications that can change the structure of a MOF can be classified as:

- Functionalisation or substitution of the organic ligand,
- Metal ions substitution,
- Composite with appropriate materials.

The modification of the organic linker of the MOF can result in higher reactivity towards the target specie, larger pore dimension, or increased stability [59,164–166]. Regarding the modification of the ligand, a possible strategy that may improve the performance of ZIF-67 could involve the addition of Brønsted acid groups such as carboxylic groups -COOH or sulfonate groups -SO_3H which could increase the chemical interaction towards ammonium ions [167,168]. However, some of these modifications were carried out on UiO-66 (Section 5.2.1) and were not effective. Considering that their applicability on industrial scale is very limited, they will not be considered in this work.

As far as the substitution of the metal is concerned, attention should be focused towards those metals that have high affinity towards nitrogen, and that can have unsaturated sites in the structure, which can be used to bind ammonia. In this regard, copper-based MOFs such as HKUST-1 and MOF-74 have been reported to be amongst the best MOFs with IRMOF-3 to attract ammonia [169]. HKUST-1 binds NH_3 to the open copper sites through chemisorption forming a diamine complex [133]. However, as mentioned in Section 5.1, Cu-based MOFs instability upon adsorption has been highlighted by several researchers, who reported that as a consequence of the new bonds and preference towards ammonia, the structure of the MOF was irreversibly affected after the adsorption [62,170]. A solution to this issue might be to modify ZIF-67 by doping copper in the structure only in low amount to exchange some cobalt ions with copper ions. This could potentially help to maintain the integrity of the structure after adsorption. This procedure has been carried out on ZIF-8 at room temperature in methanol solution by Schejn *et al.* [73].

Amongst the metals that have affinity with ammonia there is also silver, because it forms diamine complex with ammonia $[Ag(NH_3)_2]^+$. Thus, it could be embedded in the structure to increase the interactions of the material towards nitrogen [171,172].

Lastly, the adsorption capacity could be improved if ZIF-67 was in a composite configuration. A composite is a material made of two or more components that possess different properties. The combination of the two materials results in a material which has different properties compared to the individual ones. In this regard, Petit *et al.* reported improved ammonia adsorption capacity

with a composite of HKUST-1 and graphene oxide (GO) compared to the singular components [133]. They explained that this positive effect could be due to the increased porosity but also that the layers of graphene increase dispersive forces which help to retain the ammonia. It has been reported in the literature that composites of MOFs and carbon materials increase properties [173,174]. Therefore, a cheap and feasible solution compared to graphene oxide could be to synthesise a composite with recycled carbon fibres, a by-product of the automotive industry [175].

6.2 Results

6.2.1 Screening test

The outcome of the screening test on the modified structures of ZIF-67 is depicted in Figure 31 and is compared to the uptake of ZIF-67 PP (ZIF-67 purchased from Promethean Particles) previously tested.

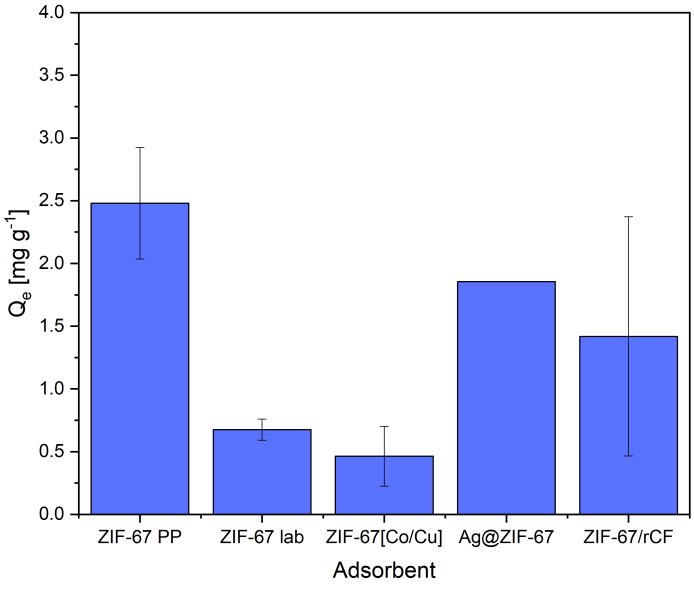

***Figure 31**: Adsorption amount at the equilibrium (Q_e) of different ZIF-67 derivatives in the following conditions: C_0= 100 mg NH_4-N L^{-1}, pH_{in} =7, loading 10 g ZIF-67 L^{-1}*

The first observation is that ZIF-67 PP outperformed all the samples synthesised in the lab, with an average adsorption capacity of 2.5 mg g^{-1} at an initial NH_4-N concentration of 100 mg L^{-1}. The uptake of ZIF-67 lab, which was expected to have a similar capacity to ZIF-67 PP, was almost one fifth of the corresponding industrially produced material. This discrepancy led to further

investigation on the morphology and of the structure of the two compounds. As can be seen in Figure 32 (left), the samples spectra almost completely overlap, showing the same peaks in the fingerprint region (1500 – 500 cm^{-1}) which correspond to the C-N and C-H bonds of the organic ligand, 2-methylimidazole [176].

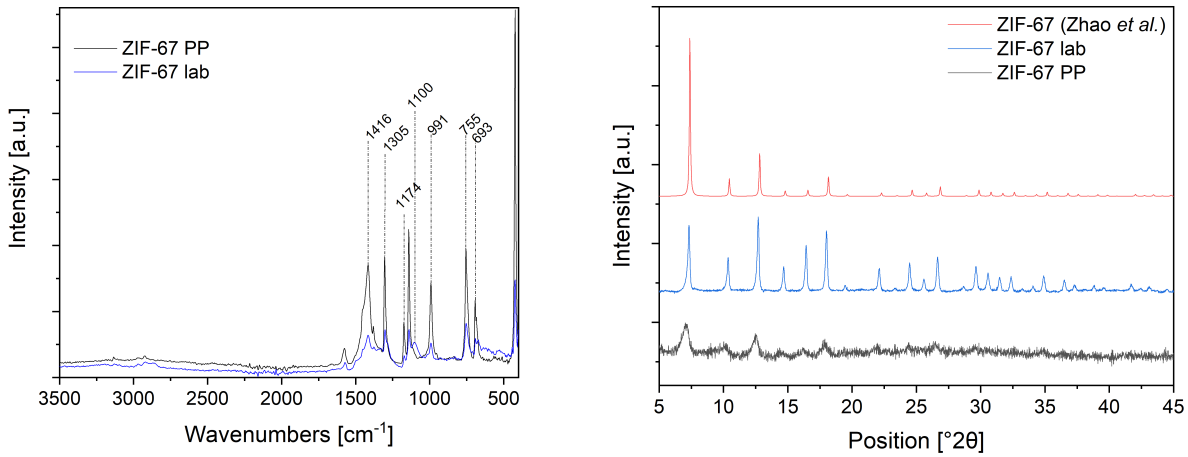

***Figure 32**: FTIR (left) of ZIF-67 PP and ZIF-67 lab; XRD (right) of the two materials compared with the literature*

Only one extra peak that was observed at 1100.5 cm^{-1} and it was attributed to organic C-C bond. The mineral phase of the samples is shown in the XRD spectra (Figure 32, right) and compared with the literature [144]. In this case, only few peaks were visible for ZIF-67 PP, indicating an amorphous structure; as opposed to ZIF-67 lab which resulted to have a crystalline structure. This was further confirmed by TEM analyses, which are illustrated in Figure 33.

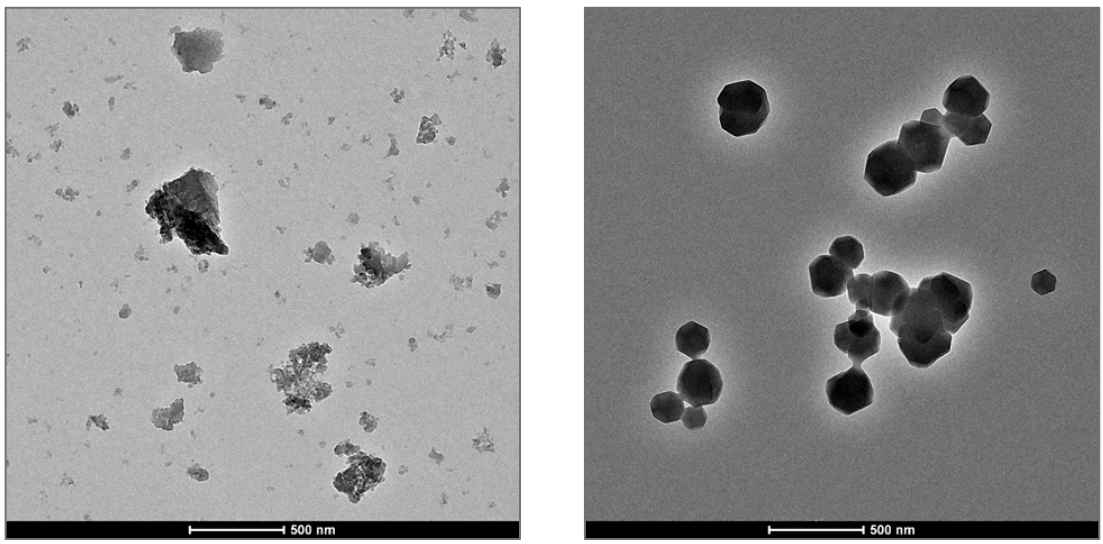

***Figure 33**: TEM images of ZIF-67 PP (left) and ZIF-67 lab (right), taken at 500 nm magnification*

The images highlight the significant difference in the morphology of the two materials. If on one hand ZIF-67 PP (left) seems to be formed by much smaller crystals and agglomerates of particles of undefined forms and shape, on the other hand ZIF-67 lab (right) shows crystals of various size up to 250 nm with rhombic dodecahedron shape, as reported in the literature [142]. Overall, this difference is likely to be due to the conditions in which the reaction takes place, where a fast reaction in a continuous reactor might not allow the opportunity for full crystal growth. Considering that this was the only significant dissimilarity detected in this work, it was hypothesised that the amorphous structure and finer grain size facilitated the adsorption of NH_4-N, resulting in a higher uptake. This has been previously highlighted in the literature for other nanomaterials [177–179].

Regarding the performance of the ZIF-67 samples that were chemically modified (Figure 31), some considerations can be made by comparing them with ZIF-67 lab. In fact, if on one hand the copper-doping modification did not improve the capacity, on the other hand the silver enhanced significantly the NH_4-N uptake, which was almost tripled. The characterisation tests of ZIF-67[Co,Cu] are shown is Appendix B (Figure B 1 and B 2). Unfortunately, there is not an error bar for this test due to the low availability of Ag NPs in Australia and their limited concentration (0.02 mg/mL) which only allowed one successful synthesis (Appendix B, Figure B 3 and B 4). Interestingly, an improvement was noticed also regarding the composite configuration of ZIF-67 and oxidised recycled carbon fibres, which more than doubled the uptake capacity. This may be due to the increased polarisation of the material due to the carboxylic groups on the surface of the fibres. In the literature, the positive effect of oxidised graphite and ZIF-67 composite has been reported recently for the application of water remediation from cationic and anionic dyes [158]. This is important data from an industrial perspective, considering that a composite configuration would facilitate ZIF-67 scalability. In fact, practically MOFs could not be applied in powder form due to the nanometre scale of the particles, which would involve high costs for filtering them at the end of the treatment. As can be seen in the SEM image below (Figure 34), the particles adhered onto the fibres forming compact purple layers of fibres of minimum 200 μm length.

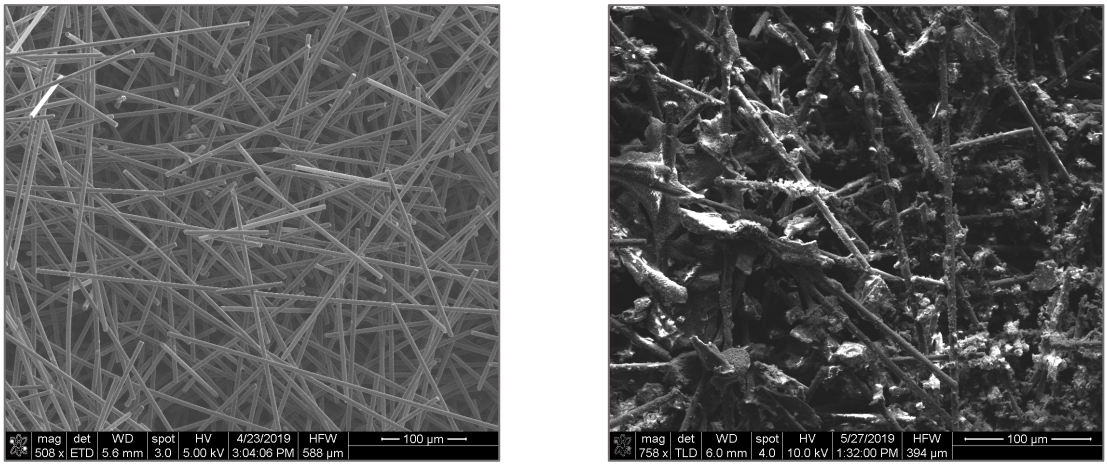

***Figure 34**: SEM of rCF (left) and rCF/ZIF-67 (right)*

Moreover, the realisation of the composite was very simple, performed by just adding the fibres to the cobalt salt precursor. Despite the fibres have to be oxidised first with sulphuric and nitric acid solutions, the cost of this material is very low (circa £ 11 kg^{-1}), as it is a by-product of the automotive industry [175].

6.2.2 Influence of temperature

Further tests were carried out on ZIF-67 PP to deepen the knowledge regarding the adsorption mechanism of this MOF and answer research question B.4.

Isothermal tests were conducted at 35 °C (308 K) and are reported in Figure 35. The results are compared to the ones gathered from tests at room temperature, already reported in Section 5.2.3.

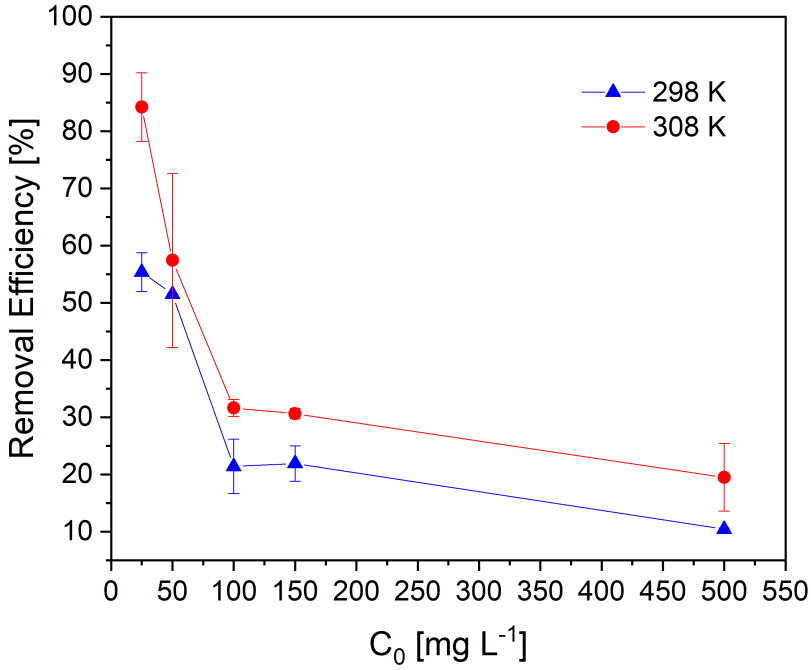

***Figure 35**: Removal efficiency of ZIF-67 PP at 298 and 308 K with respect to initial NH_4-N concentration C_0*

Overall, the temperature increase proved to have a positive effect on the adsorption performance of ZIF-67. The removal efficiency of ZIF-67 was enhanced at 35 °C throughout the tests at different initial solution concentrations, from 25 mg NH_4-N L^{-1} to 500 mg NH_4-N L^{-1}. Moreover, the NH_4-N uptake reached an average 85 % at C_0 of 25 mg L^{-1}, proving the capacity of ZIF-67 to perform in standard wastewater NH_4-N concentrations and reduce the output value to below a conservative discharge limit of 5 mg L^{-1} (in one test the final concentration of the solution was 2.5 mg L^{-1}). From an industrial point of view, this would mean that the water needs to be heated to 35 °C to achieve this effective result. Considering that the average water temperature of WWT works in the UK is typically between 10 and 12 °C [180], it may seem that this temperature would imply high energy requirements. However, this temperature is reached at some stages of WWT plants (e.g. in the liquors after the anaerobic digestion treatment); or it could be provided if low-grade heat is available on site.

The samples were characterised after this test, with particular attention to the ones which achieved removal efficiency above 80 %. FTIR confirmed that the structure of ZIF-67 was

maintained during the test (Figure 36). This result further highlights the structural integrity of the MOF in different conditions.

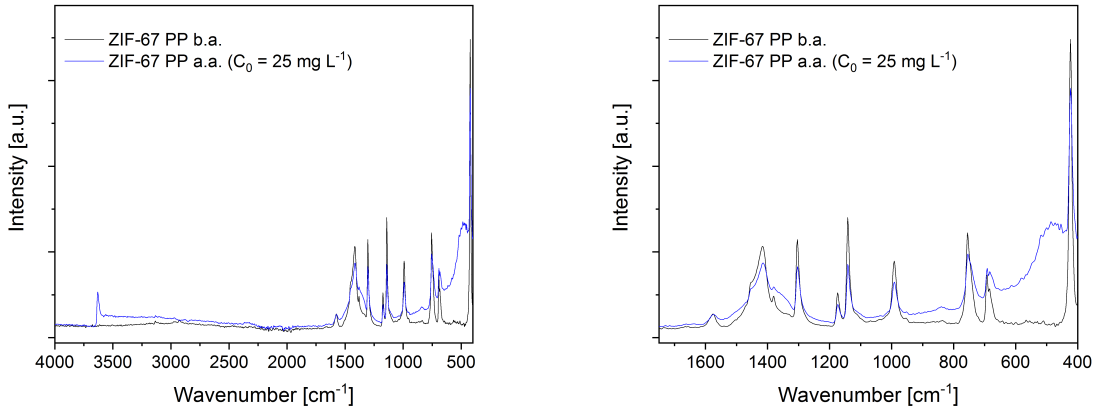

***Figure 36**: FTIR of ZIF-67 PP before (b.a.) and after (a.a.) adsorption at 35 °C with C_0 of 25 mg NH_4-N L^{-1} (left). The spectrum is zoomed in the region 1750-400 cm^{-1} (right)*

Figure 36 (right) is zoomed in the fingerprint region to highlight that all the peaks corresponding to the organic ligand were preserved, as well as the Co-N bond, confirming the integrity of the structure. An extra peak was detected at 3630 cm^{-1} in the sample tested after the test (Figure 36, left). This peak could represent the formation of a N-H bond [143], as it was noted in Section 5.2.1. However, this peak may also correspond to an O-H bond, indicating the formation of cobalt hydroxide, $Co(OH)_2$. The graph reported in Figure 37 compares the XRD patterns of ZIF-67 PP before and after the test with the spectrum of ZIF-67 found in the literature and the peaks of cobalt hydroxide.

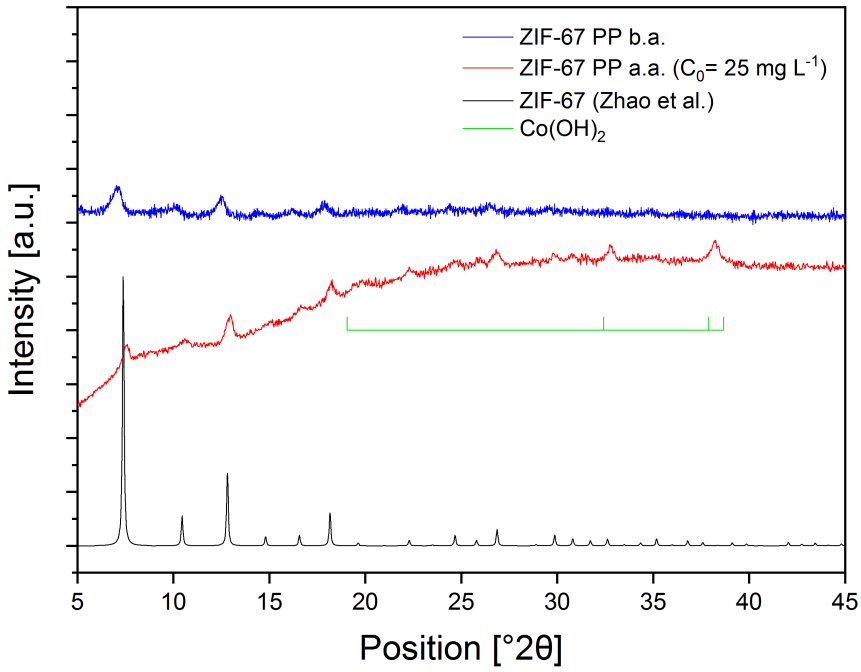

***Figure 37**: XRD patterns of ZIF-67 PP before (b.a.) and after adsorption (a.a.) at T = 308 K and C_0 = 25 mg NH_4-N L^{-1}*

Two new peaks could be detected for ZIF-67 PP a.a. at higher angles (2θ = 33° and 38°). This may indicate that the phase of the sample is not pure and that there is indeed the formation of another structure, which could be $Co(OH)_2$. Therefore, the MOF partially decomposes when tested at 35 °C. This poses a problem of durability and structural integrity of the MOF in these conditions. Moreover, the partial decomposition of ZIF-67 to $CO(OH)_2$ creates another challenge. In fact, $CO(OH)_2$ is insoluble, and it would end up in the receiving water stream contaminating the environment unless a filtration stage was added before discharge.

6.2.3 Optimisation of adsorption conditions for ZIF-67 structural stability

This paragraph reports the results of elemental analysis on ZIF-67 to identify the optimal conditions in which ZIF-67 could be used without degrading the structure. Section 5.2.4 highlighted that with initial pH of 2 and 8 cobalt was leaked in the solution, possibly due to the formation of the soluble cobalt chloride, $CoCl_2$. From an environmental point of view, the presence of cobalt in water in significant concentrations could be harmful to the environment. At present, there is not a specific regulation concerning cobalt levels in wastewater. In the case of a water stream containing high concentrations of cobalt it must be ensured that the level is below the

Environmental Quality Standard (EQS) for cobalt in natural waters, according to the Environment Agency [181]. For cobalt, the annual average EQS is 3 μg L^{-1}, whilst the maximum allowable concentration EQS is 100 μg L^{-1} for both freshwater and saltwater. However, this is applicable because currently there are no processes that are responsible for leaching cobalt during treatment. If this were to happen and a water company were to declare the presence of this metal in water effluent due to a treatment, certainly new regulation would be imposed. Nevertheless, the current regulation was used to understand the impact of this treatment and the consequences of the presence of cobalt in the effluent. The results of the ICP tests are shown in Figure 38 and report the cobalt release in solution and the cobalt release as a mass percentage of the total cobalt in the system for C_0 values of 25 mg L^{-1} (left) and 100 mg L^{-1} (right).

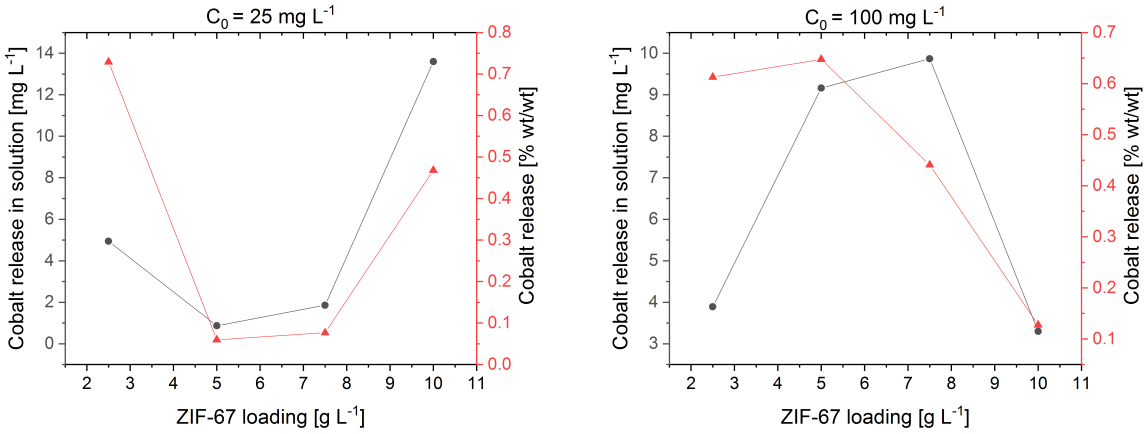

***Figure 38**: Cobalt release in the solution (mg L^{-1}) with respect to different ZIF-67 loadings and initial concentrations C_0 of 25 mg L^{-1} (left) and 100 mg L^{-1} (right). In red, cobalt release expressed as a mass percentage of the total cobalt in the system.*

From these graphs it emerges that both the adsorbent loading and the NH_4-N concentration affect the release of cobalt in the solution, and therefore the stability of the MOF. At C_0 of 25 mg NH_4-N L^{-1} adsorbent loading of 5 and 7.5 g L^{-1} result in a release of cobalt in the solution lower than 2 mg L^{-1}, which correspond to less than 0.2 % of the cobalt present in sample. Interestingly, when C_0 was 100 mg NH_4-N L^{-1} the ZIF-67 loadings that resulted in the lowest release of cobalt in solution were 2.5 and 10 g L^{-1}. These results apply to the range that was possible to test in this research. However, further tests at ZIF-67 loading of less than 2.5 g L^{-1} and more than 10 g L^{-1} could provide more information regarding the optimal adsorbent loading. Overall, all the tests positively

resulted in a release of cobalt below 0.8 % wt/wt of the cobalt present in ZIF-67. These results find confirmation in the Pourbaix diagram of the cobalt-water system, which shows the equilibrium phases of cobalt in water depending on the pH and electrochemical potential [182,183]. The electrochemical potential depends on the ions (cations and anions) present in the solution and can be calculated following the Nernst equation, therefore NH_4^+, OH^-, H^+ all have an influence on the stability of the structure.

To assess whether the cobalt release in the solution could effectively represent a problem in an industrial system, the worst value detected from the elemental analysis was used (14 mg L^{-1}) and integrated in the following equation [181]:

$$PC\ [\mu g\ L^{-1}] = \frac{RC\ [\mu g\ L^{-1}]}{ID} \quad \text{(Eq. 28)}$$

Where RC is the release concentration of the pollutant in the effluent, ID is the initial dilution factor and PC is the process contribution. Considering that the maximum allowable concentration EQS is 100 µg L^{-1}, if RC was 14,000 µg L^{-1} the minimum dilution factor could be 140, meaning that the effluent could only be discharge in large water systems. If we consider the minimum value detected (corresponding to 1,500 µg L^{-1}), then the minimum dilution factor could be 15. It is important to note that if the annual average concentration EQS (3 µg L^{-1}) was applied in the calculation, the dilution factor would have to be of over 1000. This represents a great challenge because even though the average ID in the UK is 40 [184], in England and especially in the Midlands most treatment plants have much smaller ID (many in the order of 1). Thus, further research should focus on identifying solutions to prevent ZIF-67 from degrading and leaching cobalt in the stream.

6.2.4 Adsorption mechanism

The adsorption mechanism for ZIF-67 was determined by using the data gathered in Section 5 and 6.2.2. Freundlich and Langmuir models were applied that are widely used to identify the chemical and physical nature of adsorption processes.

The parameters derived with the simulations of the Langmuir and Freundlich models that were determined at 20 and 35 °C with an adsorbent loading of 10 g L^{-1} are reported in Table 12.

***Table 12**: Langmuir and Freundlich parameters for the adsorption of NH_4-N over ZIF-67*

	Langmuir parameters				**Freundlich parameters**		
T [°C]	$Q^0{}_{max}$ [mg g^{-1}]	K_L	R^2	R_L	K_F	n	R^2
20	8.051	0.009	0.939	0.175-0.810	0.417	0.448	0.989
35	11.161	0.010	0.857	0.161-0.793	1.125	0.313	0.863

Both models revealed that the sorption mechanism is favourable, with the Freundlich parameter n below 1 and the separation factor R_L always below 1 for all initial concentrations. Langmuir model indicated a maximum concentration of 8.051 mg g^{-1}, which increased to 11.161 mg g^{-1} at 35 °C. For both isothermal conditions, Freundlich model better fitted the experimental data with the highest R^2 (98.9 %). This classifies the mechanism of adsorption as a heterogeneous multilayer adsorption mechanism. As it can be observed in Figure 39, the experimental data adequately fitted the Freundlich curve at 20 °C, whereas more uncertainty on the data points was detected at 35 °C. This could be due to the degradation of the sample at high NH_4-N concentration and higher temperature.

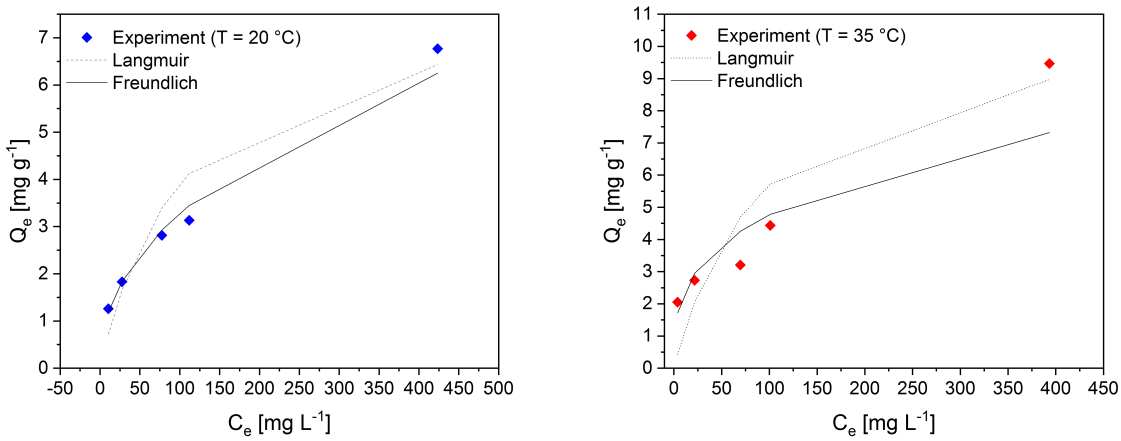

***Figure 39**: Adsorption amount at the equilibrium Q_e against the equilibrium concentration C_e at 20 °C (left) and 35 °C (right). Conditions: contact time 6 hours, neutral pH, adsorbent loading 10 g L^{-1}*

6.2.5 Adsorption with continuous flow

The adsorption of NH_4-N over ZIF-67 was also tested and validated in a continuous system with ammonia solution. In this work, the MOF was used in powder form and 2 g of media were added

to a reactor, which had a 1 µm glass microfibre filter to retain ZIF-67 in the column, inlet and outlet valves and a peristaltic pump to ensure a volumetric flow for the duration of the test (Figure 40) [185].

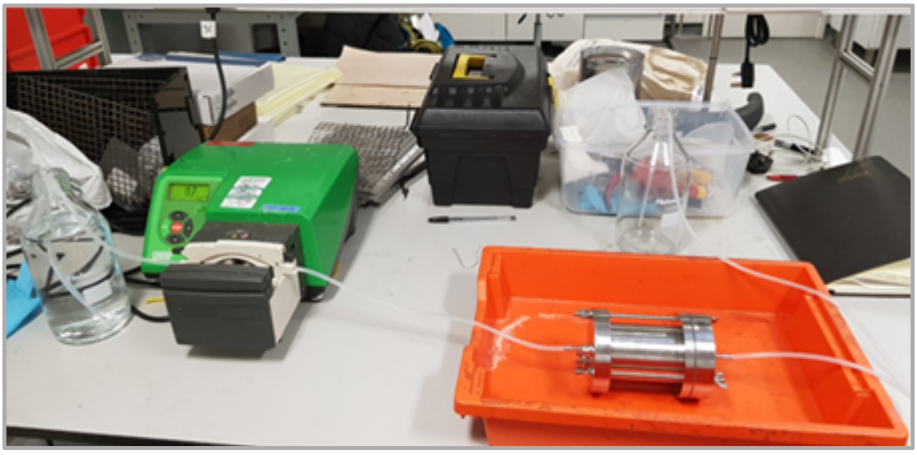

***Figure 40**: Experimental setup for a continuous-flow adsorption test. Permission granted from the author.*

In total 1 L of solution was tested over 3 hours. The initial NH_4-N concentration of the inlet solution was 26.2 mg L^{-1}, the water was pumped through the reactor at a flow rate of 5.56 mL min^{-1}, with an average retention time of 36 minutes. The outlet concentration of the solution was measured every 15 minutes. ZIF-67 successfully proved the ability to consistently remove NH_4-N throughout the test, with a peak of 70 % removal efficiency (Figure 41).

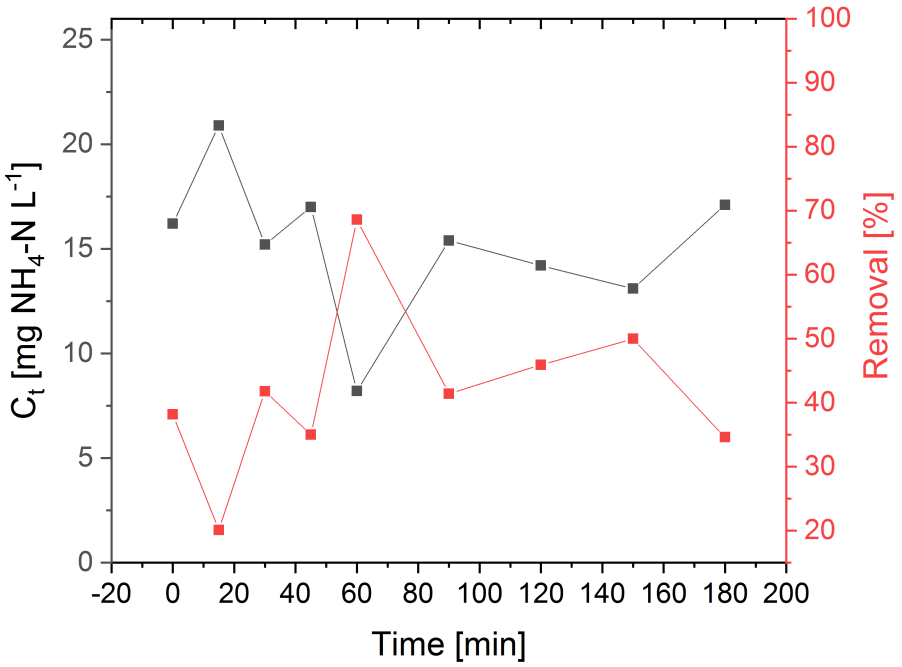

***Figure 41**: Removal efficiency [%] of ZIF-67 in a continuous system and residual % of NH_4-N in the effluent, adapted from* [185]

The limitation of this test was due to technical configuration of the system. The NH_4-N concentration was measured whilst fresh inlet flow was pumped in the reactor, mixing it with the solution which had reacted with ZIF-67. The reactor did not have an agitation system; therefore, the particles might have settled at the bottom of the chamber forming a bed. Nevertheless, the MOF positively performed for the total duration of the test, and the 1 µm glass microfibre filter adequately retained the powder, since the water that was filtered through was transparent and did not contain any particles. Overall, ZIF-67 performed quite well in these conditions, and this further proves the media as very promising for adaptation to continuous flow treatment.

6.2.6 ZIF-67 regeneration and release of ammonia

ZIF-67 was regenerated in a vacuum oven and kept at 150 °C for 2 hours. The results of the FTIR test before and after regeneration is shown in Figure 42.

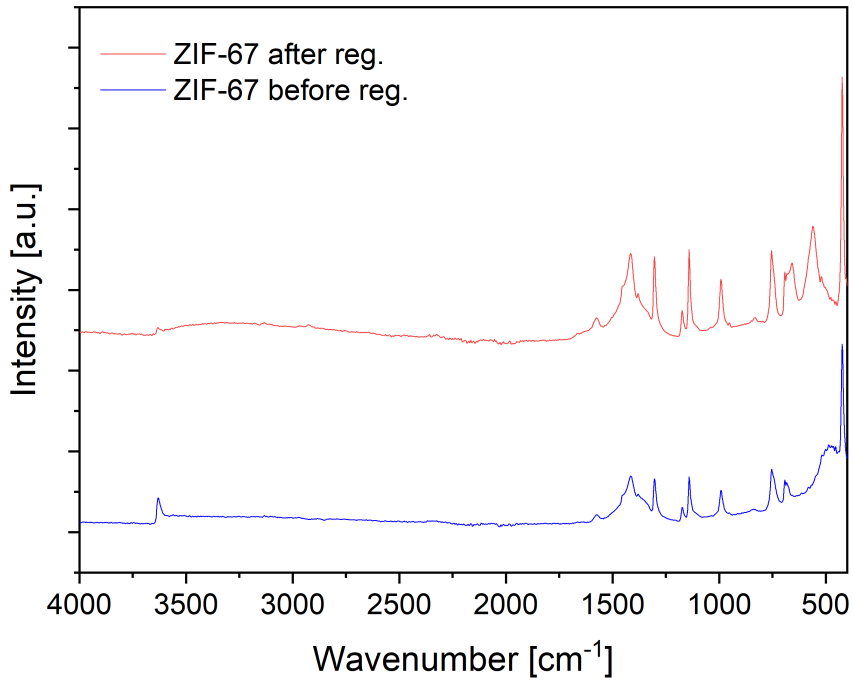

***Figure 42**: ATR-FTIR spectra of ZIF-67 before and after regeneration in a vacuum oven at 150 °C for 3 hours*

The blue pattern is the spectrum of ZIF-67 after adsorption with initial neutral pH, ZIF-67 loading of 10 g L^{-1} of NH_4-N solution, and C_0 of 25 mg L^{-1} performed at room temperature. The peak that appeared after the adsorption test at 3630 cm^{-1} had been identified in Section 5.2.1 with the formation of a N-H bond. After regeneration, it seemed that the peak almost disappeared. However, FTIR is not a quantitative analysis, so it is difficult to establish whether the ammonia was completely released. A mass balance calculation determined that the sample lost on average 7.9 % upon heating. This percentage will reasonably also include water molecules that entered the pores. Interestingly, the mass loss during regeneration increased with the initial NH_4-N concentration of the solution, when all the other conditions were kept constant (Figure 43). This possibly indicates that it is the nitrogen that is released together with the water.

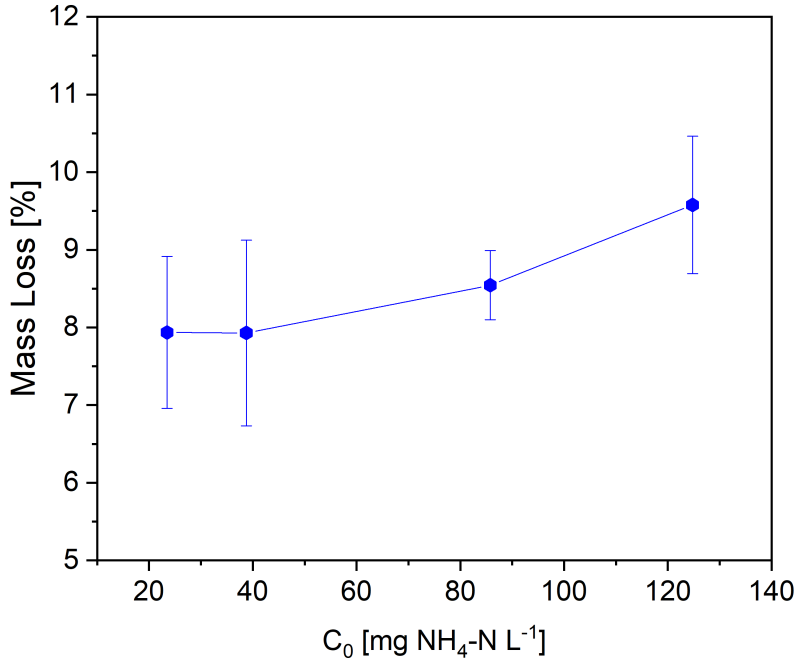

***Figure 43**: Mass loss (%) upon regeneration of ZIF-67 in a vacuum oven at 150 °C for 3 h*

Lastly, it is important to note how the structure of ZIF-67 is positively maintained after regeneration, allowing the material to be reused multiple times (Figure 42). Thermal regeneration could offer the opportunity to reduce the use of chemicals required for the ion-exchange technology, where the cost of sodium chloride needed for the regeneration of zeolites and can result in 80 % of the total operating cost [186].

6.3 Summary

In this Section, ZIF-67 was thoroughly investigated to improve its capacity to adsorb ammonium and deepen the knowledge of the adsorption and desorption mechanism. The structure of ZIF-67 was chemically modified with at room temperature to enhance the performance of the MOF. Interestingly, these modifications revealed a discrepancy between the lab-synthesised ZIF-67 and ZIF-67 PP, available commercially, since ZIF-67 lab showed much lower NH_4-N removal. After analysing the structures of the two materials it was understood that their only dissimilarity regarded the amorphous state of the commercial sample, as opposed to the crystalline ordered structure of ZIF-67 lab. Thus, it was hypothesised that the amorphous phase of the material could

positively affect the adsorption of ammonium, as previously reported in the literature for other nanomaterials.

In this work, a composite of oxidised recycled carbon fibres and ZIF-67 was successfully synthesised. The composite improved the uptake capacity of ZIF-67 lab and proved the possibility of scale up and application of this materials, since this configuration would avoid the use of costly filtration systems that would be necessary to retain the nanomaterial.

In this research, the positive effect of temperature was also revealed. Indeed at 35 °C with an initial NH_4-N concentration of 25 mg L^{-1}, ZIF-67 was able to capture on average 85 % of the total NH_4-N, thus reducing the concentration of the solution to below 5 mg L^{-1}, which is lower than the current discharge limits. Characterisation analysis showed that the structure of ZIF-67 seemed to be maintained, although two extra peaks were visible in the XRD pattern, possibly indicating the formation of a by-product. (e.g. cobalt hydroxide). From these results, further experiments, including elemental analysis were carried out to identify the optimal conditions and quantify the cobalt leakage (already detected in Section 5.2.4) to understand whether it could represent an environmental threat. This study determined the cobalt release at different ZIF-67 loadings and with initial NH_4-N concentrations C_0 of 25 and 100 mg L^{-1}. Interestingly, for every condition the release of cobalt was found to be below 0.8 % wt/wt of the cobalt present in ZIF-67. The maximum cobalt concentration in the solution was 14 mg L^{-1}, detected when ZIF-67 loading was 10 g L^{-1} and C_0 was 25 mg L^{-1}; whilst the minimum was 1.5 mg L^{-1} at 5 g ZIF-67 L^{-1} and C_0 of 25 mg L^{-1}. Since there is not a specific regulation concerning the effluent limits for cobalt, the limits are set depending on the dilution of the effluent into the receiving body. Considering that according to the Environment Agency the maximum allowable concentration is 100 µg L^{-1} for both freshwater and saltwater, the minimum dilution factor was determined for the worst- and best-case scenarios (14 and 1.5 mg L^{-1}). The minimum dilution factors were calculated to be respectively 140 and 15. This implicate that in case of relevant cobalt concentration the effluent could only be discharge in large water systems. It is important to note that if the average allowable concentration were considered, the minimum dilution factors would be much higher. In addition to this, if there was

a process that leaked cobalt and the presence of this metal in water effluent was declare because of it, certainly new regulation would be imposed. Thus, further research should thoroughly investigate how cobalt can be retained in the structure of ZIF-67.

Lastly, ZIF-67 was used in a system with continuous flow and ammonia solution for 3 hours. Importantly, the media consistently captured the ammonium present in the solution throughout the test, with a peak of 70 % removal efficiency. The material was effectively retained in the reactor by a 1 μm glass microfibre filter. This result proves the effectiveness of ZIF-67 also in a more realistic design configuration and makes this media very promising for adaptation to continuous flow treatment.

7 Cost-benefit analysis of the ZIF-67 adsorption technology

In order to validate the cost effectiveness of ZIF-67 on an industrial scale, a preliminary analysis of costs that would be involved in its application was carried out. Considering that the adsorbent is at an early stage of research and that its capacity was tested only on a laboratory scale, several assumptions had to be made to compare the costs with the conventional use of zeolites.

Firstly, it was assumed that ZIF-67 would work in a continuous system in a fixed-bed reactor, since it is the most common configuration for adsorption and ion-exchange systems [187]. The system used as benchmark was the synthetic zeolite MesoLite, which has been widely investigated for NH_4-N recovery also at pilot scale [188–190]. MesoLite acts as cation-exchanger by replacing the sodium ions Na^+ in its structure with NH_4^+. The cost of this technology is limited by the use of chemicals to regenerate the spent zeolite. A solution of brine, NaCl, is needed to wash out the NH_4^+ to reuse the media [191]. However, it can happen that some NH_4^+ remains trapped in the zeolite depending on the time of regeneration, the pH and the chemical used [186]. Furthermore, it has been reported that the use of chemicals can result in up to 80 % of the operating cost of this process [186]. In the case of ZIF-67, desorption and regeneration of the MOF would be achieved thermally, as shown in Section 6.2.6. A summary of the key analogies and differences of the two systems is reported in Table 13.

***Table 13**: Comparison of the key aspects of the adsorption system using ZIF-67 and the ion-exchange process with MesoLite*

Technology	Adsorption	Ion-Exchange
Media	ZIF-67	MesoLite
Configuration	Fixed-bed	Fixed-bed
Flow	Continuous	Continuous
Media regeneration	Thermal (150 °C, 2 h)	Chemical (NaCl solution)

The key parameters affecting the chemical costs of the technology can be summarised as:

- Adsorbent cost
- Regeneration cost
- Practical loading

The main difference from an economic perspective is the cost of the media. Since MOFs have only recently been developed on industrial scale, their cost is much higher than zeolites. ZIF-67 can be purchased on a kg scale for £ 2500 kg^{-1}, although for larger orders the price may be cheaper [192]. The cost of MesoLite is assumed to be similar to the one of other synthetic zeolites (e.g. Zeolite 13X) and is £ 1.93 kg^{-1} (2.50 USD kg^{-1}) [193]. Despite the large difference, it is reasonable to think that the cost of MOFs, which is an emerging technology will decrease rapidly in the near future as it has happened for the price of innovations such as television or mobile phones in the last 50 years [194]. In fact, publications and research on production processes and application has risen exponentially in the past 20 years. Moreover, compared to the conventional solvothermal processes for zeolites production, new synthesis techniques that would help reducing the production costs involve solvent-free technologies [125,195]. Solvent-free but also water-based production technologies will help also from an environmental point of view, since the processing and management of solvent waste is an issue, also for the production of zeolites. Furthermore, despite the use of MOFs would currently be uneconomic, the demand for these materials is increasing at pace, and their market is expected to be worth 410 million USD by 2024 [196]. This indicates that the price of MOFs could decrease as fast as it has happened for example in the case of televisions or mobile phones.

As far as the process is concerned, it was assumed that the MOF would be used in a composite configuration with recycled carbon fibre to form a bed. This research has developed the composite as an innovative solution to use ZIF-67 on a larger scale. In fact, it would be uneconomic to filter out the fine particles, but it was positively demonstrated in Section 6.2.1 that the MOF can easily form a dense structure with oxidised carbon fibres.

The adsorption process would be applied as a polishing treatment to reduce the NH_4-N concentration to a conservative limit of 1 mg L^{-1}. The analysis was directed for a small WWT plant that would serve 2,000 PE, with a flow rate of 1200 m^3 day^{-1} [190]. The flow rate was determined by assuming the rate of a full flow treatment (FFT), which is the maximum rate of flow that WWT works can accept for settlement and biological treatment. This value was set as triple the dry weather flow (200 L $head^{-1}$ day^{-1}). The concentration of the influent was assumed 5 mg L^{-1}. To achieve 1 mg L^{-1} in the outlet would correspond to an 80 % removal efficiency. As it was observed in Section 6.2.2, ZIF-67 would require a temperature of 35 °C and conservatively 60 minutes contact time to reach 90 % of its equilibrium adsorption capacity (Section 5.2.1). This parameter is called Empty Bed Contact Time (EBCT) and is the time during which the water is in contact with the medium. The volume of ZIF-67 needed was calculated according to the literature following the equation below [197]:

$$Media\ [m^3] = Flow\ rate\ [m^3\ h^{-1}] \times EBCT\ [h] \quad \text{(Eq. 29)}$$

A summary of the principal design parameters is reported in Table 14.

Table 14: *Design parameters for the adsorption column with ZIF-67 and MesoLite*

Parameter		**Notes**		**Notes**
Media	ZIF-67	This work	MesoLite	[190]
Media cost [£ kg^{-1}]	2500	[192]	1.93	Alibaba
Plant size [PE]	2000	Assumed	2000	Assumed
Flow rate [m^3 day^{-1}]	1200	Assumed	1200	Assumed
Q_{max} [g kg^{-1}]	11.16	This work	51	[188]
C_0 [mg L^{-1}]	5	Assumed	5	Assumed
C_e [mg L^{-1}]	1	Assumed	1	Assumed
Contact time [min]	60	Experiment	15	Experiment
Media [m^3]	50	Calculated	12.5	Calculated
Life of the media	50	Assumed	50	Assumed

From Eq. 29 the volume of ZIF-67 needed was indeed calculated from the flow rate 50 m^3 h^{-1} (converted from 1200 m^3 day^{-1}), multiplied by the contact time (60 minutes, thus one hour). In the same way, 12.5 m^3 were calculated for MesoLite. The quantity required of ZIF-67 was

calculated from the EBCT, the flow rate Q and the adsorbent loading ($\rho_{ZIF\text{-}67}$). From the batch tests, the optimal ZIF-67 loading was determined to be 5 g L^{-1} of NH_4-N solution (Section 5.2.2) and was used for the following calculation:

$$Mass\ of\ ZIF-67\ in\ the\ bed\ [g] = Flow\ rate\ [L\ h^{-1}] \times EBCT\ [h] \times \rho_{ZIF-67}[g\ L^{-1}] = \\ = 50{,}000\ L\ h^{-1} \times 1\ h \times 5\ gL^{-1} = 250{,}000\ g = 250\ kg \quad \text{(Eq. 30)}$$

The usage rate of ZIF-67 could be calculated by using the information provided by the Freundlich parameters K_f and n identified from the batch experiments (K_f= 1.125 and n = 0.313, Section 6.2.4) which define q_e (the adsorbate phase concentration at equilibrium in mg of adsorbate per g of adsorbent):

$$Usage\ rate\ [g\ L^{-1}] = \frac{C_0 - C_e}{q_e} = \frac{C_0 - C_e}{K_f {C_e}^n} = 3.55\ g\ L^{-1} \quad \text{(Eq. 31)}$$

If we divide the mass of ZIF-67 by the usage rate it is possible to calculate the volume of water treated:

$$Volume\ of\ water\ treated\ [L] = \frac{Mass\ of\ ZIF-67\ [g]}{Usage\ rate\ [g\ L^{-1}]} = \frac{250{,}000\ g}{3.55\ g\ L^{-1}} 70{,}422\ L \quad \text{(Eq. 32)}$$

Finally, the bed life in days is derived by dividing the volume of water treated within the defined EBCT by the daily flow rate, as below:

$$Bed\ life\ [days] = \frac{Volume\ of\ water\ treated\ [L]}{Flow\ rate\ [L\ d^{-1}]} = 0.06\ days \quad \text{(Eq. 33)}$$

The result is very low, indicating that the media would need to be changed multiple times within the day. However, this is a starting point which enables us to understand the current baseline with respect to the batch tests and the capacity of the media at its early stage in the research. The following calculations assume that the ZIF-67 could be used for 50 cycles as MesoLite to understand the impact of the other variables.

Given the limited amount of data available for ZIF-67, the approach taken to estimate the costs was similar to the one proposed by Kumar *et al.* [198]. The chemical cost of adsorption, which does not consider the capital cost of the equipment, can be expressed as:

$$Cost\ [£\ g^{-1}NH_4 - N] = \frac{x+ny}{n+1} \quad \text{(Eq. 34)}$$

Where x is the cost of one adsorption cycle measured in £ g^{-1} of NH_4-N, y is the cost of the regeneration cycle (£ g^{-1} of NH_4-N) and n is the number of regeneration cycles before replacing the media. The function x can be defined as:

$$x = \frac{x_1}{x_2} \quad \text{(Eq. 35)}$$

With x_1 being the cost of the adsorbent (£ kg^{-1}) and x_2 is the adsorption capacity (g NH_4-N kg^{-1}). A simulation of the cost was run using Eq. 35. It was assumed an adsorption capacity of 51 mg g^{-1} for MesoLite and 11.14 for ZIF-67, as result of the isotherm study (Section 6.2.4). If the cost of ZIF-67 remained 2500 £ kg^{-1}, an increase in the adsorption capacity would not be sufficient to compete with the overall cost of MesoLite, which is 0.038 £ g^{-1} of NH_4-N adsorbed (Figure 44, left).

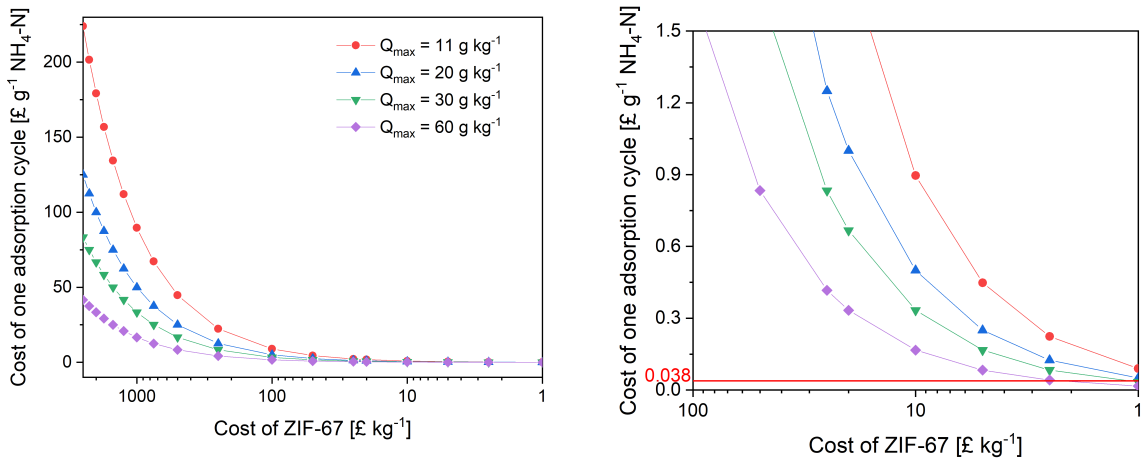

***Figure 44**: Cost of one adsorption cycle with respect to the cost of ZIF-67 at different Q_{max}* (left); the same graph zoomed in the area of interest (right)

From the graph, it emerges how ZIF-67 would become competitive if the price of the media decreased to below £ 5 kg^{-1}. If Q_{max} increased to 20 g kg^{-1}, the price of ZIF-67 should drop to £ 1 kg^{-1} to result in an overall cost equal to the one of MesoLite (red horizontal line in Figure 44, right). Moreover, ZIF-67 would be competitive if the adsorption capacity improved to 30 or 60 mg g^{-1} also at £ 2.5 kg^{-1}. It is important to note that these estimates are conservative, as the overall price of MesoLite does not include the cost of the required pre-treatment with sodium chloride, which would be avoided if using ZIF-67.

With regard to the regeneration, the regeneration cost function y can be split as:

$$y = \frac{(y_1 + y_2)}{x_2} \quad \text{(Eq. 36)}$$

Where y_1 is equal to cost of desorption of one cycle (£ kg of media^{-1} cycle^{-1}), y_2 is the cost of NH_4-N recovery (£ kg of media^{-1} cycle^{-1}). In this study, it is assumed that the cost of the recovery process with sulfuric acid solution (y_2) was the same for ZIF-67 and MesoLite. As far as the regeneration process is concerned, it was assumed that the spent ZIF-67 would be regenerated thermally at 150 °C for 2 hours, as mentioned previously. The value of energy was calculated as the integral of the DSC curve of a ZIF-67 sample after adsorption (Appendix C, Figure C 1) up to 150 °C and was determined as 33.55 kJ kg^{-1}. This value is equal to 0.009 kWh kg^{-1}. Considering that the cost of electricity is assumed as 10 p kWh^{-1} (data provided by Severn Trent), the total energy required per kg of ZIF-67 can be calculated as:

$$Regeneration\ cost_{ZIF-67}\ [£\ kg^{-1}] = 0.009\frac{kWh}{kg} \times £\ 0.1\ kWh^{-1} = £\ 0.0009\ kg^{-1}cycle^{-1}$$
$$= £\ 0.9\ tonne^{-1}cycle^{-1} \quad \text{(Eq. 37)}$$

In case of regeneration of the spent MesoLite, a solution NaCl and NaOH was used, which resulted in a total annual operating cost of £ 66,000 if the brine solution is not reused. The cost dropped to £ 32,000 when the solution was utilised three times [190]. Those values can be converted to the cost per kg of media as below:

$$Regeneration\ cost_{MesoLite}\ [£\ kg^{-1}] = \frac{£66{,}000\ year}{365.25\ day/year} \times \frac{1}{12500\ kg\ day^{-1} \times 49\ cycles}$$
$$= £\ 0.00029\ kg^{-1}cycle^{-1} = £\ 0.29\ tonne^{-1}cycle^{-1} \quad \text{(Eq. 38)}$$

The value decreases to £ 0.14 tonne^{-1} cycle^{-1} if the brine is recycled three times. Thus, the function y expressed in Eq. 36 can be derived by dividing these values by the adsorption capacity. Then the function y can be inserted in Eq. 34 to calculate the overall cost. For this calculation, it was assumed that the adsorption capacity remained the same throughout the number of cycles.

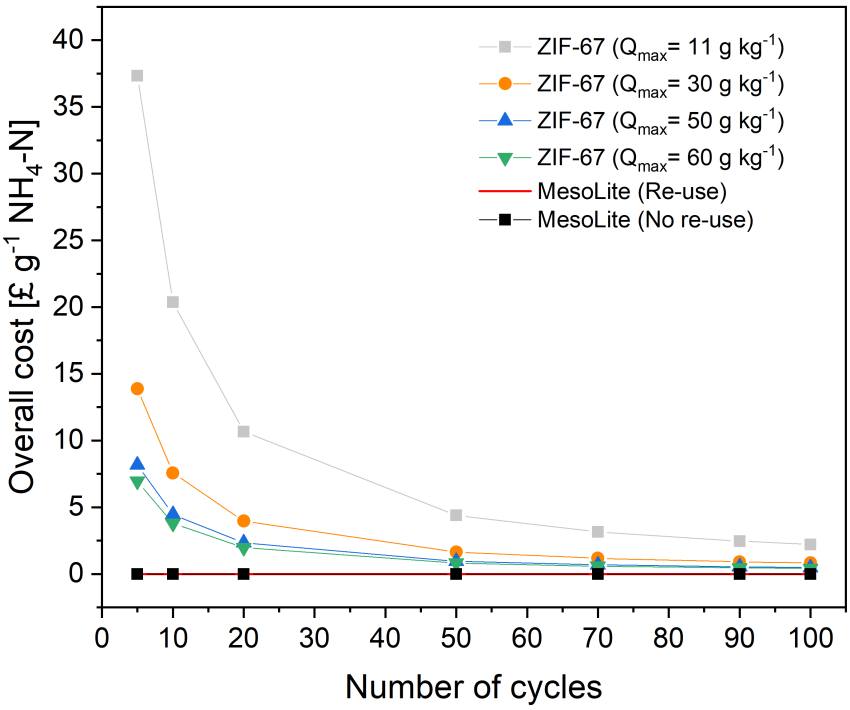

***Figure 45**: Overall cost of the adsorption technology expressed in £ g^{-1} of ZIF-67 at different Q_{max} and MesoLite with respect to the number of regeneration cycles. The cost of the media is £ 2500 kg^{-1} for ZIF-67 and 1.93 £ kg^{-1} for MesoLite*

The overall cost of MesoLite with and without the reuse of chemicals for the regeneration was sensibly lower compared to the cost of the technology with ZIF-67 (Figure 45). However, if the adsorption capacity improved to 30 g kg^{-1} the MOF would become more competitive with an overall cost below £ 2.5 g^{-1} of NH_4-N and 50 regeneration cycles. It is important to note that of the overall cost, 99.9 % is attributed to the adsorption step and therefore the cost of the media. Thus, Figure 46 shows the impact of the cost of ZIF-67 on the total cost of the technology.

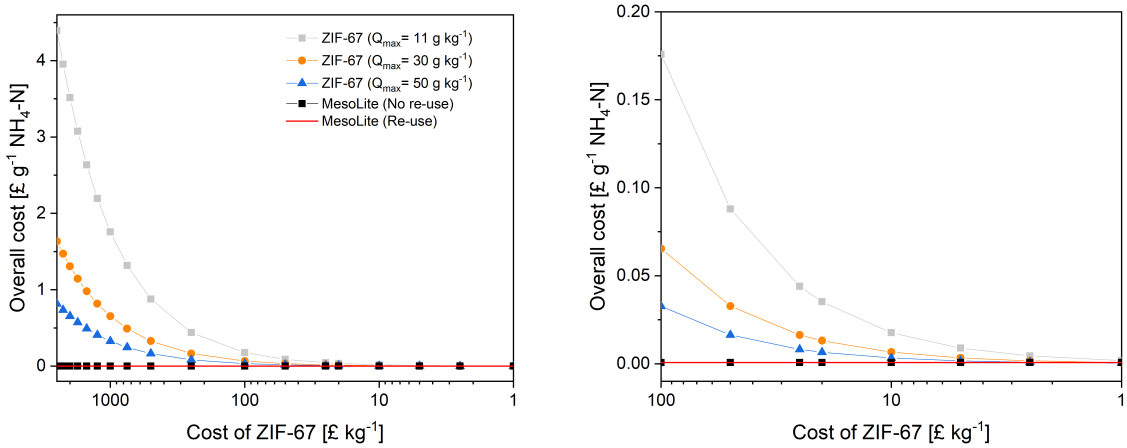

***Figure 46**: Impact of the cost of ZIF-67 and Q_{max} on the overall cost (left) with 50 regeneration cycles;* the same graph zoomed in the area of interest (right)

Interestingly, the overall cost is greatly reduced to below £ 0.2 g^{-1} when the price of ZIF-67 becomes £ 100 kg. Moreover, if ZIF-67 had the same adsorption capacity of MesoLite (51 g kg^{-1}) the overall cost equal to the one of the zeolite would be reached when the ZIF-67 was worth £ 5 kg^{-1} (Figure 46, right). From an environmental point of view, the energy used to regenerate ZIF-67 could be provided by renewable sources and would avoid the use of brine, making it a more sustainable option.

These preliminary considerations are only an estimation of the order of magnitude of the costs involved in the use of ZIF-67 in comparison with MesoLite. Ultimately, this data provided insights into the differences and potential advantages of the ZIF-67 adsorption process. To make this process viable and competitive, both the cost of the media and the adsorption capacity will need to be improved. Nevertheless, the initial estimates show promising trends, which will be key for future development.

8 Research challenges and recommendations

This research has looked at two different ammonia recovery technologies: chemical precipitation and adsorption. Chemical precipitation is a widespread and consolidated technique also on industrial scale, applied in nutrients-rich streams. The challenges regarding this process involved the use of magnesium chloride ($MgCl_2$) needed for the precipitation and the low quality of the solid product, struvite, which could be sold as slow release fertiliser. This research provided new insight and potential solutions to these challenges by looking at thermally decomposing struvite and recover more valuable products (e.g. ammonia solution). During this study, the decomposition reactions were identified, and the energy required for each step was found. The temperature of the decomposition of struvite to magnesium hydrogen phosphate ($MgHPO_4$) still remains a challenge for WWT industry. In fact, it was found from the thermal analysis that the temperature must be up to 250 °C to perform the first reaction. However, the energy needed for the first reaction was found to be 5 % of the total energy requirement for a plant that serves 800,000 PE and that generates 1000 kg of struvite per day. This study proposed a first stage decomposition at 75 °C to evaporate most of the water, followed by a second step at 250 °C to complete the first reaction and recover all the ammonia. The recovery would then be completed with a condensation step. However, this conceptual design is only a preliminary process-flow, created based on the results of this study.

Future research should look more in details into the design of the thermal decomposition technology by considering this new knowledge, especially with regard to the kinetics. This work proved that the first reaction is characterised by a diffusion mechanism. This means that the reaction could be facilitated by agitation. Thus, a stirred-tank reactor would be preferred for this stage. Furthermore, $MgHPO_4$ could be reused in the feed for multiple cycles to reduce the use of $MgCl_2$. However, it would be important to assess the effectiveness of $MgHPO_4$ on industrial scale to identify the optimal number of cycles in which $MgHPO_4$ can be reused, before being recovered

from the system. Thus, future research should focus on a pilot-scale study to assess how these parameters influence the design of the technology.

As far as the adsorption process is concerned, this project looked at uncovering new possible materials that could be used as an alternative to conventional adsorbents, such as zeolites. This work demonstrated for the first time the potential of Metal-Organic Frameworks (MOFs) in the adsorption of ammonium nitrogen (NH_4-N) from wastewater. Several highly water-stable MOFs were tested. The screening test highlighted how challenging it is to find a suitable adsorbent. In particular, high surface area and water stability are not enough to guarantee the capture of NH_4-N. From this screening it was understood that there has to be chemical interaction with the guest specie to compete with the water molecules and trap the adsorbate in the pores. In this study it was demonstrated the effective NH_4-N uptake of ZIF-67, a MOF which has a zeolitic-like structure with a cobalt cluster and methylimidazolate linkers. This MOF could successfully capture NH_4-N in various conditions of pH, adsorbent loading, temperature, initial NH_4-N concentrations. This study provided a proof of concept that this material could be considered in the future as an alternative material for this application. However, research is at an early stage and future studies should focus for example on understanding the behaviour of ZIF-67 in more realistic conditions (e.g. presence of competing cations or other contaminants). It is important indeed to mention that the results obtained in this research are based on tests carried out in ammonia solution and future studies should analyse the MOF behaviour in synthetic and real wastewater. In this research project ZIF-67 was positively synthesised for the first time in a composite configuration with oxidised recycled carbon fibres. This configuration did not affect the capacity to adsorb NH_4-N, and actually improved the capacity of the corresponding ZIF-67 synthesised in the lab. This composite provides the advantage of overcoming the limitation of nanoscale particles that would be an issue in industry. Thus, research should investigate this composite, which could facilitate the scalability of this material to industrial scale. Lastly, future work should regard thorough investigation of the reusability of the material, to also allow for a more detailed cost/benefits analysis. The cost analysis was conducted with data collected in this research at laboratory scale,

in addition to data and assumptions from the literature to the best of the author's knowledge. Therefore, the accuracy of the cost analysis was limited by data availability and the number of assumptions used for the calculations. Data obtained at a larger scale of implementation would help to develop a more accurate picture for the technology.

9 Conclusions

This research had the principal aim of providing new knowledge to develop more sustainable solutions for the recovery of ammonia from wastewater. To do so, the chemical precipitation and adsorption technology were studied during the EngD.

The optimisation of the chemical precipitation technology involved the thermal decomposition in the solid state of the precipitate, struvite. Struvite deposits together with heavy metals which lower its economic value. In addition to this, magnesium chloride has to be dosed to allow the precipitation. Moreover, high levels of ammonium are left in the stream due to the limiting reagent (phosphate ion). The objectives of this research involved the assessment of struvite thermal decomposition as an option to recover more valuable products whilst recycling the magnesium source, thus reducing the operating costs of struvite precipitation. The study involved the characterisation of the decomposition products; the identification of the decomposition mechanism and of the energy required for the process; the assessment of the reusability of struvite calcination products to reduce the use of magnesium.

This innovation report highlights that it is possible to thermally decompose struvite and recover ammonia and water in vapour form (objective A.1). Interestingly, 42 % out of the total mass loss (54.5 %) can be evaporated by heating struvite at 75 °C. Elemental analysis revealed that nitrogen (2.5 % of the sample) remains in the solid at that temperature, whilst a temperature of at least 250 °C is needed to evaporate all the ammonia. The thermal analysis on struvite, combined with a kinetic study also accomplished objective A.2 by revealing the presence of a two-step decomposition process. The two-step thermal degradation proposed in this study is the following:

$$MgNH_4PO_4 \cdot 6H_2O_{(s)} \rightarrow MgHPO_{4\,(s)} + NH_{3(g)} \uparrow + 6H_2O_{(g)} \uparrow$$

$$2MgHPO_{4\,(g)} \rightarrow Mg_2P_2O_{7(s)} + H_2O_{(g)} \uparrow$$

The energy required for both steps was identified, and the kinetics of the first reaction was found to be controlled by diffusion. From an industrial point of view, a diffusion-controlled

reaction means that the decomposition can be sped up under agitation. This information is important from a design point of view, thus it helped fulfilling objective A.3.

The first reaction transforms struvite into magnesium hydrogen phosphate ($MgHPO_4$) and is completed at circa 250 °C. This step was considered for a conceptual design of the struvite decomposition technology, since the product of the second reaction, magnesium pyrophosphate ($Mg_2P_2O_7$), is insoluble in water and could hardly be reused to recover more ammonia. This Innovation Report highlights how the energy required for the first reaction would be 5 % of the total energy required for a WWT plant serving 800,000 PE and producing 1 tonne of struvite per day. Thus, a preliminary design of the technology was suggested (objective A.3), which would use low-grade heat as a first step to evaporate most of the water and small part of the ammonia at 75 °C. Afterwards, a second heating unit would bring the compound up to 250 °C to complete the transformation to $MgHPO_4$. Highly pure ammonia solution could be recovered, whilst $MgHPO_4$ could be reused for several times to reduce the use of magnesium chloride needed for the struvite precipitation. Moreover, this would result in the recovery of larger amounts of ammonium, which is usually left in the stream due to the limiting concentration of phosphate ions.

The research which regarded the adsorption technology focused particularly on the adsorbent media. The main research question was: what new materials could potentially be applied for the adsorption of ammonium? This project investigated the potential of a new class of porous nanomaterials, Metal-Organic Frameworks (MOFs), which had only been tested for the recovery of ammonia in gaseous form. This study had the principal aim of understanding their ability to capture NH_4-N and define the characteristics of these MOFs that enhance the adsorption towards ammonium and ammonia. Several water-stable MOFs were tested with a batch screening experiment carried out in fixed conditions in ammonia solution. Their performance was evaluated with characterisation tests on the structure before and after adsorption (objective B.1). From this test one MOF in particular, ZIF-67, emerged as the most suitable for this application, capturing 40 % of ammonium present in solution. The uptake was

lower but still comparable with the conventional natural zeolite clinoptilolite, which reached 48 % removal efficiency in six hours (objective B.2). Interestingly, ZIF-67 has the same structure of ZIF-8(Zn), which gave an unstable behaviour and did not remove any ammonium. The only difference lies in the metal cluster, which for ZIF-67 is constituted by cobalt. The same consideration could be done for CPO-27(Zn) and CPO-27(Ni). The nickel-based CPO-27 achieved better removal performance compared to CPO-27(Zn), which had an unstable behaviour in the solution. This led to the conclusion that the metal cluster has a key role in enhancing the chemical interactions towards ammonium and retaining the contaminant in the structure. The project then posed the attention on ZIF-67, which was investigated with more detailed tests. The effectiveness of this material for this application was assessed for the first time to the best of the author's knowledge. This research has proven that ZIF-67 can effectively uptake ammonium in different conditions of initial pH, initial ammonium concentration, adsorbent loading and temperature. The structure was retained in most cases and the optimal range of conditions was evaluated. The optimal adsorbent loading was found to be at 5 g of ZIF-67 L^{-1}, before the adsorption capacity drops considerably at higher loadings. At room temperature, it emerged that 56 % removal efficiency could be achieved when the ammonium was 25 mg L^{-1}, average value found in wastewater mainstreams. Interestingly, this performance increased to an average of 85 % removal at 35 °C, taking the NH_4-N below a conservative discharge limit of 5 mg L^{-1}. This would make the MOF suitable for a polishing treatment, to remove residual ammonium before the clean effluent is discharged.

Lastly, the kinetics of the adsorption process with ZIF-67 were investigated, by using the pseudo-first order and pseudo-second order kinetic models. The experimental data fitted well the pseudo-second order model. This indicated that, that chemisorption is the mechanism governing the process, as for zeolites. This means that the uptake of ammonium depends on the number of active sites, and on the exchange of electrons between ZIF-67 and the guest specie.

In this work, ZIF-67 was successfully synthesised in a composite configuration with oxidised recycled carbon fibres. This configuration will help to overcome the challenge in the industrial use of this nanomaterial. In fact, it would avoid the need for ultrafiltration, which would greatly lower the operating cost.

A preliminary economic evaluation was carried out by comparing the use of ZIF-67 with the conventional MesoLite. Currently, the price of ZIF-67 is uneconomic (£ 2500 kg^{-1}) compared to zeolites because its industrial scale production has only recently reached the market. However, the demand for these innovative materials is rising; thus, it is reasonable to think the cost will lower in future years, as it has been the case for other innovations (e.g. televisions or mobile phones). This work revealed that the cost needs to drop to below £ 5 kg^{-1} for ZIF-67 to be competitive. Another important parameter that influences the industrial applicability is the adsorption capacity. In this study, it was found that the adsorption capacity of the MOF has to be improved to 30 mg g^{-1} and the cost of the media should decrease to £ 5 kg^{-1} for this process to be viable. However, as opposed to MesoLite, ZIF-67 would not require the use of chemicals for the regeneration but could release gaseous ammonia and be reactivated thermally. Moreover, the energy to reactivate the MOF could come from renewable sources, further reducing the environmental impact of the technology. Currently, the cost of the media represents 99.9 % of the overall cost of the process, which considered adsorption and desorption costs. To the author's knowledge, this was the first study regarding the use of ZIF-67 for the capture of ammonium in the liquid phase, which positively established the potential of this material for this application.

References

[1] A. Zouboulis, A. Tolkou, Effect of Climate Change in Wastewater Treatment Plants: Reviewing the Problems and Solutions, in: S. Shrestha, A.K. Anal, P.A. Salam, M. van der Valk (Eds.), Manag. Water Resour. under Clim. Uncertain. Examples from Asia, Eur. Lat. Am. Aust., Springer International Publishing, 2015: pp. 197–220.

[2] The United Nations Department of Economic and Social Affairs, Sustainable Development Goal 6, Sustain. Dev. Knowl. Platf. (2019). https://www.un.org/sustainabledevelopment/water-and-sanitation/ (accessed November 15, 2019).

[3] Foresight, The Future Of Manufacturing: a new era of opportunity and challenge for the UK, London, 2013.

[4] S. Fields, Global Nitrogen: Cycling out of control, Environ. Health Perspect. 112 (2004) 556–563. doi:10.1289/ehp.112-a556.

[5] A. Vieira, C.F. Galinha, A. Oehmen, G. Carvalho, The link between nitrous oxide emissions, microbial community profile and function from three full-scale WWTPs, Sci. Total Environ. 651 (2019) 2460–2472. doi:10.1016/j.scitotenv.2018.10.132.

[6] Y. Law, L. Ye, Y. Pan, Z. Yuan, Nitrous oxide emissions from wastewater treatment processes, Philos. Trans. R. Soc. B Biol. Sci. 367 (2012) 1265–1277. doi:10.1098/rstb.2011.0317.

[7] M. Appl, Complete Ammonia Production Plants, in: Ammon. Princ. Ind. Pract., Wiley, 1999: pp. 177–204. http://onlinelibrary.wiley.com/book/10.1002/9783527613885.

[8] S. Matassa, D.J. Batstone, T. Hülsen, J. Schnoor, W. Verstraete, Can direct conversion of used nitrogen to new feed and protein help feed the world?, Environ. Sci. Technol. 49 (2015) 5247–5254. doi:10.1021/es505432w.

[9] J.W. Erisman, M. a. Sutton, J. Galloway, Z. Klimont, W. Winiwarter, How a century of ammonia synthesis changed the world, Nat. Geosci. 1 (2008) 636–639.

doi:10.1038/ngeo325.

[10] G. Schnitkey, Nitrogen Prices, Rates Cuts, and 2018 Fertilizer Costs., Farmdoc Dly. (8)58. (2018).

[11] Metcalf & Eddie, Wastewater Characteristics, in: Wastewater Eng. - Treat. Resour. Recover., Fifth Edit, McGraw-Hill Education, 2014: pp. 59–180.

[12] C.M. Mehta, W.O. Khunjar, V. Nguyen, S. Tait, D.J. Batstone, Technologies to recover nutrients from waste streams: A critical review, Crit. Rev. Environ. Sci. Technol. 45 (2015) 385–427. doi:10.1080/10643389.2013.866621.

[13] D.. Hand, Q. Zhang, J.. Mihelcic, Water Treatment, in: Environ. Eng., John Wiley & Sons, 2010: pp. 397–458.

[14] Metcalf & Eddie, Fundamentals of Biological Treatment, in: Wastewater Eng. - Treat. Resour. Recover., Fifth Edit, McGraw-Hill Education, 2014: pp. 615–647.

[15] European Commission, Nitrogen Pollution and the European Environment: Implications for Air Quality Policy, Bristol, 2013.

[16] EEC Council, 91/271/EEC of 21 May 1991 concerning urban waste-water treatment, 1991. doi:http://eur-lex.europa.eu/legal-content/en/ALL/?uri=CELEX:31991L0271.

[17] European Parliament, Directive 2000/60/EC of the European Parliament and of the Council of 23 October 2000, 2000.

[18] J. Lear, Bacteria to help meet the ammonia wastewater challenge, WWTonline. (2017). https://wwtonline.co.uk/Blog/bacteria-to-help-meet-the-ammonia-wastewater-challenge (accessed October 20, 2019).

[19] M.K. Winkler, L. Straka, New directions in biological nitrogen removal and recovery from wastewater, Curr. Opin. Biotechnol. 57 (2019) 50–55. doi:10.1016/j.copbio.2018.12.007.

[20] L. Miao, G. Yang, T. Tao, Y. Peng, Recent advances in nitrogen removal from landfill leachate using biological treatments – A review, J. Environ. Manage. 235 (2019) 178–185. doi:10.1016/j.jenvman.2019.01.057.

[21] J. Huang, C. Shang, Air Stripping, in: L.K. Wang, Y.-T. Hung, N.K. Shammas (Eds.), Adv. Physicochem. Treat. Process., The Humana Press Inc., Totowa, NJ, 2007: pp. 47–79. doi:10.1016/S0166-1116(08)70529-6.

[22] S. Gustin, R. Marinsek-Logar, Effect of pH, temperature and air flow rate on the continuous ammonia stripping of the anaerobic digestion effluent, Process Saf. Environ. Prot. 89 (2011) 61–66. doi:10.1016/j.psep.2010.11.001.

[23] L. Kinidi, I.A.W. Tan, N.B. Abdul Wahab, K.F. Bin Tamrin, C.N. Hipolito, S.F. Salleh, Recent Development in Ammonia Stripping Process for Industrial Wastewater Treatment, Int. J. Chem. Eng. 2018 (2018). doi:10.1155/2018/3181087.

[24] M. Rezakazemi, S. Shirazian, S.N. Ashrafizadeh, Simulation of ammonia removal from industrial wastewater streams by means of a hollow-fiber membrane contactor, Desalination. 285 (2012) 383–392. doi:10.1016/j.desal.2011.10.030.

[25] S.N. Ashrafizadeh, Z. Khorasani, Ammonia removal from aqueous solutions using hollow-fiber membrane contactors, Chem. Eng. J. 162 (2010) 242–249. doi:10.1016/j.cej.2010.05.036.

[26] M. Darestani, V. Haigh, S.J. Couperthwaite, G.J. Millar, L.D. Nghiem, Hollow fibre membrane contactors for ammonia recovery: Current status and future developments, J. Environ. Chem. Eng. 5 (2017) 1349–1359. doi:10.1016/j.jece.2017.02.016.

[27] I. Sancho, E. Licon, C. Valderrama, N. de Arespacochaga, S. López-Palau, J.L. Cortina, Recovery of ammonia from domestic wastewater effluents as liquid fertilizers by integration of natural zeolites and hollow fibre membrane contactors, Sci. Total Environ. 584–585 (2017) 244–251. doi:10.1016/j.scitotenv.2017.01.123.

[28] J. Lubensky, M. Ellersdorfer, K. Stocker, Ammonium recovery from model solutions and sludge liquor with a combined ion exchange and air stripping process, J. Water Process Eng. 32 (2019) 100909. doi:10.1016/j.jwpe.2019.100909.

[29] T. Cai, S.Y. Park, Y. Li, Nutrient recovery from wastewater streams by microalgae: Status and prospects, Renew. Sustain. Energy Rev. 19 (2013) 360–369.

doi:10.1016/j.rser.2012.11.030.

[30] J. Shi, B. Podola, M. Melkonian, Removal of nitrogen and phosphorus from wastewater using microalgae immobilized on twin layers: An experimental study, J. Appl. Phycol. 19 (2007) 417–423. doi:10.1007/s10811-006-9148-1.

[31] L. de S. Leite, M.T. Hoffmann, L.A. Daniel, Microalgae cultivation for municipal and piggery wastewater treatment in Brazil, J. Water Process Eng. 31 (2019) 1–7. doi:10.1016/j.jwpe.2019.100821.

[32] I.H. Chang, D. Jung, T.S. Ahn, Improving the effectiveness of a nutrient removal system composed of Microalgae and Daphnia by an artificial illumination, Sustain. 6 (2014) 1346–1358. doi:10.3390/su6031346.

[33] P. Kuntke, P. Zamora, M. Saakes, C.J.N. Buisman, H.V.M. Hamelers, Gas-permeable hydrophobic tubular membranes for ammonia recovery in bio-electrochemical systems, Environ. Sci. Water Res. Technol. 2 (2016) 261–265. doi:10.1039/C5EW00299K.

[34] Y. Ye, H.H. Ngo, W. Guo, Y. Liu, S.W. Chang, D.D. Nguyen, J. Ren, Y. Liu, X. Zhang, Feasibility study on a double chamber microbial fuel cell for nutrient recovery from municipal wastewater, Chem. Eng. J. 358 (2019) 236–242. doi:10.1016/j.cej.2018.09.215.

[35] P. Zamora, T. Georgieva, A. Ter Heijne, T.H.J.A. Sleutels, A.W. Jeremiasse, M. Saakes, C.J.N. Buisman, P. Kuntke, Ammonia recovery from urine in a scaled-up Microbial Electrolysis Cell, J. Power Sources. 356 (2017) 491–499. doi:10.1016/j.jpowsour.2017.02.089.

[36] M. Rodríguez Arredondo, P. Kuntke, A.W. Jeremiasse, T.H.J.A. Sleutels, C.J.N. Buisman, A. Ter Heijne, Bioelectrochemical systems for nitrogen removal and recovery from wastewater, Environ. Sci. Water Res. Technol. 1 (2015) 22–33. doi:10.1039/c4ew00066h.

[37] P. Kuntke, T.H.J.A. Sleutels, M. Rodríguez Arredondo, S. Georg, S.G. Barbosa, A. Heijne, (Bio)electrochemical ammonia recovery: progress and perspectives, Appl. Microbiol. Biotechnol. 2 (2018) 3865–3878. doi:https://doi.org/10.1007/s00253-018-8888-6.

[38] K.J. Howe, D.W. Hand, J.C. Crittenden, R. Rhodes Trussel, G. Tchobanoglous, Adsorption

and Ion Exchange, in: Princ. Water Treat., Wiley, 2012: pp. 369–435.

[39] S. Wasielewski, E. Rott, R. Minke, H. Steinmetz, Evaluation of different clinoptilolite zeolites as adsorbent for ammonium removal from highly concentrated synthetic wastewater, Water (Switzerland). 10 (2018) 1–17. doi:10.3390/w10050584.

[40] R. Taddeo, S. Prajapati, R. Lepistö, Optimizing ammonium adsorption on natural zeolite for wastewaters with high loads of ammonium and solids, J. Porous Mater. 24 (2017) 1545–1554. doi:10.1007/s10934-017-0394-1.

[41] A. Alshameri, C. Yan, Y. Al-Ani, A.S. Dawood, A. Ibrahim, C. Zhou, H. Wang, An investigation into the adsorption removal of ammonium by salt activated Chinese (Hulaodu) natural zeolite: Kinetics, isotherms, and thermodynamics, J. Taiwan Inst. Chem. Eng. 45 (2014) 554–564. doi:10.1016/j.jtice.2013.05.008.

[42] F. Mazloomi, M. Jalali, Ammonium removal from aqueous solutions by natural Iranian zeolite in the presence of organic acids, cations and anions, J. Environ. Chem. Eng. 4 (2016) 1664–1673. doi:10.1016/j.jece.2015.11.031.

[43] M. Murkani, M. Nasrollahi, M. Ravanbakhsh, P. Bahrami, N. Jaafarzadeh, Evaluation of natural zeolite clinoptilolite efficiency for the removal of ammonium and nitrate from aquatic solutions, Environ. Heal. Eng. Manag. J. 2 (2015) 17–22.

[44] J.S. Cyrus, G.B. Reddy, Sorption and desorption of ammonium by zeolite: Batch and column studies, J. Environ. Sci. Heal. Part A. 46 (2011) 408–414. doi:10.1080/02773813.2010.542398.

[45] Y. Lin, M. Guo, N. Shah, D.C. Stuckey, Economic and environmental evaluation of nitrogen removal and recovery methods from wastewater, Bioresour. Technol. 215 (2016) 227–238. doi:10.1016/j.biortech.2016.03.064.

[46] J.D. Doyle, S.A. Parsons, Struvite formation, control and recovery, Water Res. 36 (2002) 3925–3940. doi:10.1016/S0043-1354(02)00126-4.

[47] L. Pastor, D. Mangin, J. Ferrer, A. Seco, Struvite formation from the supernatants of an anaerobic digestion pilot plant, Bioresour. Technol. 101 (2010) 118–125.

doi:10.1016/j.biortech.2009.08.002.

[48] M. V. Ramlogan, A.A. Rouff, An investigation of the thermal behavior of magnesium ammonium phosphate hexahydrate, J. Therm. Anal. Calorim. 123 (2016) 145–152. doi:10.1007/s10973-015-4860-1.

[49] J.P. van der Hoek, R. Duijff, O. Reinstra, Nitrogen recovery from wastewater: Possibilities, competition with other resources, and adaptation pathways, Sustain. 10 (2018). doi:10.3390/su10124605.

[50] P. Šimon, Isoconversional methods: Fundamentals, meaning and application, J. Therm. Anal. Calorim. 76 (2004) 123–132. doi:10.1023/B:JTAN.0000027811.80036.6c.

[51] C.H. Bamford, C.F.H. Tipper, Theory of solid state reaction kinetics, in: C.H. Bamford, C.F.H. Tipper (Eds.), Compr. Chem. Kinet. Vol. 22, React. Solid State, Elsevier, Amsterdam; Oxford; New York, 1980: pp. 41–113.

[52] A.K. Burnham, Introduction to Chemical Kinetics, in: Glob. Chem. Kinet. Foss. Fuels How to Model Matur. Pyrolysis, 2017: pp. 25–74. doi:10.1007/978-3-319-49634-4.

[53] S. Vyazovkin, C.A. Wight, Model-free and model-fitting approaches to kinetic analysis of isothermal and nonisothermal data, Thermochim. Acta. 340–341 (1999) 53–68. doi:10.1016/S0040-6031(99)00253-1.

[54] M.E. Brown, D. Dollimore, A. Galwey, Reactions in the solid state. Comprehensive Chemical Kinetics, 1980. doi:10.1016/S0167-6881(99)80004-4.

[55] B. Mu, Synthesis and Gas Adsorption Study of Porous Metal-Organic Framework Materials (Ph.D Thesis), Georgia Institute of Technology, Atlanta, 2011.

[56] H. Jasuja, G.W. Peterson, J.B. Decoste, M.A. Browe, K.S. Walton, Evaluation of MOFs for air purification and air quality control applications: Ammonia removal from air, Chem. Eng. Sci. 124 (2015) 118–124. doi:10.1016/j.ces.2014.08.050.

[57] X. Dyosiba, J. Ren, N.M. Musyoka, H.W. Langmi, M. Mathe, M.S. Onyango, Feasibility of Varied Polyethylene Terephthalate Wastes as a Linker Source in Metal–Organic Framework UiO-66(Zr) Synthesis, Ind. Eng. Chem. Res. 58 (2019) 17010–17016.

doi:10.1021/acs.iecr.9b02205.

[58] X. Liu, N.K. Demir, Z. Wu, K. Li, Highly Water-Stable Zirconium Metal-Organic Framework UiO-66 Membranes Supported on Alumina Hollow Fibers for Desalination, J. Am. Chem. Soc. 137 (2015) 6999–7002. doi:10.1021/jacs.5b02276.

[59] Y. Khabzina, J. Dhainaut, M. Ahlhelm, H.J. Richter, H. Reinsch, N. Stock, D. Farrusseng, Synthesis and Shaping Scale-up Study of Functionalized UiO-66 MOF for Ammonia Air Purification Filters, Ind. Eng. Chem. Res. 57 (2018) 8200–8208. doi:10.1021/acs.iecr.8b00808.

[60] J. Li, Y.N. Wu, Z. Li, B. Zhang, M. Zhu, X. Hu, Y. Zhang, F. Li, Zeolitic imidazolate framework-8 with high efficiency in trace arsenate adsorption and removal from water, J. Phys. Chem. C. 118 (2014) 27382–27387. doi:10.1021/jp508381m.

[61] G. Zhong, D. Liu, J. Zhang, The application of ZIF-67 and its derivatives: Adsorption, separation, electrochemistry and catalysts, J. Mater. Chem. A. 6 (2018) 1887–1899. doi:10.1039/c7ta08268a.

[62] M.J. Katz, A.J. Howarth, P.Z. Moghadam, J.B. Decoste, R.Q. Snurr, J.T. Hupp, O.K. Farha, High volumetric uptake of ammonia using Cu-MOF-74/Cu-CPO-27, Dalt. Trans. 45 (2016) 4150–4153. doi:10.1039/x0xx00000x.

[63] S. Hindocha, S. Poulston, Study of the scale-up, formulation, ageing and ammonia adsorption capacity of MIL-100(Fe), Cu-BTC and CPO-27(Ni) for use in respiratory protection filters, Faraday Discuss. 201 (2017) 113–125. doi:10.1039/c7fd00090a.

[64] L. Garzón-Tovar, A. Carné-Sánchez, C. Carbonell, I. Imaz, D. Maspoch, Optimised room temperature, water-based synthesis of CPO-27-M metal-organic frameworks with high space-time yields, J. Mater. Chem. A. 3 (2015) 20819–20826. doi:10.1039/c5ta04923g.

[65] Y. Chen, L. Li, J. Li, K. Ouyang, J. Yang, Ammonia capture and flexible transformation of M-2(INA) (M=Cu, Co, Ni, Cd) series materials, J. Hazard. Mater. 306 (2016) 340–347. doi:10.1016/j.jhazmat.2015.12.046.

[66] E. Borfecchia, S. Maurelli, D. Gianolio, E. Groppo, M. Chiesa, F. Bonino, C. Lamberti,

Insights into adsorption of NH3 on HKUST-1 metal-organic framework: A multitechnique approach, J. Phys. Chem. C. 116 (2012) 19839–19850. doi:10.1021/jp305756k.

[67] Y. Chen, X. Mu, E. Lester, T. Wu, High efficiency synthesis of HKUST-1 under mild conditions with high BET surface area and CO2 uptake capacity, Prog. Nat. Sci. Mater. Int. 28 (2018) 584–589. doi:10.1016/j.pnsc.2018.08.002.

[68] P. Kumar, A. Pournara, K.H. Kim, V. Bansal, S. Rapti, M.J. Manos, Metal-organic frameworks: Challenges and opportunities for ion-exchange/sorption applications, Prog. Mater. Sci. 86 (2017) 25–74. doi:10.1016/j.pmatsci.2017.01.002.

[69] Y. Chen, F. Zhang, Y. Wang, C. Yang, J. Yang, J. Li, Recyclable ammonia uptake of a MIL series of metal-organic frameworks with high structural stability, Microporous Mesoporous Mater. 258 (2018) 170–177. doi:10.1016/j.micromeso.2017.09.013.

[70] S. Moribe, Z. Chen, S. Alayoglu, Z.H. Syed, T. Islamoglu, O.K. Farha, Ammonia Capture within Isoreticular Metal–Organic Frameworks with Rod Secondary Building Units, ACS Mater. Lett. 1 (2019) 476–480. doi:10.1021/acsmaterialslett.9b00307.

[71] M. Sánchez-Sánchez, N. Getachew, K. Díaz, M. Díaz-García, Y. Chebude, I. Díaz, Synthesis of metal–organic frameworks in water at room temperature: salts as linker sources, Green Chem. 17 (2015) 1500–1509. doi:10.1039/C4GC01861C.

[72] J. Yao, M. He, K. Wang, R. Chen, Z. Zhong, H. Wang, High-yield synthesis of zeolitic imidazolate frameworks from stoichiometric metal and ligand precursor aqueous solutions at room temperature, CrystEngComm. 15 (2013) 3601–3606. doi:10.1039/c3ce27093a.

[73] A. Schejn, A. Aboulaich, L. Balan, V. Falk, J. Lalevée, G. Medjahdi, L. Aranda, K. Mozet, R. Schneider, Cu2+-doped zeolitic imidazolate frameworks (ZIF-8): Efficient and stable catalysts for cycloadditions and condensation reactions, Catal. Sci. Technol. 5 (2015) 1829–1839. doi:10.1039/c4cy01505c.

[74] J. Qian, F. Sun, L. Qin, Hydrothermal synthesis of zeolitic imidazolate framework-67 (ZIF-

67) nanocrystals, Mater. Lett. 82 (2012) 220–223. doi:10.1016/j.matlet.2012.05.077.

[75] G. Zhang, S. Sun, D. Yang, J.P. Dodelet, E. Sacher, The surface analytical characterization of carbon fibers functionalized by H2SO4/HNO3 treatment, Carbon N. Y. 46 (2008) 196–205. doi:10.1016/j.carbon.2007.11.002.

[76] M. Zhang, H. Zhang, D. Xu, L. Han, D. Niu, B. Tian, J. Zhang, L. Zhang, W. Wu, Removal of ammonium from aqueous solutions using zeolite synthesized from fly ash by a fusion method, Desalination. 271 (2011) 111–121. doi:10.1016/j.desal.2010.12.021.

[77] Y. Zheng, Y. Xie, A. Wang, Rapid and wide pH-independent ammonium-nitrogen removal using a composite hydrogel with three-dimensional networks, Chem. Eng. J. 179 (2012) 90–98. doi:10.1016/j.cej.2011.10.064.

[78] Y. Zheng, A. Wang, Preparation and ammonium adsorption properties of biotite-based hydrogel composites, Ind. Eng. Chem. Res. 49 (2010) 6034–6041. doi:10.1021/ie9016336.

[79] Merck, Equivalency of Ammonia (Ammonium) Spectroquant ® Test Kits : Ammonia (Ammonium) by Indophenol Reaction and Photometry, (n.d.) 1–36.

[80] S. Lagergeen, Zur theorie der sogenannten adsorption gelöster stoffe, K. Sven. Vetenskapsakademiens. Handl. 24 (1898) 1–39.

[81] Y.S. Ho, Citation review of Lagergren kinetic rate equation on adsorption reactions, Scientometrics. 59 (2004) 171–177. doi:10.1023/B:SCIE.0000013305.99473.cf.

[82] Y.S. Ho, G. McKay, Pseudo-second order model for sorption processes, Process Biochem. 34 (1999) 451–465. doi:10.1016/S0032-9592(98)00112-5.

[83] H. Freundlich, Of the adsorption of gases. Section II. Kinetics and energetics of gas adsorption, Trans. Faraday Soc. 28 (1932) 195–201.

[84] I. Langmuir, The constitution and fundamental properties of solids and liquids, J. Am. Chem. Soc. 38 (1916) 2221–2295.

[85] H.N. Tran, S.J. You, A. Hosseini-Bandegharaei, H.P. Chao, Mistakes and inconsistencies regarding adsorption of contaminants from aqueous solutions: A critical review, Water

Res. 120 (2017) 88–116. doi:10.1016/j.watres.2017.04.014.

[86] A. Zarebska, D. Romero Nieto, K. V Christensen, L. Fjerbæk Søtoft, B. Norddahl, D.R. Nieto, K. V Christensen, L.F. Sotoft, B. Norddahl, Ammonium Fertilizers Production from Manure: A Critical Review, Crit. Rev. Environ. Sci. Technol. 45 (2014) 1469–1521. doi:10.1080/10643389.2014.955630.

[87] M.S. Romero-Güiza, S. Tait, S. Astals, R. del Valle-Zermeño, M. Martínez, J. Mata-Alvarez, J.M. Chimenos, Reagent use efficiency with removal of nitrogen from pig slurry via struvite: A study on magnesium oxide and related by-products, Water Res. 84 (2015) 286–294. doi:10.1016/j.watres.2015.07.043.

[88] J. Borgerding, Phosphate deposits in digestion systems, J. Wastewater Pollut. Control Fed. 44 (1972) 813 – 819.

[89] R.D.B. M. I. H. Bhuiyan, D. S. Mavinic, A Solubility and Thermodynamic Study of Struvite, Environ. Technol. 28 (2007) 1015–1026. doi:10.1080/09593332808618857.

[90] E. V. Munch, K. Barr, Controlled Struvite Crystallisation for Removing Phosphorus From Anaerobic Digestion Sidestreams, Water Res. 35 (2001) 151–159. doi:10.1016/S0043-1354(00)00236-0.

[91] B. Li, I. Boiarkina, W. Yu, H.M. Huang, T. Munir, G.Q. Wang, B.R. Young, Phosphorous recovery through struvite crystallization: Challenges for future design, Sci. Total Environ. 648 (2019) 1244–1256. doi:10.1016/j.scitotenv.2018.07.166.

[92] A. Uysal, Y.D. Yilmazel, G.N. Demirer, The determination of fertilizer quality of the formed struvite from effluent of a sewage sludge anaerobic digester, J. Hazard. Mater. 181 (2010) 248–254. doi:10.1016/j.jhazmat.2010.05.004.

[93] R.L. Frost, M.L. Weier, K.L. Erickson, Thermal decomposition of struvite, J. Therm. Anal. Calorim. 76 (2004) 1025–1033. doi:10.1023/B:JTAN.0000032287.08535.b3.

[94] M.I.H. Bhuiyan, D.S. Mavinic, F. a. Koch, Thermal decomposition of struvite and its phase transition, Chemosphere. 70 (2008) 1347–1356. doi:10.1016/j.chemosphere.2007.09.056.

[95] Y. Chen, J. Tang, W. Li, Z. Zhong, J. Yin, Thermal decomposition of magnesium ammonium phosphate and adsorption properties of its pyrolysis products toward ammonia nitrogen, Trans. Nonferrous Met. Soc. China. 25 (2015) 497–503. doi:10.1016/S1003-6326(15)63630-5.

[96] S. Sugiyama, M. Yokoyama, H. Ishizuka, K.-I. Sotowa, T. Tomida, N. Shigemoto, Removal of aqueous ammonium with magnesium phosphates obtained from the ammonium-elimination of magnesium ammonium phosphate, J. Colloid Interface Sci. 292 (2005) 133–8. doi:10.1016/j.jcis.2005.05.073.

[97] R. Kumar, P. Pal, Turning hazardous waste into value-added products: Production and characterization of struvite from ammoniacal waste with new approaches, J. Clean. Prod. 43 (2013) 59–70. doi:10.1016/j.jclepro.2013.01.001.

[98] S. He, Y. Zhang, M. Yang, W. Du, H. Harada, Repeated use of MAP decomposition residues for the removal of high ammonium concentration from landfill leachate, Chemosphere. 66 (2007) 2233–2238. doi:10.1016/j.chemosphere.2006.09.016.

[99] K.S. Le Corre, E. Valsami-Jones, P. Hobbs, S.A. Parsons, Impact of calcium on struvite crystal size, shape and purity, J. Cryst. Growth. 283 (2005) 514–522. doi:10.1016/j.jcrysgro.2005.06.012.

[100] T. Zhang, L. Ding, H. Ren, Pretreatment of ammonium removal from landfill leachate by chemical precipitation, J. Hazard. Mater. 166 (2009) 911–915. doi:10.1016/j.jhazmat.2008.11.101.

[101] A. Matynia, B. Wierzbowska, N. Hutnik, A. Mazienczuk, A. Kozik, K. Piotrowski, Separation of Struvite from Mineral Fertilizer Industry Wastewater, Procedia Environ. Sci. 18 (2013) 766–775. doi:10.1016/j.proenv.2013.04.103.

[102] M.I. Ali, Struvite Crystallization in Fed-Batch Pilot Scale and Description of Solution Chemistry of Struvite, Chem. Eng. Res. Des. 85 (2007) 344–356. doi:10.1205/cherd06031.

[103] M.M. Rahman, M.A.M. Salleh, U. Rashid, A. Ahsan, M.M. Hossain, C.S. Ra, Production of

slow release crystal fertilizer from wastewaters through struvite crystallization - A review, Arab. J. Chem. 7 (2014) 139–155. doi:10.1016/j.arabjc.2013.10.007.

[104] Ostara Nutrient Recovery Technologies Inc., Turn Problematic Struvite Into Premium, High Value, Market-Ready Fertiliser, 2018. http://ostara.com/wp-content/uploads/2018/04/EU_Ostara_Crystal-Green_Handout.pdf.

[105] European Commission, Regulation (EC) No 2003/2003 of the European Parliament and of the Council of 13 October 2003 relating to fertilisers, 2003.

[106] M.T. Munir, B. Li, I. Boiarkina, S. Baroutian, W. Yu, B.R. Young, Phosphate recovery from hydrothermally treated sewage sludge using struvite precipitation, Bioresour. Technol. 239 (2017) 171–179. doi:10.1016/j.biortech.2017.04.129.

[107] R. Yu, H. Ren, Y. Wang, L. Ding, J. Geng, K. Xu, Y. Zhang, A kinetic study of struvite precipitation recycling technology with NaOH/Mg(OH)2 addition, Bioresour. Technol. 143 (2013) 519–524. doi:10.1016/j.biortech.2013.06.042.

[108] B. Boonchom, Kinetic and thermodynamic studies of MgHPO4 ·3H2O by non-isothermal decomposition data, J. Therm. Anal. Calorim. 98 (2009) 863. doi:10.1007/s10973-009-0108-2.

[109] A. Khawan, R.D. Flanagan, Solid-State kinetic Models: Basic and Mathematical Fundamentals, J.Phys.Chem.B. 110 (2006) 17315–17328. doi:10.1021/jp062746a.

[110] B.E. Poling, G.H. Thomson, D.G. Friend, R.L. Rowley, W.V. Wilding, Physical and Chemical Data, in: D. Green, R. Perry (Eds.), Perry's Chem. Eng. Handb., 8th Editio, 2007: pp. 2–17.

[111] H. Huang, J. Liu, C. Xu, F. Gao, Recycling struvite pyrolysate obtained at negative pressure for ammonia nitrogen removal from landfill leachate, Chem. Eng. J. 284 (2016) 1204–1211. doi:10.1016/j.cej.2015.09.080.

[112] P.S. Liu, G.F. Chen, General Introduction to Porous Materials, in: Porous Mater., First Edit, Elsevier Inc., 2014: pp. 1–20. doi:10.1016/b978-0-12-407788-1.00001-0.

[113] C.N. Vignoli, J.M.C.F. Bahé, M.R.C. Marques, Evaluation of ion exchange resins for removal and recuperation of ammonium-nitrogen generated by the evaporation of landfill

leachate, Polym. Bull. 72 (2015) 3119–3134. doi:10.1007/s00289-015-1456-7.

[114] J. Liu, Y. Su, Q. Li, Q. Yue, B. Gao, Preparation of wheat straw based superabsorbent resins and their applications as adsorbents for ammonium and phosphate removal, Bioresour. Technol. 143 (2013) 32–39. doi:10.1016/j.biortech.2013.05.100.

[115] H. Zhang, A. Li, W. Zhang, C. Shuang, Combination of Na-modified zeolite and anion exchange resin for advanced treatment of a high ammonia-nitrogen content municipal effluent, J. Colloid Interface Sci. 468 (2016) 128–135. doi:10.1016/j.jcis.2015.10.006.

[116] Y. Ding, M. Sartaj, Optimization of ammonia removal by ion-exchange resin using response surface methodology, Int. J. Environ. Sci. Technol. 13 (2016) 985–994. doi:10.1007/s13762-016-0939-x.

[117] N.P.G.N. Chandrasekara, R.M. Pashley, Study of a new process for the efficient regeneration of ion exchange resins, Desalination. 357 (2015) 131–139. doi:10.1016/j.desal.2014.11.024.

[118] T.C. Jorgensen, L.R. Weatherley, Continuous removal of ammonium ion by ion exchange in the presence of organic compounds in packed columns, J. Chem. Technol. Biotechnol. 81 (2006) 1151–1158. doi:10.1002/jctb.1481.

[119] P. Vassileva, D. Voikova, Investigation on natural and pretreated Bulgarian clinoptilolite for ammonium ions removal from aqueous solutions, J. Hazard. Mater. 170 (2009) 948–953. doi:10.1016/j.jhazmat.2009.05.062.

[120] H. Cruz, P. Luckman, T. Seviour, W. Verstraete, B. Laycock, I. Pikaar, Rapid removal of ammonium from domestic wastewater using polymer hydrogels, Sci. Rep. 8 (2018) 1–6. doi:10.1038/s41598-018-21204-4.

[121] R.R. Karri, J.N. Sahu, V. Chimmiri, Critical review of abatement of ammonia from wastewater, J. Mol. Liq. 261 (2018) 21–31. doi:10.1016/j.molliq.2018.03.120.

[122] M. Rubio-Martinez, C. Avci-Camur, A.W. Thornton, I. Imaz, D. Maspoch, M.R. Hill, New synthetic routes towards MOF production at scale, Chem. Soc. Rev. 46 (2017) 3453–3480. doi:10.1039/c7cs00109f.

[123] Y. Chen, S. Li, X. Pei, J. Zhou, X. Feng, S. Zhang, Y. Cheng, H. Li, R. Han, B. Wang, A Solvent-Free Hot-Pressing Method for Preparing Metal-Organic-Framework Coatings, Angew. Chemie - Int. Ed. 55 (2016) 3419–3423. doi:10.1002/anie.201511063.

[124] P.A. Julien, C. Mottillo, T. Friščić, Metal-Organic Frameworks meet scalable and sustainable synthesis, Green Chem. 19 (2017) 2729–2747. doi:10.1039/c7gc01078h.

[125] I. Stassen, N. Campagnol, J. Fransaer, P. Vereecken, D. De Vos, R. Ameloot, Solvent-free synthesis of supported ZIF-8 films and patterns through transformation of deposited zinc oxide precursors, CrystEngComm. 15 (2013) 9308–9311. doi:10.1039/c3ce41025k.

[126] R. Zhang, C.A. Tao, R. Chen, L. Wu, X. Zou, J. Wang, Ultrafast synthesis of Ni-MOF in one minute by ball milling, Nanomaterials. 8 (2018) 1–11. doi:10.3390/NANO8121067.

[127] C.J. Kepert, Metal-Organic Framework Materials, in: D.W. Bruce, D. O'Hare, R.I. Walton (Eds.), Porous Mater., Wiley, 2010: pp. 1–67.

[128] A.J. Rieth, M. Dinca, Controlled Gas Uptake in Metal-Organic Frameworks with Record Ammonia Sorption, J. Am. Chem. Soc. 140 (2018) 3461–3466. doi:10.1021/jacs.8b00313.

[129] K. Vikrant, V. Kumar, K.H. Kim, D. Kukkar, Metal-organic frameworks (MOFs): Potential and challenges for capture and abatement of ammonia, J. Mater. Chem. A. 5 (2017) 22877–22896. doi:10.1039/c7ta07847a.

[130] A.J. Rieth, Y. Tulchinsky, M. Dinca, High and Reversible Ammonia Uptake in Mesoporous Azolate Metal-Organic Frameworks with Open Mn, Co, and Ni Sites, J. Am. Chem. Soc. 138 (2016) 9401–9404. doi:10.1021/jacs.6b05723.

[131] Y. Chen, Y. Wang, C. Yang, S. Wang, J. Yang, J. Li, Antenna-Protected Metal-Organic Squares for Water/Ammonia Uptake with Excellent Stability and Regenerability, ACS Sustain. Chem. Eng. 5 (2017) 5082–5089. doi:10.1021/acssuschemeng.7b00460.

[132] T.J. Bandosz, C. Petit, MOF/graphite oxide hybrid materials: Exploring the new concept of adsorbents and catalysts, Adsorption. 17 (2011) 5–16. doi:10.1007/s10450-010-

9267-5.

[133] C. Petit, B. Mendoza, T.J. Bandosz, Reactive adsorption of ammonia on Cu-based MOF/graphene composites, Langmuir. 26 (2010) 15302–15309. doi:10.1021/la1021092.

[134] J.R. Li, J. Sculley, H.C. Zhou, Metal-Organic Frameworks for separations, Chem. Rev. 112 (2012) 869–932. doi:10.1021/cr200190s.

[135] P. Kumar, V. Bansal, K.H. Kim, E.E. Kwon, Metal-organic frameworks (MOFs) as futuristic options for wastewater treatment, J. Ind. Eng. Chem. 62 (2018) 130–145. doi:10.1016/j.jiec.2017.12.051.

[136] M. Kadhom, B. Deng, Metal-Organic Frameworks in water filtration membranes for desalination and other applications, Appl. Mater. Today. 11 (2018) 219–230. doi:https://doi.org/10.1016/j.apmt.2018.02.008.

[137] Y. Bian, N. Xiong, G. Zhu, Technology for the remediation of water pollution: A review on the fabrication of metal organic frameworks, Processes. 6 (2018). doi:10.3390/pr6080122.

[138] N. Yin, K. Wang, Y. Xia, Z. Li, Novel melamine modified metal-organic frameworks for remarkably high removal of heavy metal Pb (II), Desalination. 430 (2018) 120–127. doi:10.1016/j.desal.2017.12.057.

[139] S. Bo, W. Ren, C. Lei, Y. Xie, Y. Cai, S. Wang, J. Gao, Q. Ni, J. Yao, Flexible and porous cellulose aerogels/zeolitic imidazolate framework (ZIF-8) hybrids for adsorption removal of Cr(IV) from water, J. Solid State Chem. 262 (2018) 135–141. doi:10.1016/j.jssc.2018.02.022.

[140] Y.Y. Xiong, J.Q. Li, L. Le Gong, X.F. Feng, L.N. Meng, L. Zhang, P.P. Meng, M.B. Luo, F. Luo, Using MOF-74 for Hg2+ removal from ultra-low concentration aqueous solution, J. Solid State Chem. 246 (2017) 16–22. doi:10.1016/j.jssc.2016.10.018.

[141] A. Karimi, V. Vatanpour, A. Khataee, M. Safarpour, Contra-diffusion synthesis of ZIF-8 layer on polyvinylidene fluoride ultrafiltration membranes for improved water

purification, J. Ind. Eng. Chem. 73 (2019) 95–105. doi:10.1016/j.jiec.2019.01.010.

[142] K. Zhou, B. Mousavi, Z. Luo, S. Phatanasri, S. Chaemchuen, F. Verpoort, Characterization and properties of Zn/Co zeolitic imidazolate frameworks vs. ZIF-8 and ZIF-67, J. Mater. Chem. A. 5 (2017) 952–957. doi:10.1039/C6TA07860E.

[143] B.H. Stuart, Inorganic Molecules, in: Infrared Spectrosc. Fundam. Appl., Wiley, 2004: pp. 95–111. doi:10.1002/0470011149.

[144] H. Zhao, Y. Wang, L. Zhao, Magnetic Nanocomposites Derived from Hollow ZIF-67 and Core-Shell ZIF-67@ZIF-8: Synthesis, Properties, and Adsorption of Rhodamine B, Eur. J. Inorg. Chem. 2017 (2017) 4110–4116. doi:10.1002/ejic.201700587.

[145] M.L. Nguyen, C.C. Tanner, Ammonium removal from wastewaters using natural New Zealand zeolites, New Zeal. J. Agric. Res. 41 (1998) 427–446. doi:10.1080/00288233.1998.9513328.

[146] K.Y. Hor, J.M.C. Chee, M.N. Chong, B. Jin, C. Saint, P.E. Poh, R. Aryal, Evaluation of physicochemical methods in enhancing the adsorption performance of natural zeolite as low-cost adsorbent of methylene blue dye from wastewater, J. Clean. Prod. 118 (2016) 197–209. doi:10.1016/j.jclepro.2016.01.056.

[147] X. Liu, Z. Ni, C. Xie, R. Wang, R. Guo, Controlled Synthesis and Selective Adsorption Properties of Pr2CuO4 Nanosheets: a Discussion of Mechanism, Nanoscale Res. Lett. 13 (2018). doi:10.1186/s11671-018-2697-9.

[148] P.M. Usov, C. McDonnell-Worth, F. Zhou, D.R. MacFarlane, D.M. D'Alessandro, The electrochemical transformation of the zeolitic imidazolate framework ZIF-67 in aqueous electrolytes, Electrochim. Acta. 153 (2015) 433–438. doi:10.1016/j.electacta.2014.11.150.

[149] K.Y.A. Lin, H.A. Chang, Zeolitic Imidazole Framework-67 (ZIF-67) as a heterogeneous catalyst to activate peroxymonosulfate for degradation of Rhodamine B in water, J. Taiwan Inst. Chem. Eng. 53 (2015) 40–45. doi:10.1016/j.jtice.2015.02.027.

[150] K.Y.A. Lin, H.A. Chang, Ultra-high adsorption capacity of zeolitic imidazole framework-

67 (ZIF-67) for removal of malachite green from water, Chemosphere. 139 (2015) 624–631. doi:10.1016/j.chemosphere.2015.01.041.

[151] J. Dhainaut, C. Avci-Camur, J. Troyano, A. Legrand, J. Canivet, I. Imaz, D. Maspoch, H. Reinsch, D. Farrusseng, Systematic study of the impact of MOF densification into tablets on textural and mechanical properties, CrystEngComm. 19 (2017) 4211–4218. doi:10.1039/C7CE00338B.

[152] M.R. Ryder, J.-C. Tan, Nanoporous metal organic framework materials for smart applications, Mater. Sci. Technol. 30 (2014) 1598–1612. doi:10.1179/1743284714Y.0000000550.

[153] W.P. Mounfield, M. Taborga Claure, P.K. Agrawal, C.W. Jones, K.S. Walton, Synergistic Effect of Mixed Oxide on the Adsorption of Ammonia with Metal–Organic Frameworks, Ind. Eng. Chem. Res. 55 (2016) 6492–6500. doi:10.1021/acs.iecr.6b01045.

[154] N.C. Burtch, H. Jasuja, K.S. Walton, Water stability and adsorption in metal-organic frameworks, Chem. Rev. 114 (2014) 10575–10612. doi:10.1021/cr5002589.

[155] C. Wang, X. Liu, N. Keser Demir, J.P. Chen, K. Li, Applications of water stable metal–organic frameworks, Chem. Soc. Rev. 45 (2016) 5107–5134. doi:10.1039/C6CS00362A.

[156] O. Kolmykov, N. Chebbat, J.M. Commenge, G. Medjahdi, R. Schneider, ZIF-8 nanoparticles as an efficient and reusable catalyst for the Knoevenagel synthesis of cyanoacrylates and 3-cyanocoumarins, Tetrahedron Lett. 57 (2016) 5885–5888. doi:10.1016/j.tetlet.2016.11.070.

[157] C.S. Wu, Z.H. Xiong, C. Li, J.M. Zhang, Zeolitic imidazolate metal organic framework ZIF-8 with ultra-high adsorption capacity bound tetracycline in aqueous solution, RSC Adv. 5 (2015) 82127–82137. doi:10.1039/c5ra15497a.

[158] Q. Yang, R. Lu, S.S. Ren, C. Chen, Z. Chen, X. Yang, Three dimensional reduced graphene oxide/ZIF-67 aerogel: Effective removal cationic and anionic dyes from water, Chem. Eng. J. 348 (2018) 202–211. doi:10.1016/j.cej.2018.04.176.

[159] P. Krokidas, M. Castier, S. Moncho, D.N. Sredojevic, E.N. Brothers, H.T. Kwon, H.K. Jeong,

J.S. Lee, I.G. Economou, ZIF-67 Framework: A Promising New Candidate for Propylene/Propane Separation. Experimental Data and Molecular Simulations, J. Phys. Chem. C. 120 (2016) 8116–8124. doi:10.1021/acs.jpcc.6b00305.

[160] C. Liang, X. Zhang, P. Feng, H. Chai, Y. Huang, ZIF-67 derived hollow cobalt sulfide as superior adsorbent for effective adsorption removal of ciprofloxacin antibiotics, Chem. Eng. J. 344 (2018) 95–104. doi:10.1016/j.cej.2018.03.064.

[161] Y. Pan, H. Li, X.X. Zhang, Z. Zhang, X.S. Tong, C.Z. Jia, B. Liu, C.Y. Sun, L.Y. Yang, G.J. Chen, Large-scale synthesis of ZIF-67 and highly efficient carbon capture using a ZIF-67/glycol-2-methylimidazole slurry, Chem. Eng. Sci. 137 (2015) 504–514. doi:10.1016/j.ces.2015.06.069.

[162] K.Y. Andrew Lin, W. Der Lee, Self-assembled magnetic graphene supported ZIF-67 as a recoverable and efficient adsorbent for benzotriazole, Chem. Eng. J. 284 (2016) 1017–1027. doi:10.1016/j.cej.2015.09.075.

[163] J. Zhang, Y. Cai, K. Liu, Extremely Effective Boron Removal from Water by Stable Metal Organic Framework ZIF-67, Ind. Eng. Chem. Res. 58 (2019) 4199–4207. doi:10.1021/acs.iecr.8b05656.

[164] T.H. Chen, I. Popov, W. Kaveevivitchai, O.Š. Miljanić, Metal-organic frameworks: Rise of the ligands, Chem. Mater. 26 (2014) 4322–4325. doi:10.1021/cm501657d.

[165] V. Guillerm, H. Xu, J. Albalad, I. Imaz, D. Maspoch, Postsynthetic Selective Ligand Cleavage by Solid-Gas Phase Ozonolysis Fuses Micropores into Mesopores in Metal-Organic Frameworks, J. Am. Chem. Soc. 140 (2018) 15022–15030. doi:10.1021/jacs.8b09682.

[166] H. Jasuja, Y.G. Huang, K.S. Walton, Adjusting the stability of metal-organic frameworks under humid conditions by ligand functionalization, Langmuir. 28 (2012) 16874–16880. doi:10.1021/la304151r.

[167] J.F. Van Humbeck, T.M. McDonald, X. Jing, B.M. Wiers, G. Zhu, J.R. Long, Ammonia capture in porous organic polymers densely functionalized with Bronsted acid groups, J. Am.

Chem. Soc. 136 (2014) 2432–2440. doi:10.1021/ja4105478.

[168] G. Barin, G.W. Peterson, V. Crocellà, J. Xu, K.A. Colwell, A. Nandy, J.A. Reimer, S. Bordiga, J.R. Long, Highly effective ammonia removal in a series of Brønsted acidic porous polymers: investigation of chemical and structural variations, Chem. Sci. (2017) 4399–4409. doi:10.1039/C6SC05079D.

[169] D. Britt, D. Tranchemontagne, O.M. Yaghi, Metal-organic frameworks with high capacity and selectivity for harmful gases, Proc. Natl. Acad. Sci. 105 (2008) 11623–11627. doi:10.1073/pnas.0804900105.

[170] G.W. Peterson, G.W. Wagner, A. Balboa, J. Mahle, T. Sewell, C.J. Karwacki, Ammonia Vapor Removal by Cu3 (BTC)2 and Its Characterization by MAS NMR, J Phys Chem C Nanomater Interfaces. 113 (2009) 13906–13917. doi:10.1021/jp902736z.Ammonia.

[171] A. Buccolieri, A. Serra, G. Giancane, D. Manno, Colloidal solution of silver nanoparticles for label-free colorimetric sensing of ammonia in aqueous solutions, Beilstein J. Nanotechnol. 9 (2018) 499–507. doi:10.3762/bjnano.9.48.

[172] L. Chetia, D. Kalita, G.A. Ahmed, Synthesis of Ag nanoparticles using diatom cells for ammonia sensing, Sens. Bio-Sensing Res. 16 (2017) 55–61. doi:10.1016/j.sbsr.2017.11.004.

[173] X.W. Liu, T.J. Sun, J.L. Hu, S.D. Wang, Composites of metal-organic frameworks and carbon-based materials: Preparations, functionalities and applications, J. Mater. Chem. A. 4 (2016) 3584–3616. doi:10.1039/c5ta09924b.

[174] I. Ahmed, S.H. Jhung, Composites of metal-organic frameworks: Preparation and application in adsorption, Mater. Today. 17 (2014) 136–146. doi:10.1016/j.mattod.2014.03.002.

[175] ELG, ELG Carbon Fibre Ltd., (2019). http://www.elgcf.com/ (accessed October 20, 2019).

[176] A. Khan, M. Ali, A. Ilyas, P. Naik, I.F.J. Vankelecom, M.A. Gilani, M.R. Bilad, Z. Sajjad, A.L. Khan, ZIF-67 filled PDMS mixed matrix membranes for recovery of ethanol via

pervaporation, Sep. Purif. Technol. 206 (2018) 50–58. doi:10.1016/j.seppur.2018.05.055.

[177] W. Zhang, R. Fu, L. Wang, J. Zhu, J. Feng, W. Yan, Rapid removal of ammonia nitrogen in low-concentration from wastewater by amorphous sodium titanate nano-particles, Sci. Total Environ. 668 (2019) 815–824. doi:10.1016/j.scitotenv.2019.03.051.

[178] B. Pan, Q. Zhang, W. Du, W. Zhang, B. Pan, Q. Zhang, Z. Xu, Q. Zhang, Selective heavy metals removal from waters by amorphous zirconium phosphate: Behavior and mechanism, Water Res. 41 (2007) 3103–3111. doi:10.1016/j.watres.2007.03.004.

[179] Q. Chen, K. Zhou, Y. Chen, A. Wang, F. Liu, Removal of ammonia from aqueous solutions by ligand exchange onto a Cu(ii)-loaded chelating resin: kinetics, equilibrium and thermodynamics, RSC Adv. 7 (2017) 12812–12823. doi:10.1039/c6ra28287c.

[180] S.F. Ali, A. Gillich, Determining the UK's Potential for Heat Recovery from Wastewater using Steady State and Dynamic Modelling - Preliminary Results, WEENTECH Proc. Energy. 5 (2019) 107–121. doi:10.32438/WPE.58181.

[181] Environment Agency, H1 Annex D-Basic Surface water discharges, GEHO0810BSXL-E-E v2.2. (2011). http://www.devon.gov.uk/core-doc-s3-h1-annex-d-basic-surface-water-discharges.pdf.

[182] L.-F. Huang, J.M. Rondinelli, Reliable electrochemical phase diagrams of magnetic transition metals and related compounds from high-throughput ab initio calculations, Npj Mater. Degrad. 3 (2019). doi:10.1038/s41529-019-0088-z.

[183] J. Chivot, L. Mendoza, C. Mansour, T. Pauporté, M. Cassir, New insight in the behaviour of Co-H 2 O system at 25-150 °C, based on revised Pourbaix diagrams, Corros. Sci. 50 (2008) 62–69. doi:10.1016/j.corsci.2007.07.002.

[184] V.D.J. Keller, R.J. Williams, C. Lofthouse, A.C. Johnson, Worldwide estimation of river concentrations of any chemical originating from sewage-treatment plants using dilution factors, Environ. Toxicol. Chem. 33 (2014) 447–452. doi:10.1002/etc.2441.

[185] C. Manchanayake, The design and build of a reusable container that can be used to

recover nitrogen-based compounds from wastewater - ES327 Technical Report, University of Warwick, 2019.

[186] Q. Deng, B.R. Dhar, E. Elbeshbishy, H.S. Lee, Ammonium nitrogen removal from the permeates of anaerobic membrane bioreactors: Economic regeneration of exhausted zeolite, Environ. Technol. (United Kingdom). 35 (2014) 2008–2017. doi:10.1080/09593330.2014.889759.

[187] M.D. LeVan, G. Carta, Adsorption and Ion Exchange, in: D.W. Green, R.H. Perry (Eds.), Perry's Chem. Eng. Handb., 8th Editio, 2007: pp. 16-1,16-69.

[188] A. Thornton, P. Pearce, S.A. Parsons, Ammonium removal from solution using ion exchange on to MesoLite, an equilibrium study, J. Hazard. Mater. 147 (2007) 883–889. doi:10.1016/j.jhazmat.2007.01.111.

[189] A. Thornton, P. Pearce, S.A. Parsons, Ammonium removal from digested sludge liquors using ion exchange, Water Res. 41 (2006) 433–439. doi:10.1016/j.watres.2006.10.021.

[190] J. Canellas-Garriga, Tertiary Ammonium Removal with Zeolites (Ph.D Thesis), Cranfield University, 2018.

[191] A.R. Rahmani, A.H. Mahvi, A.R. Mesdaghinia, S. Nasseri, Investigation of ammonia removal from polluted waters by Clinoptilolite zeolite, Int. J. Environ. Sci. Technol. 1 (2013) 125–133. doi:10.1007/BF03325825.

[192] Promethean Particles Ltd, Shop, Prometh. Part. Ltd. (2019). https://www.prometheanparticles.co.uk/shop/page/2/ (accessed October 30, 2019).

[193] Alibaba.com, Alibaba, (2019).

[194] Castle Cover, The Changing Prices of Products in the UK from the 50s to the Present Day, (2019). https://www.castlecover.co.uk/historic-home-utility-prices/ (accessed November 20, 2019).

[195] K. Rademann, M. Klimakow, P. Klobes, A.F. Th, Mechanochemical Synthesis of Metal - Organic Frameworks : A Fast and Facile Approach toward Quantitative Yields and High Specific Surface Areas, (2010) 5216–5221. doi:10.1021/cm1012119.

[196] MarketWatch, Metal-organic Frameworks (MOF) Market Size Soaring at 34.3% CAGR to Reach 410 million USD by 2024, MarketWatch. (2019). https://www.marketwatch.com/press-release/metal-organic-frameworks-mof-market-size-soaring-at-343-cagr-to-reach-410-million-usd-by-2024-2019-05-09 (accessed October 25, 2019).

[197] Metcalf & Eddie, Adsorption, in: Wastewater Eng. - Treat. Resour. Recover., Fifth Edit, McGraw-Hill Education, 2014: pp. 1224–1245.

[198] P.S. Kumar, L. Korving, M.C.M. van Loosdrecht, G.J. Witkamp, Adsorption as a technology to achieve ultra-low concentrations of phosphate: Research gaps and economic analysis, Water Res. X. 4 (2019) 100029. doi:10.1016/j.wroa.2019.100029.

Appendix A

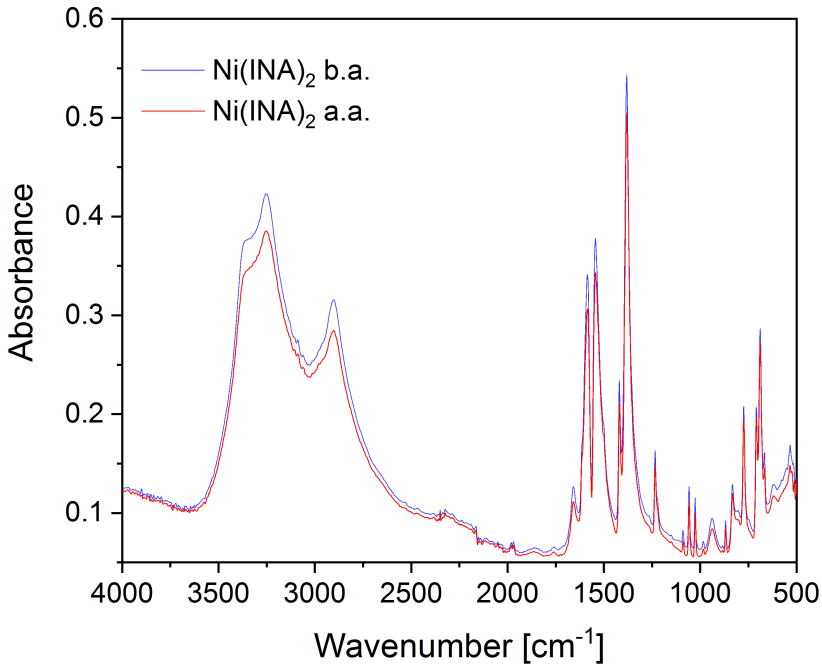

***Figure A 1**: FTIR spectra of $Ni(INA)_2$ before adsorption (b.a.) and after adsorption (a.a.)*

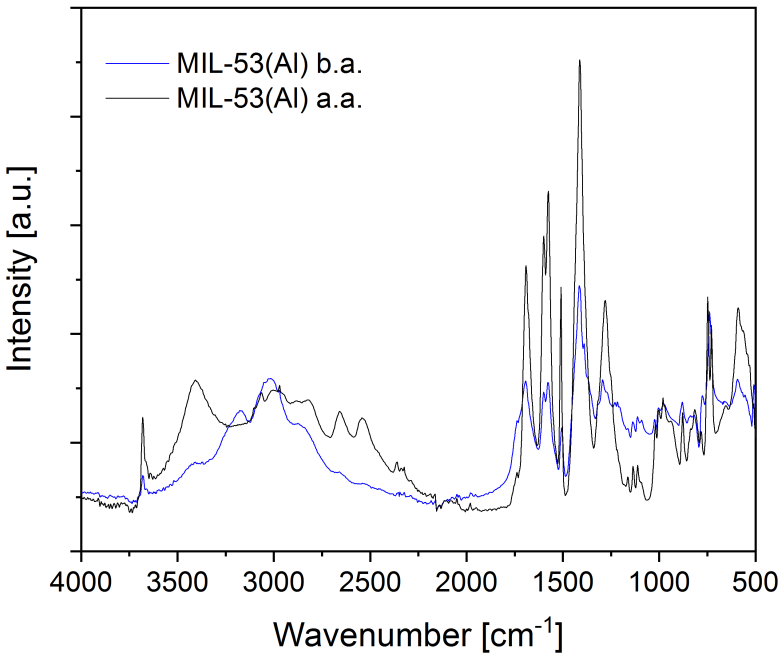

***Figure A 2**: FTIR spectra of MIL-53(Al) before (b.a.) and after (a.a.) adsorption*

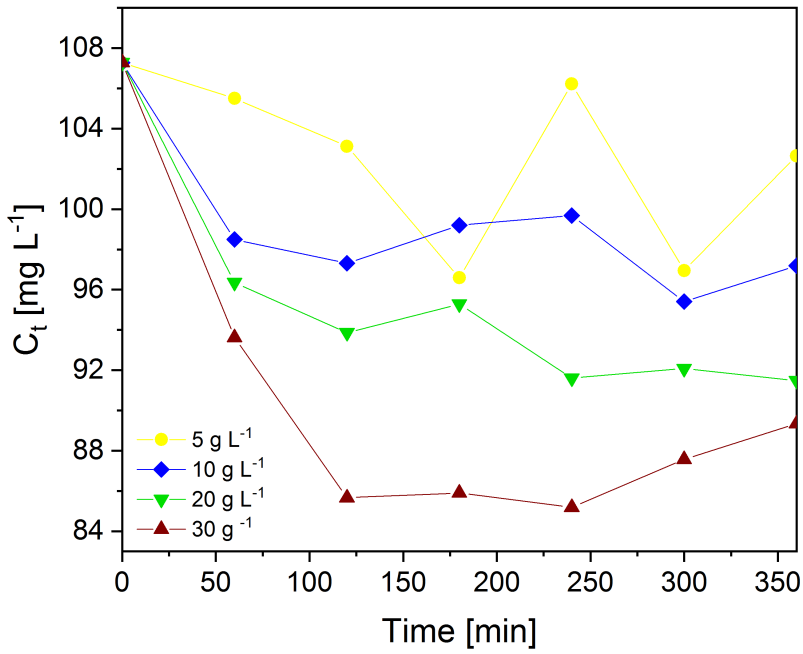

***Figure A 3**: Residual concentration C_t over time for CPO-27(Ni) at different MOF loadings*

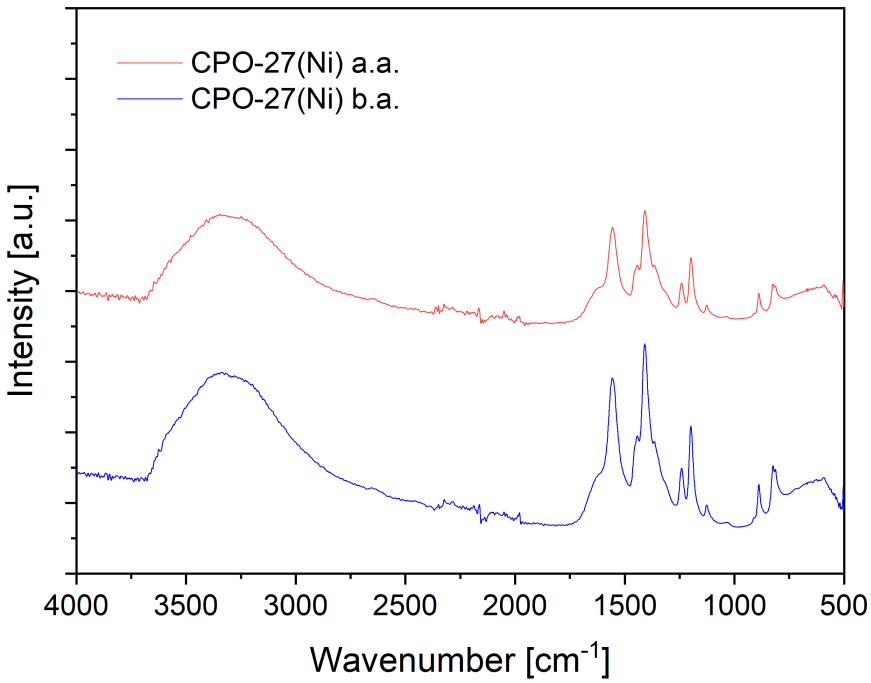

***Figure A 4**: FTIR of CPO-27(Ni) before (b.a.) and after (a.a.) adsorption*

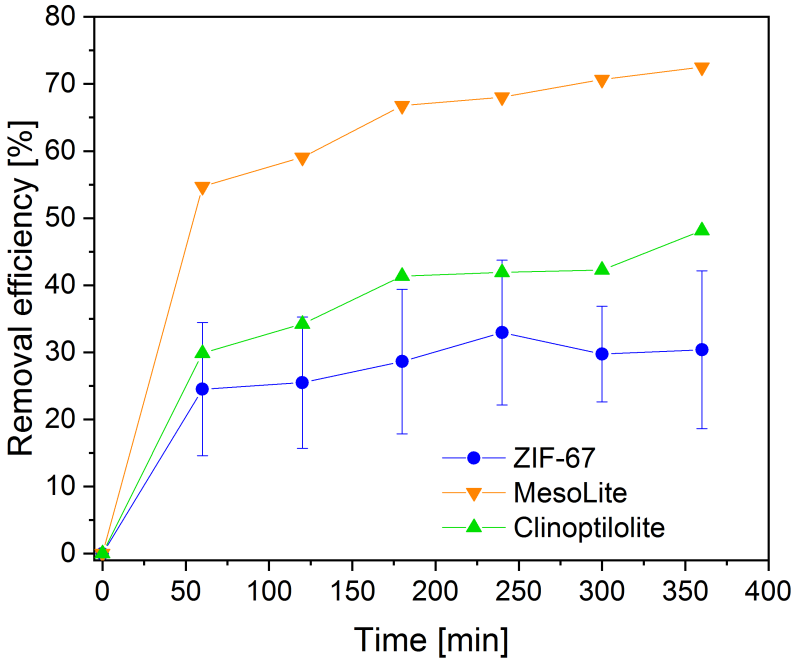

***Figure A 5**: Removal efficiency over time of ZIF-67, clinoptilolite and MesoLite*

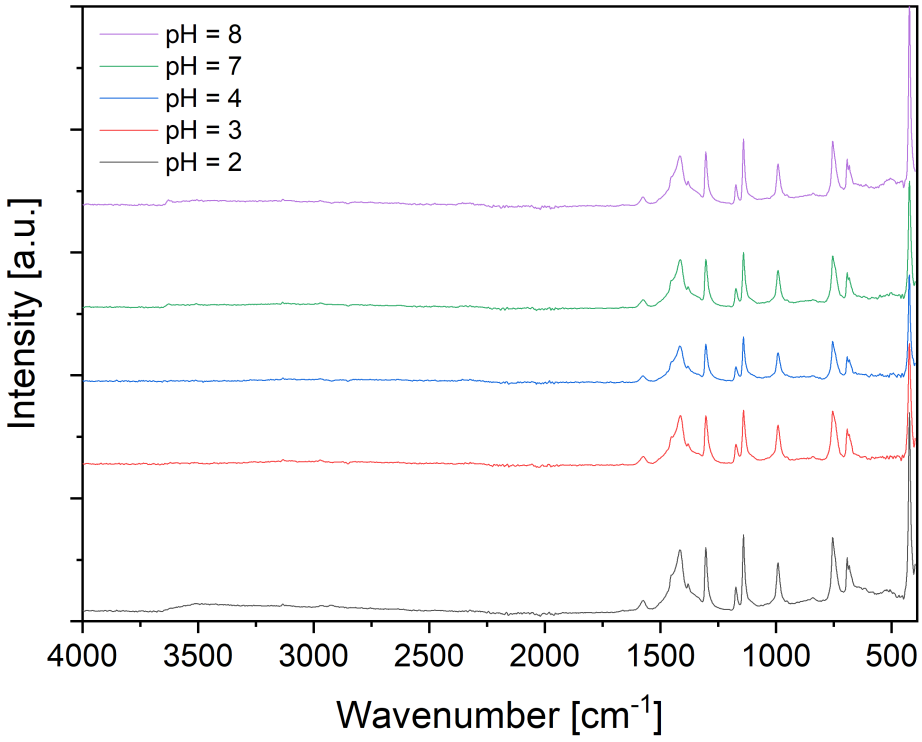

***Figure A 6**: FTIR of ZIF-67 after adsorption with different initial pHs*

Appendix B

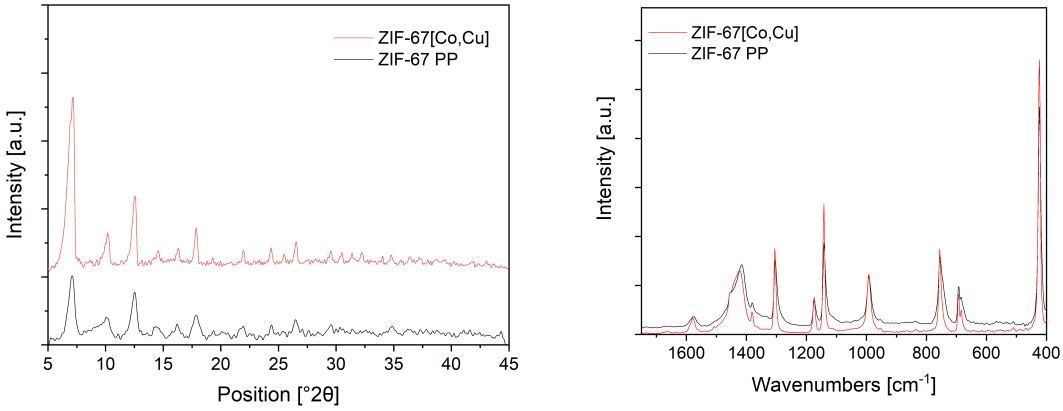

***Figure B 1**: XRD (left) and FTIR (right) of ZIF-67[Co,Cu] compared to ZIF-67 PP*

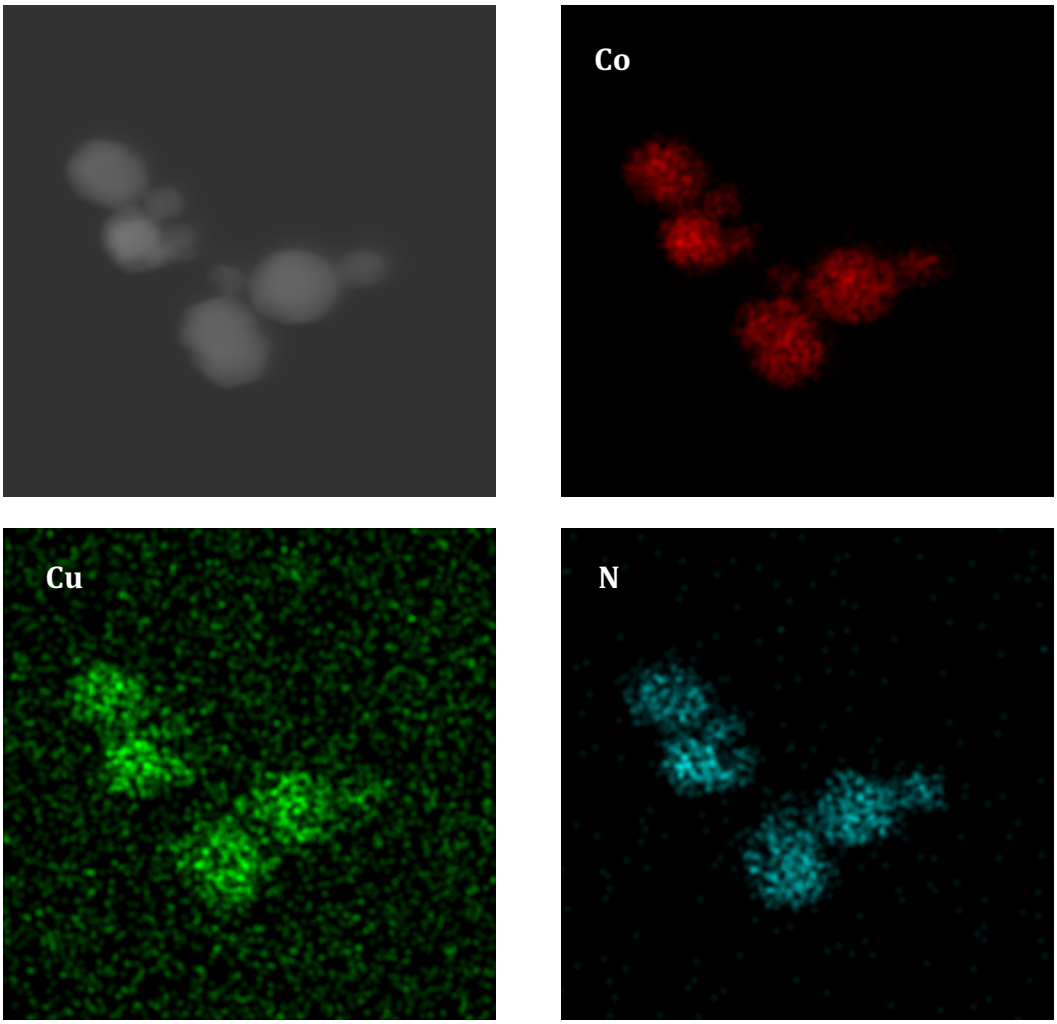

***Figure B 2**: EDS-TEM elemental mapping images of ZIF-67[Co,Cu]*

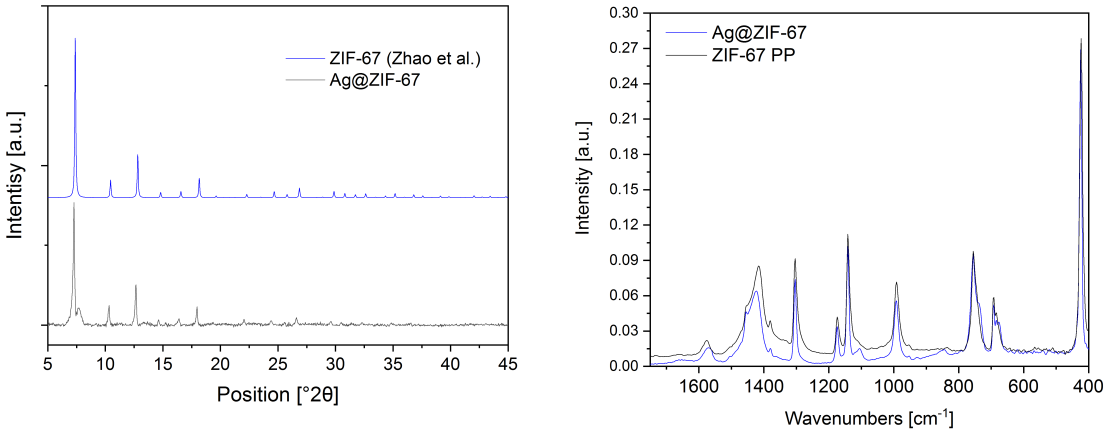

***Figure B 3**: XRD (left) and FTIR (right) of Ag@ZIF-67 compared to ZIF-67 PP*

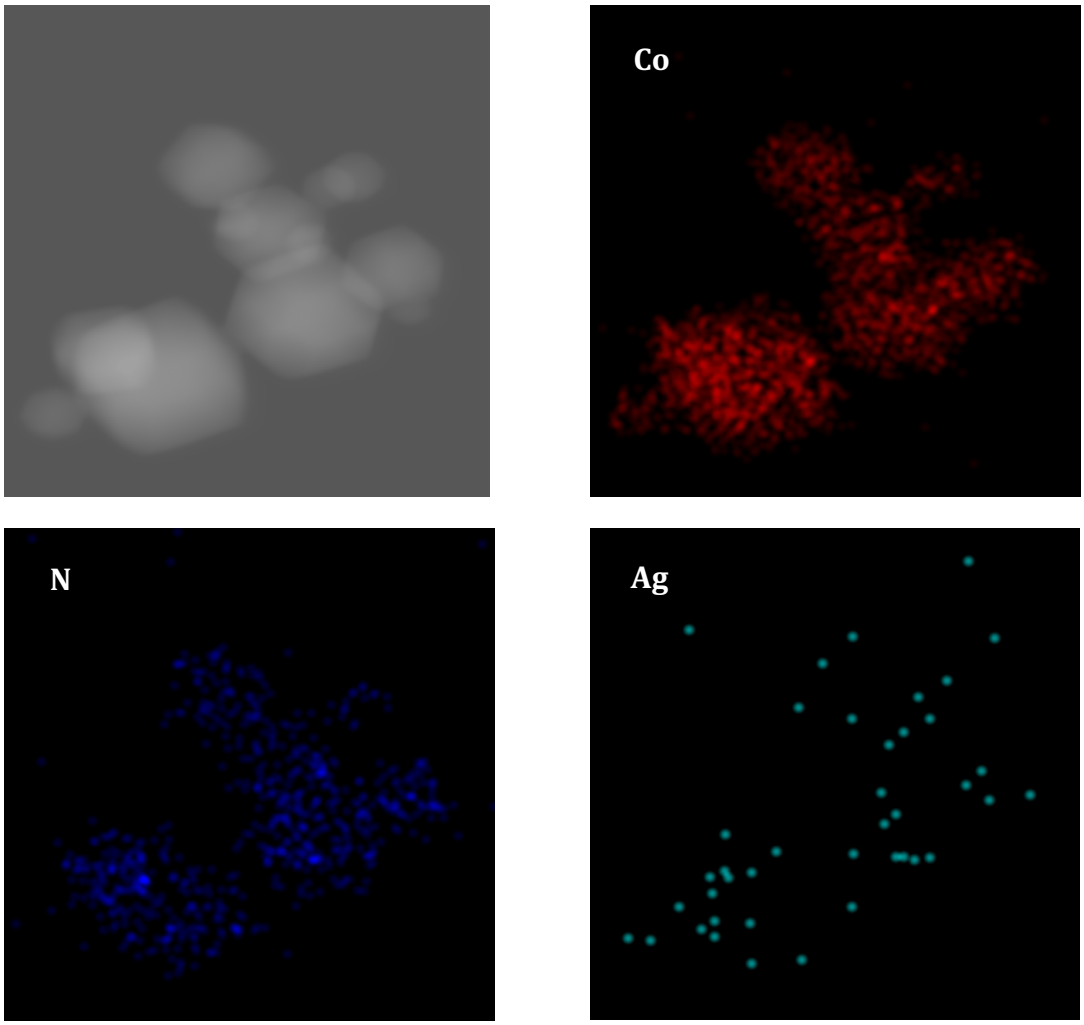

***Figure B 4**: EDS-TEM elemental mapping images of Ag@ZIF-67*

Appendix C

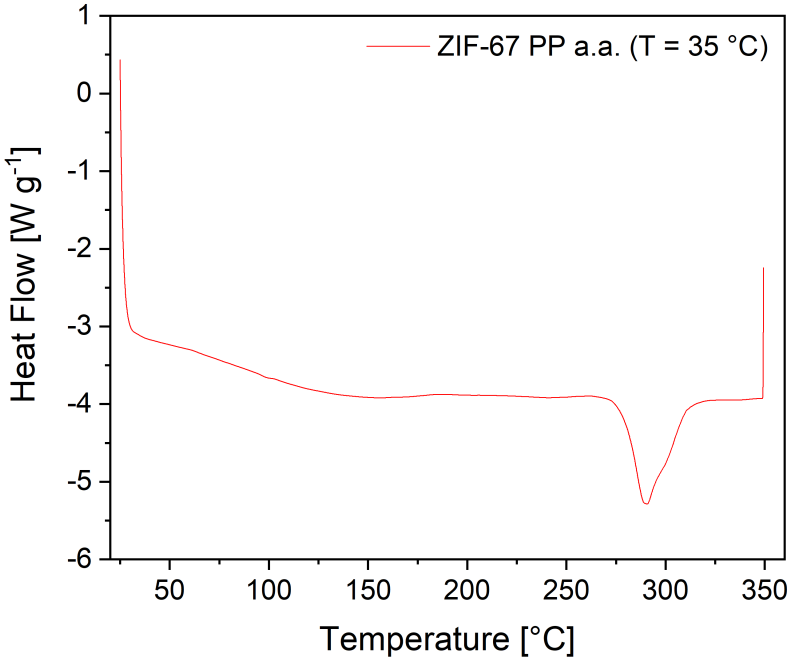

***Figure C 1**: DSC curve of ZIF-67 PP after adsorption at 35 °C*